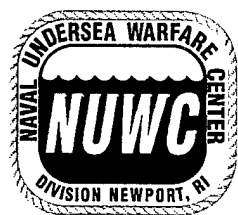


Detection Performance of Or-ing Device with Pre- and Post-Averaging: Part III – Deterministic Signal

Albert H. Nuttall
Surface Undersea Warfare Department



**Naval Undersea Warfare Center Division
Newport, Rhode Island**

Approved for public release; distribution is unlimited.

DTIC QUALITY INSPECTED 4

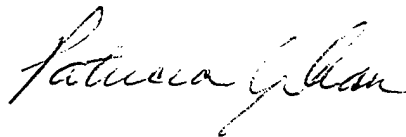
20001002 026

PREFACE

The work described in this report was sponsored by the Independent Research Program of the Naval Undersea Warfare Center (NUWC) Division, Newport, RI, Project No. C622480, "Performance Analysis of Or-ing with Arbitrary Amounts of Pre-Averaging and Post-Averaging," principal investigator Albert H. Nuttall (Code 31A). The Independent Research Program is funded by the Office of Naval Research; the NUWC Division Newport program manager is Richard B. Philips (Code 102). This report was also partially funded by Project No. A196200, "Passive Advanced Processing Build," principal investigator Walter R. Lane (Code 2123). The sponsoring activity is the Program Executive Office, Undersea Warfare, Advanced Systems and Technology Office (ASTO-D1), program manager Robert Zarnich.

The technical reviewer for this report was William A. Struzinski (Code 2123).

Reviewed and Approved: 18 September 2000



Patricia J. Dean
Director, Surface Undersea Warfare



REPORT DOCUMENTATION PAGEForm Approved
OMB No. 0704-0188

Public reporting burden for this collection of information is estimated to average 1 hour per response, including the time for reviewing instructions, searching existing data sources, gathering and maintaining the data needed, and completing and reviewing the collection of information. Send comments regarding this burden estimate or any other aspect of this collection of information, including suggestions for reducing this burden, to Washington Headquarters Services, Directorate for Information Operations and Reports, 1215 Jefferson Davis Highway, Suite 1204, Arlington, VA 22202-4302, and to the Office of Management and Budget, Paperwork Reduction Project (0704-0188), Washington, DC 20503.

1. AGENCY USE ONLY (Leave Blank)		2. REPORT DATE 18 September 2000	3. REPORT TYPE AND DATES COVERED Final	
4. TITLE AND SUBTITLE Detection Performance of Or-ing Device with Pre- and Post-Averaging: Part III – Deterministic Signal			5. FUNDING NUMBERS	
6. AUTHOR(S) Albert H. Nuttall				
7. PERFORMING ORGANIZATION NAME(S) AND ADDRESS(ES) Naval Undersea Warfare Center Division 1176 Howell Street Newport, RI 02841-1708			8. PERFORMING ORGANIZATION REPORT NUMBER TR 11,248	
9. SPONSORING/MONITORING AGENCY NAME(S) AND ADDRESS(ES) Office of Naval Research 800 North Quincy Street Arlington, VA 22217-5160 Program Executive Office for Undersea Warfare (ASTO D1) 2531 Jefferson Davis Highway Arlington, VA 22242-5160			10. SPONSORING/MONITORING AGENCY REPORT NUMBER	
11. SUPPLEMENTARY NOTES				
12a. DISTRIBUTION/AVAILABILITY STATEMENT Approved for public release; distribution is unlimited.			12b. DISTRIBUTION CODE	
13. ABSTRACT (Maximum 200 words) <p>The detection performance of an or-ing device with pre-averaging and post-averaging has been determined in the form of numerous receiver operating characteristics covering a wide range of input deflections (signal-to-noise ratios). Numerical evaluation of the false alarm probability P_f and detection probability P_d has been conducted for the case of a deterministic signal in the presence of additive Gaussian noise for a wide range of values of K, the amount of pre-averaging before or-ing; N, the number of channels or-ed; and M, the amount of post-averaging after or-ing. A MATLAB program that can be used to extend these results to parameter values outside the range studied here is also provided.</p> <p>The tradeoffs associated with switching from post-averaging to pre-averaging, or vice versa, have been thoroughly investigated and tabulated for a standard operating point ($P_f = 1E-3$, $P_d = 0.5$) and for a high-quality operating point ($P_f = 1E-6$, $P_d = 0.9$). The losses associated with performing too little pre-averaging can be severe, especially for large numbers, N, of or-ed channels.</p>				
14. SUBJECT TERMS Signal Processing Or-ing Deterministic Signals Pre-averaging Post-averaging			15. NUMBER OF PAGES 80	
			16. PRICE CODE	
17. SECURITY CLASSIFICATION OF REPORT Unclassified	18. SECURITY CLASSIFICATION OF THIS PAGE Unclassified	19. SECURITY CLASSIFICATION OF ABSTRACT Unclassified	20. LIMITATION OF ABSTRACT SAR	

TABLE OF CONTENTS

	Page
LIST OF ILLUSTRATIONS	ii
LIST OF TABLES	iii
LIST OF ABBREVIATIONS, ACRONYMS, AND SYMBOLS	iii
INTRODUCTION	1
Background	1
Scope	3
INPUT DATA MODELS	5
Deterministic Signal in Gaussian Noise	5
Optimum Processing of Available Data	6
PERFORMANCE ANALYSIS FOR BLOCK PROCESSING.	7
Deterministic Signal	10
A Shortcut in Tabulated Results.	11
Special Cases	12
Numerical Approach	13
QUANTITATIVE PERFORMANCE RESULTS	15
Required Input Deflections	15
Tradeoff Between Pre- and Post-Averaging	22
SUMMARY	25
APPENDIX A — ROCs FOR DETERMINISTIC SIGNAL	A-1
APPENDIX B — MATLAB PROGRAM FOR EVALUATION OF RECEIVER OPERATING CHARACTERISTICS	B-1
APPENDIX C — SHIFTED DECISION VARIABLES	C-1
REFERENCES	R-1

LIST OF ILLUSTRATIONS

Figure		Page
1	Or-ing with Pre- and Post-Averaging	2
2	Required Input Deflection $d(K,N,M)$ for $P_f = 1E-3$, $P_d = 0.5$, $KM = 4$, Deterministic Signal.	17
3	Required Input Deflection $d(K,N,M)$ for $P_f = 1E-6$, $P_d = 0.9$, $KM = 4$, Deterministic Signal.	17
4	Required Input Deflection $d(K,N,M)$ for $P_f = 1E-3$, $P_d = 0.5$, $KM = 16$, Deterministic Signal	18
5	Required Input Deflection $d(K,N,M)$ for $P_f = 1E-6$, $P_d = 0.9$, $KM = 16$, Deterministic Signal	18
6	Required Input Deflection $d(K,N,M)$ for $P_f = 1E-3$, $P_d = 0.5$, $KM = 64$, Deterministic Signal	19
7	Required Input Deflection $d(K,N,M)$ for $P_f = 1E-6$, $P_d = 0.9$, $KM = 64$, Deterministic Signal	19
8	Required Input Deflection $d(K,N,M)$ for $P_f = 1E-3$, $P_d = 0.5$, $KM = 256$, Deterministic Signal.	20
9	Required Input Deflection $d(K,N,M)$ for $P_f = 1E-6$, $P_d = 0.9$, $KM = 256$, Deterministic Signal.	20
10	Required Input Deflection $d(K,N,M)$ in Decibels for $P_f = 1E-3$, $P_d = 0.5$, $KM = 256$, Deterministic Signal . .	21
11	Required Input Deflection $d(K,N,M)$ in Decibels for $P_f = 1E-6$, $P_d = 0.9$, $KM = 256$, Deterministic Signal . .	21

LIST OF TABLES

Table	Page
1 Required Input Deflection $d_1(N,M)$ for $P_f = 1E-3$, $P_d = 0.5$, $K = 1$, Deterministic Signal	16
2 Required Input Deflection $d_1(N,M)$ for $P_f = 1E-6$, $P_d = 0.9$, $K = 1$, Deterministic Signal	16

LIST OF ABBREVIATIONS, ACRONYMS, AND SYMBOLS

c_0, c_1	Cumulative distribution functions of $y_n(t)$, equation (6)
CDF	Cumulative distribution function
CF	Characteristic function
c_v	Cumulative distribution function of $v(t)$, equation (6)
d, d_k	Deflection, equations (2) and (3)
$d(K,N,M)$	Required input deflection, equations (23) and (24)
$d_1(N,M)$	Required input deflection for $K = 1$, equation (23)
\underline{d}	Deflection at pre-averager output, $\underline{d} = \sqrt{K} d$
dB	Decibel
EDF	Exceedance distribution function
e_v	Exceedance distribution function of $v(t)$, equations (9) and (10)
e_w	Exceedance distribution function of $w(t)$, equations (13) and (14)
FFT	Fast Fourier transform

LIST OF ABBREVIATIONS, ACRONYMS, AND SYMBOLS (Cont'd)

f_v	Characteristic function of $v(t)$, equation (11)
f_w	Characteristic function of $w(t)$, equation (12)
$\{g_k\}$	Gaussian random variables, equations (2) and (3)
H_0, H_1	Signal-absent, signal-present hypotheses
HOP	High-quality operating point, $P_f = 1E-6$ and $P_d = 0.9$
K	Amount of pre-averaging, figure 1
M	Amount of post-averaging, figure 1
N	Total number of channels or-ed, figure 1
or-ing	Pass only the largest of N inputs, figure 1
p_0, p_1	Probability density functions of $y_n(t)$, equations (7) and (8)
p, PDF	Probability density function
P_d	Detection probability
P_f	False alarm probability
p_v	Probability density function of $v(t)$, equations (7) and (8)
ROC	Receiver operating characteristic
RV	Random variable
SNR	Signal-to-noise ratio
SOP	Standard operating point, $P_f = 1E-3$ and $P_d = 0.5$
t	Time instant, equation (1)
T	Available time-bandwidth product (= KM), equation (4)
$v(t)$	Or-ing output, figure 1 and equation (1)
$w(t)$	System output, figure 1
$x_n(t)$	Input data in n-th channel, figure 1 and equation (2)

LIST OF ABBREVIATIONS, ACRONYMS, AND SYMBOLS (Cont'd)

$y_n(t)$	Pre-averager output in n-th channel, figure 1
α, β	Auxiliary parameters, equation (27)
Δ_ξ	Sampling increment in ξ
Δ_u	Sampling increment in u
ϕ, Φ	Gaussian probability functions, equation (15)
$\tilde{\Phi}$	Inverse Φ function, equation (26)
ξ	Argument of characteristic functions, equation (11)
boldface	Random variable
overbar	Ensemble average

DETECTION PERFORMANCE OF OR-ING DEVICE WITH PRE- AND
POST-AVERAGING: PART III - DETERMINISTIC SIGNAL

INTRODUCTION

BACKGROUND

The need to process and condense large amounts of data is encountered frequently in modern Navy systems that employ multiple beams, frequency bins, range cells, et cetera. One way of accomplishing this goal is by or-ing a number of inputs into a single output - that is, allowing only the largest of a set of quantities to pass on for further processing and completely rejecting the remainder. However, since this or-ing operation is highly nonlinear, destroys information, and tends to cause small-signal suppression, some pre-averaging of the inputs to the or-ing device is often employed in an effort to build up the signal-to-noise ratio (SNR) prior to the maximum comparison. Furthermore, at the or-ing output, some additional post-averaging is frequently used, this time in an effort to build up the SNR before a threshold comparison is made for the purpose of declaring a signal present or absent (hypothesis H_1 or H_0 , respectively). The pertinent block diagram is displayed in figure 1.

There are N channels of real input data available for processing, namely, $\{x_n(t)\}$ for $n=1:N$, where time t has been

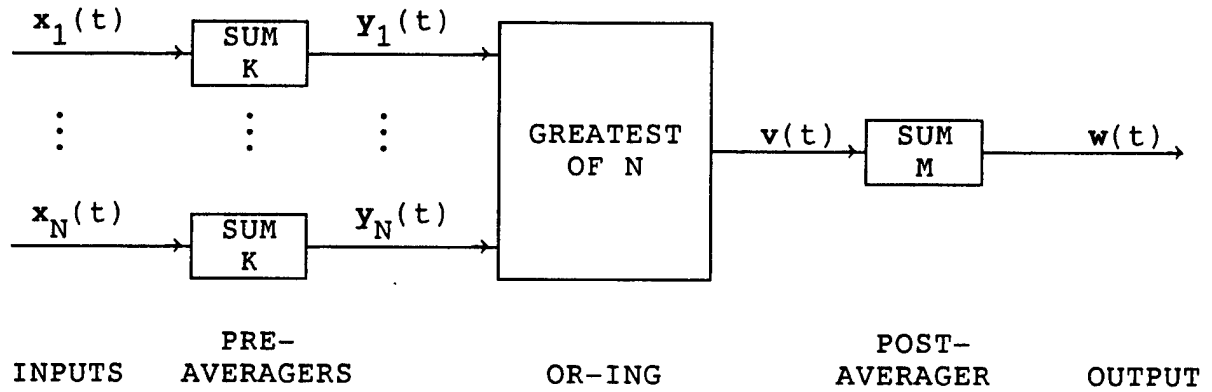


Figure 1. Or-ing with Pre- and Post-Averaging

normalized so that time-sampling instant t is an integer. Under hypothesis H_0 , there is only Gaussian noise in all the inputs, whereas under hypothesis H_1 , a signal is also present in one (unknown) channel. The goal of the processor in figure 1 is to determine signal presence with a high detection probability P_d , while realizing a specified acceptable low false alarm probability P_f .

Each pre-averager accumulates K statistically independent consecutive time samples of its corresponding input $x_n(t)$, yielding output $y_n(t)$, which is then subjected to or-ing amongst N competitors. The or-ing output at time t is

$$v(t) = \max\{y_1(t), \dots, y_N(t)\} . \quad (1)$$

Finally, the post-averager accumulates M samples of its input $v(t)$ and compares its output $w(t)$ with a fixed threshold. It is

presumed that the post-averager waits for all the K input data samples to be summed and or-ed before an input is received; then, another block of K input samples is summed and or-ed, leading to the next input to the post-averager. That is, block processing is presumed.

SCOPE

This technical report constitutes part III of a series of three investigations of or-ing with pre- and post-averaging. In particular, three different input signal models in additive Gaussian noise are of interest:

- (I) Random (Gaussian) signal,
- (II) Phase-incoherent signal, and
- (III) Coherent (deterministic) signal.

Results for part I, the Gaussian signal, have been documented in reference 1. Specifically, the details on block and overlap processing, as well as a scaling property and the standard of comparison for the or-ing system in figure 1, are presented here, along with references to related past results. Part II, the phase-incoherent signal, was documented in reference 2. The reader should be familiar with the contents of both of these earlier documents.

The current report addresses part III, the deterministic signal in noise, and presents numerous receiver operating characteristics (ROCs) that completely quantify the performance of the or-ing system in figure 1. For all three signal models above, the optimum processors have been determined, as shown in appendix A of reference 1. Thus, the exact losses that the or-ing procedure causes can be accurately quantified.

For the block processing in figure 1, expressions are derived that allow for accurate evaluation of the false alarm probability P_f and the detection probability P_d for the decision variable $w(t)$. Furthermore, these evaluations are accomplished for arbitrary amounts of pre-averaging K , arbitrary amounts of or-ing N , arbitrary amounts of post-averaging M , and arbitrary input SNRs. No approximations are involved, the analysis is not limited to mean and variance calculations, and no appeal is made to the central limit theorem. Rather, the approach employs a judicious combination of analysis and computer-aided numerical calculations. The accuracy of the end result is limited only by the accuracy of the computer. An entire ROC can be generated in minutes.

INPUT DATA MODELS

In this section, g_k is a zero-mean, unit-variance Gaussian random variable (RV).

DETERMINISTIC SIGNAL IN GAUSSIAN NOISE

Here, in part III, the signal channel input at time k under H_1 is amplitude variate

$$x_k = g_k + d_k , \quad (2)$$

where d_k is nonrandom. The input mean is $\overline{x_k} = d_k$, while the input variance is $\text{var}(x_k) = 1$. Thus, d_k is an input amplitude SNR measure, while d_k^2 (or $d_k^2/2$) is an input power SNR measure. For the noise channels, $x_k = g_k$, with zero mean and unit variance. Thus, d_k can be interpreted as a per-sample difference in mean inputs that is divided by the common input standard deviation. This quantity, d_k , will be called the input deflection.

When $d_k = d$ for all k (that is, a common input deflection d over time, or a constant signal amplitude with time), the pre-averager output under H_1 for the signal channel is

$$y = \sum_{k=1}^K x_k = \sum_{k=1}^K g_k + K d = y^0 + K d , \quad (3)$$

where y^0 is the corresponding noise-only pre-averager output. The ROCs can be parameterized by input deflection d or input power SNR measure d^2 (or $d^2/2$). More generally, the single

parameter value $d_T = \sum_k d_k$ characterizes the performance of the processor when the individual input deflections $\{d_k\}$ are unequal and arbitrary. However, this observation is of limited utility unless all of the M sums of $\{d_k\}$, one for each post-averaging interval, are identical.

OPTIMUM PROCESSING OF AVAILABLE DATA

The optimum processor for signal model (2) has been derived in appendix A of reference 1 for the case where channel occupancy identification is required, as well as for the alternative case where channel identification is irrelevant. For all situations, the optimum processor is essentially given by the threshold comparison

$$\max_{n=1:N} \left\{ \sum_{t=1}^T x_n(t) \right\} \begin{matrix} > \\ < \end{matrix} u ; \quad (4)$$

see equations (A-13), (A-19), and (A-26) of reference 1. This operation is equivalent to performing all pre-averaging and no post-averaging in figure 1, that is, taking $K = T$, the total time-bandwidth product available, and $M = 1$. Doing so defers the nonlinearity (or-ing) until after all possible linear combining (pre-averaging) has been accomplished. This case will be thoroughly evaluated numerically and will serve as the basis of comparison for the various combinations of pre-averaging and post-averaging, that is, $K < T$ or $M > 1$.

PERFORMANCE ANALYSIS FOR BLOCK PROCESSING

Due to the pre-averaging, each RV $y_n(t)$ in figure 1 is a sum of K independent RVs with identical statistics. Also, all N channel inputs are statistically independent of each other. For or-ing to be present, $N \geq 2$ is required for the following calculations and considerations.

For a noise-only channel, let p_0 be the probability density function (PDF) of pre-averager output $y_n(t)$, and let c_0 be the corresponding cumulative distribution function (CDF), namely, $c_0(u) = \text{Prob}\{y_n(t) < u | H_0\}$. For a signal present in channel 1, say, let p_1 and c_1 be the corresponding PDF and CDF of $y_1(t)$.

The or-ing output $v(t)$ in figure 1 is

$$v(t) = \max\{y_1(t), \dots, y_N(t)\} . \quad (5)$$

Its CDF for signal present, that is, hypothesis H_1 , is

$$c_{v1}(u) = c_1(u) [c_0(u)]^{N-1} , \quad (6)$$

which leads to the corresponding PDF of $v(t)$ under H_1 as

$$\begin{aligned} p_{v1}(u) &= c'_{v1}(u) = p_1(u) [c_0(u)]^{N-1} + c_1(u) (N-1) [c_0(u)]^{N-2} p_0(u) \\ &= [c_0(u)]^{N-2} [p_1(u) c_0(u) + (N-1) p_0(u) c_1(u)] . \end{aligned} \quad (7)$$

The signal-absent PDF of $v(t)$ under H_0 follows immediately as

$$p_{v0}(u) = N p_0(u) [c_0(u)]^{N-1} . \quad (8)$$

The corresponding exceedance distribution functions (EDFs) (namely, $e_v(u) = 1 - c_v(u)$ for or-ing output $v(t)$) can be expressed in terms of the following series expansions, which are useful for very small EDF values:

$$e_{v1}(u) = e_1(u) - c_1(u) \sum_{n=1}^{N-1} \binom{N-1}{n} [-e_0(u)]^n, \quad (9)$$

$$e_{v0}(u) = - \sum_{n=1}^N \binom{N}{n} [-e_0(u)]^n. \quad (10)$$

The characteristic function (CF) of or-ing output $v(t)$ is given by the Fourier transform

$$f_v(\xi) = \overline{\exp(i\xi v(t))} = \int du \exp(i\xi u) p_v(u), \quad (11)$$

where either relevant form, p_{v1} or p_{v0} above, is to be used. Finally, for the block processing in figure 1, there is no overlap of the data used in the post-averager, meaning that the processor output $w(t)$ is the sum of M independent identically distributed RVs. Therefore, the CF of the decision variable $w(t)$ in the figure is simply

$$f_w(\xi) = [f_v(\xi)]^M. \quad (12)$$

One final Fourier transform is required to manipulate CF $f_w(\xi)$ into the desired EDF $e_w(u)$ of processor output $w(t)$; see references 3 and 4. This EDF will be the false alarm probability P_f or the detection probability P_d of the or-ing processor, depending on whether PDF p_{v0} or p_{v1} is used, respectively.

The fundamental Fourier transform in equation (11) will generally have to be accomplished numerically by means of a fast Fourier transform (FFT). If pre-averager output statistics p_0 and c_0 can be found in closed form or a readily computed form, a cascaded FFT approach will lead to exact false alarm probability results for the or-ing processor in figure 1. If pre-averager output probability functions p_1 and c_1 can also be readily evaluated, accurate detection probability results can be similarly calculated as well. Some important numerical considerations for this cascaded FFT approach are presented in appendix B of reference 1.

For the special case of $M = 1$ (no post-averaging), processor output RV $w(t) = v(t)$ in figure 1, and the corresponding EDFs follow, for any K and N , as

$$e_{w1}(u) = 1 - c_1(u) [c_0(u)]^{N-1}, \quad (13)$$

$$e_{w0}(u) = 1 - [c_0(u)]^N. \quad (14)$$

Now, return to arbitrary values of K , N , and M , and specialize the general results above to the deterministic signal model of interest here, namely, equations (2) and (3).

DETERMINISTIC SIGNAL

Define $\underline{d} = \sqrt{K} d$ and auxiliary Gaussian functions

$$\phi(x) = (2\pi)^{-\frac{1}{2}} \exp(-x^2/2) , \quad \Phi(x) = \int_{-\infty}^x du \phi(u) . \quad (15)$$

Then, for constant signal amplitudes, the requisite probability functions for pre-averager outputs $\{y_n(t)\}$ for any K and u are

$$p_0(u) = \frac{1}{(2\pi K)^{\frac{1}{2}}} \exp\left(-\frac{u^2}{2K}\right) = \frac{1}{\sqrt{K}} \phi\left(\frac{u}{\sqrt{K}}\right) , \quad (16)$$

$$p_1(u) = \frac{1}{(2\pi K)^{\frac{1}{2}}} \exp\left(-\frac{(u - Kd)^2}{2K}\right) = \frac{1}{\sqrt{K}} \phi\left(\frac{u}{\sqrt{K}} - \underline{d}\right) , \quad (17)$$

$$c_0(u) = \Phi\left(\frac{u}{\sqrt{K}}\right) , \quad c_1(u) = \Phi\left(\frac{u}{\sqrt{K}} - \underline{d}\right) . \quad (18)$$

Using equations (8) and (7), the PDFs for or-ing output $v(t)$ for any K and N , under H_0 and H_1 , are, respectively,

$$p_{v0}(u) = \frac{N}{\sqrt{K}} \phi\left(\frac{u}{\sqrt{K}}\right) \Phi\left(\frac{u}{\sqrt{K}}\right)^{N-1} , \quad (19)$$

$$p_{v1}(u) = \frac{1}{\sqrt{K}} \phi\left(\frac{u}{\sqrt{K}}\right)^{N-2} \left[\phi\left(\frac{u}{\sqrt{K}} - \underline{d}\right) \Phi\left(\frac{u}{\sqrt{K}}\right) + (N-1) \phi\left(\frac{u}{\sqrt{K}}\right) \Phi\left(\frac{u}{\sqrt{K}} - \underline{d}\right) \right] . \quad (20)$$

The corresponding CFs are given in integral form as

$$f_{v0}(\xi) = N \int dx \exp(i\xi K^{\frac{1}{2}}x) \phi(x) \Phi(x)^{N-1} , \quad (21)$$

$$f_{v1}(\xi) = \int dx \exp(i\xi K^{\frac{1}{2}}x) \phi(x)^{N-2} [\phi(x-\underline{d}) \Phi(x) + (N-1) \phi(x) \Phi(x-\underline{d})] . \quad (22)$$

Equation (12) can now be utilized to obtain the CFs of output decision variable $w(t)$ in figure 1 under both hypotheses, H_0 and H_1 .

A SHORTCUT IN TABULATED RESULTS

For a specified P_f and P_d , let $d(K,N,M)$ be the input deflection required to achieve that operating point. In particular, let

$$d_1(N,M) = d(1,N,M) \quad (23)$$

be the input deflection required for $K = 1$. Also, observe from the forms of equations (16) through (18) that the effect of adding K independent Gaussian RVs is simply to scale the input deflection measure by \sqrt{K} , which means that the required input deflection satisfies the relation

$$d(K,N,M) = \frac{d(1,N,M)}{\sqrt{K}} = \frac{d_1(N,M)}{\sqrt{K}} \quad (24)$$

Therefore, it is only necessary to evaluate ROCs and tabulate numerical results for the case of $K = 1$; N and M can be general integers. This observation significantly reduces the amount of computations and graphs that need to be investigated and catalogued. In the following, the ROCs will be computed solely for $K = 1$ and labeled with the corresponding values of input deflection $d_1(N,M)$. However, these labels could be replaced by $\sqrt{K} d(K,N,M)$ for any K , and the same ROCS would still apply for any selected value of integer K .

SPECIAL CASES

When $M = 1$ (no post-averaging), the EDFs in equations (13) and (14) can be combined with the results in equation (18) to immediately yield closed-form expressions for P_f and P_d for any K , N , and input deflection d , namely,

$$P_f = 1 - [\Phi(u/\sqrt{K})]^N, \quad P_d = 1 - \Phi(u/\sqrt{K} - \underline{d}) [\Phi(u/\sqrt{K})]^{N-1}. \quad (25)$$

Here, $\underline{d} = d/\sqrt{K}$. Furthermore, these equations can be solved explicitly for the required threshold u and the required input deflection d to realize a specified P_f and P_d :

$$u = \sqrt{K} \tilde{\Phi}(\alpha), \quad d(K, N, 1) = \frac{\tilde{\Phi}(\alpha) - \tilde{\Phi}(\alpha\beta)}{\sqrt{K}} = \frac{d_1(N, 1)}{\sqrt{K}}, \quad (26)$$

where $\tilde{\Phi}$ is the inverse Φ function, and the auxiliary parameters α and β are defined as

$$\alpha = \alpha(N) \equiv (1 - P_f)^{1/N}, \quad \beta \equiv \frac{1 - P_d}{1 - P_f}. \quad (27)$$

For $N = 1$, no or-ing, and arbitrary K and M , under H_1 , the results above simplify to system output PDF

$$p_{w1}(u) = \frac{1}{(2\pi T)^{1/2}} \exp\left(-\frac{(u - Td)^2}{2T}\right), \quad T = KM, \quad (28)$$

and output EDF

$$P_d(v) = \int_v^\infty du p_{w1}(u) = \Phi\left(qd - \frac{v}{q}\right), \quad q = T^{1/2} = (KM)^{1/2}. \quad (29)$$

Obviously, for $N = 1$, only the product KM matters, at least for unity weights in both the pre- and post-averagers.

For the special case of $N = 2$, the integrals in equations (21) and (22) can be evaluated in terms of the error function of complex argument $w(\)$; see reference 5, chapter 7. The CFs follow as

$$f_{v0}(\xi) = \exp(-\gamma^2) w(\gamma) \quad (30)$$

and

$$f_{v1}(\xi) = \frac{1}{2} \exp(-\gamma^2 - \nu^2 + i2\gamma\nu) [w(\gamma + i\nu) + w(\gamma - i\nu)] , \quad (31)$$

where $\gamma = K^{\frac{1}{2}}\xi/2$ and $\nu = K^{\frac{1}{2}}d/2$. The amount of pre-averaging K is arbitrary. The CFs of decision variable $w(t)$ are given by the M -th powers of the above two results under H_0 and H_1 , respectively, when $N = 2$.

NUMERICAL APPROACH

When the CF $f_v(\xi)$ of or-ing output $v(t)$ can be derived in closed form, such as in the special cases (30) and (31), $f_v(\xi)$ can be used directly in equation (12) to find the closed-form CF of decision variable $w(t)$. This route is preferred because CF $f_v(\xi)$ can decay rather slowly with ξ for some values of K and N , making the use of equation (11) difficult.

Therefore, closed-form results for CF $f_v(\xi)$, when available, can be very useful in terms of avoiding some numerical problems in the discrete Fourier transform of $p_v(u)$ according to equation (11). When this is not possible, the closed-form results for the or-ing output PDFs given in equations (19) and (20) are used, instead, in the cascaded FFT procedure outlined in equations (11) and (12).

QUANTITATIVE PERFORMANCE RESULTS

REQUIRED INPUT DEFLECTIONS

This section gives specific quantitative detectability results with various amounts of or-ing N and post-averaging M , while the amount of pre-averaging is kept at $K = 1$. In particular, 54 ROCs are presented in appendix A for the cases of

$$\begin{aligned} N &= 1, 2, 4, 8, 16, 32, \\ M &= 1, 2, 4, 8, 16, 32, 64, 128, 256. \end{aligned}$$

A standard operating point (SOP) is defined here as $P_f = 1E-3$ and $P_d = 0.5$, while a high-quality operating point (HOP) is defined as $P_f = 1E-6$ and $P_d = 0.9$. The required input deflection values $d_1(N, M)$ for the SOP and HOP have been extracted from the ROCs in appendix A and are presented in tables 1 and 2, respectively. These results for $K = 1$ can be used to find the required input deflection for general integer K according to

$$d(K, N, M) = \frac{d_1(N, M)}{\sqrt{K}}. \quad (32)$$

In conjunction with equation (32), the input deflections in tables 1 and 2 form the basis for the plots in figures 2 through 9 for both the SOP and HOP cases of $KM = 4, 16, 64$, and 256. Figures 10 and 11 are identical to figures 8 and 9, except that the ordinates are now in decibels according to

Table 1. Required Input Deflection $d_1(N,M)$ for
 $P_f = 1E-3$, $P_d = 0.5$, $K = 1$, Deterministic Signal

M	N	1	2	4	8	16	32
1		3.09	3.29	3.48	3.66	3.83	4.00
2		2.19	2.44	2.67	2.90	3.10	3.30
4		1.55	1.82	2.08	2.33	2.56	2.77
8		1.09	1.37	1.63	1.89	2.13	2.35
16		0.773	1.02	1.28	1.53	1.78	2.01
32		0.546	0.756	0.994	1.24	1.49	1.72
64		0.386	0.557	0.766	0.998	1.24	1.47
128		0.273	0.407	0.584	0.794	1.02	1.25
256		0.193	0.296	0.440	0.623	0.833	1.05

Table 2. Required Input Deflection $d_1(N,M)$ for
 $P_f = 1E-6$, $P_d = 0.9$, $K = 1$, Deterministic Signal

M	N	1	2	4	8	16	32
1		6.03	6.17	6.31	6.44	6.57	6.69
2		4.27	4.46	4.64	4.82	4.98	5.15
4		3.02	3.27	3.50	3.71	3.91	4.11
8		2.13	2.42	2.68	2.93	3.15	3.37
16		1.51	1.80	2.08	2.34	2.58	2.81
32		1.07	1.35	1.62	1.89	2.14	2.37
64		0.754	1.00	1.26	1.53	1.78	2.02
128		0.533	0.742	0.980	1.23	1.48	1.72
256		0.377	0.546	0.753	0.986	1.23	1.46

dB = 20 log(d), since d is an amplitude SNR measure. Additional figures could also be plotted for the intermediate cases of $KM = 2, 8, 32$, and 128, if desired, by use of tables 1 and 2.

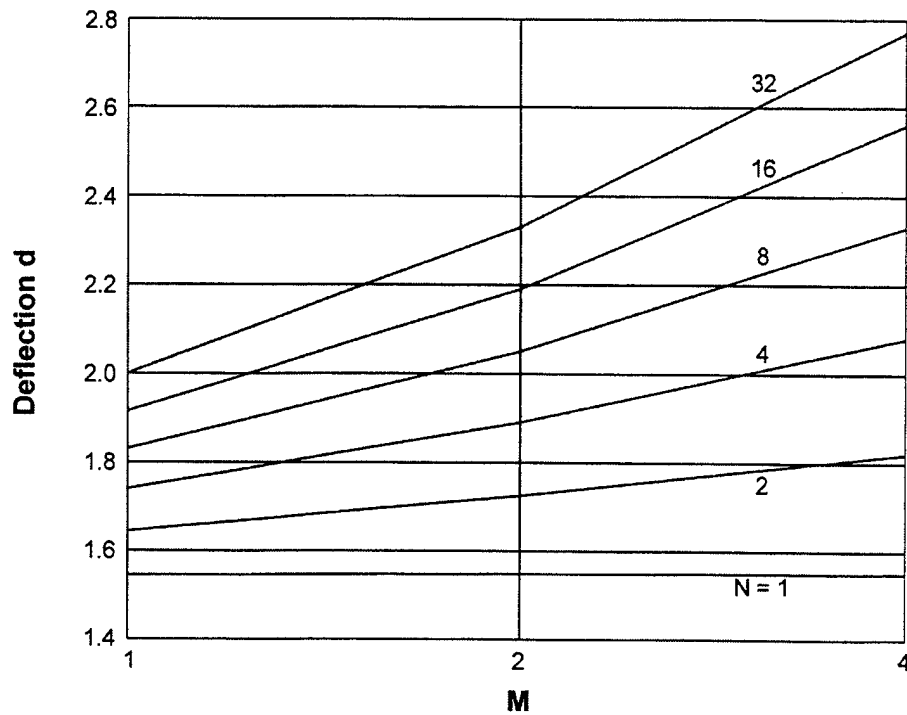


Figure 2. Required Input Deflection $d(K,N,M)$ for $P_f = 1E-3$, $P_d = 0.5$, $KM = 4$, Deterministic Signal

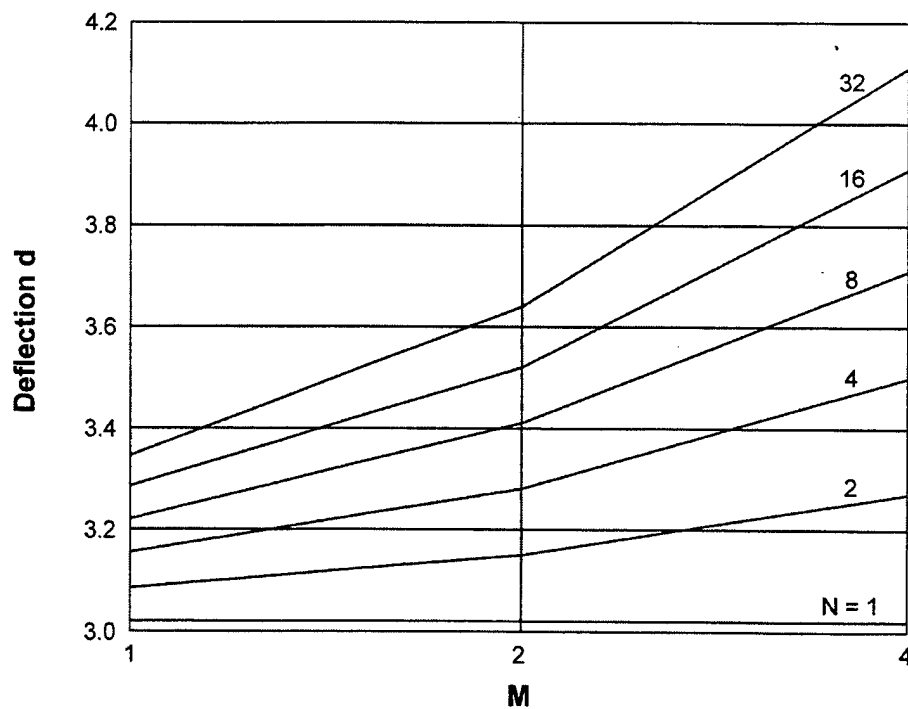


Figure 3. Required Input Deflection $d(K,N,M)$ for $P_f = 1E-6$, $P_d = 0.9$, $KM = 4$, Deterministic Signal

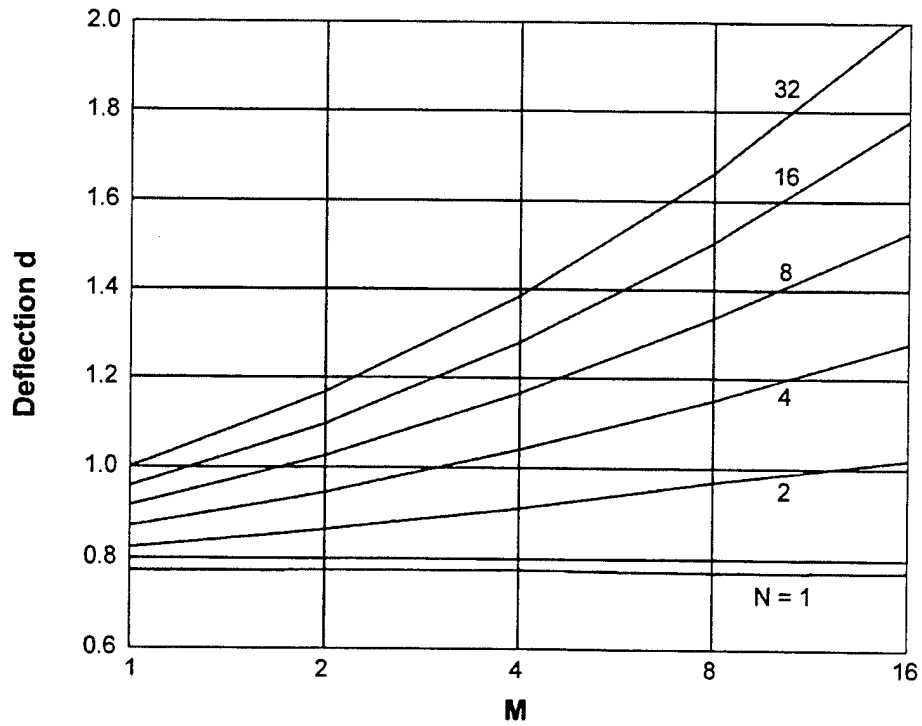


Figure 4. Required Input Deflection $d(K, N, M)$ for $P_i = 1E-3$, $P_d = 0.5$, $KM = 16$, Deterministic Signal

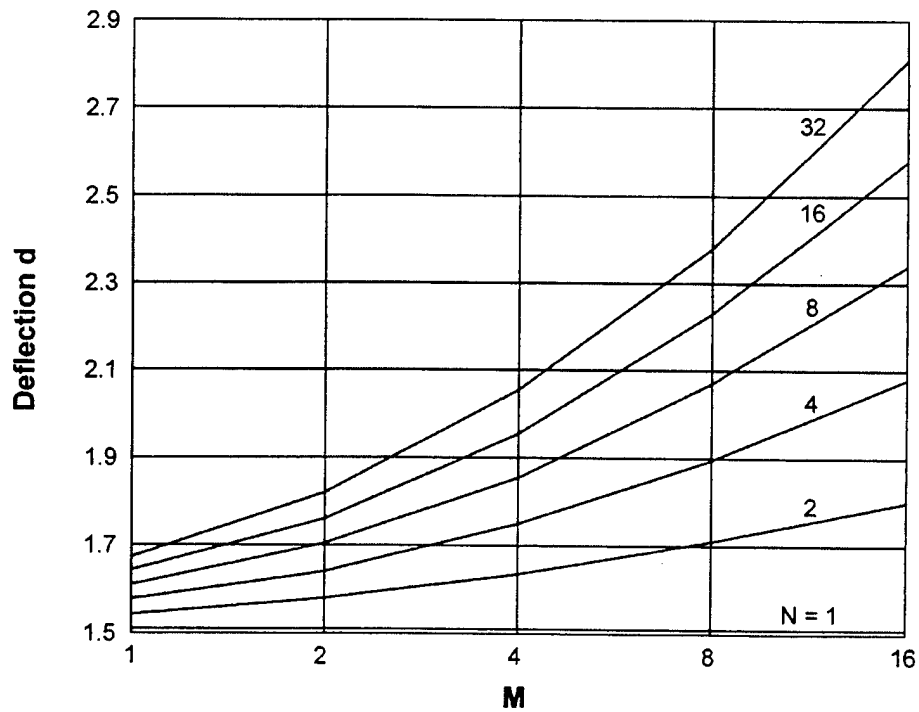


Figure 5. Required Input Deflection $d(K, N, M)$ for $P_i = 1E-6$, $P_d = 0.9$, $KM = 16$, Deterministic Signal

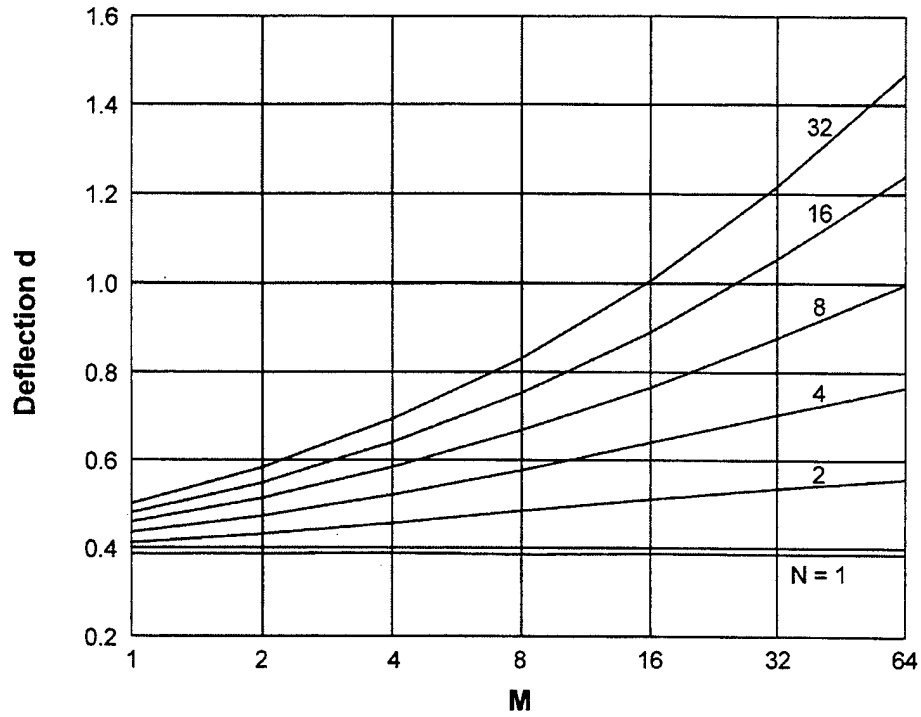


Figure 6. Required Input Deflection $d(K, N, M)$
for $P_f = 1E-3$, $P_d = 0.5$, $KM = 64$, Deterministic Signal

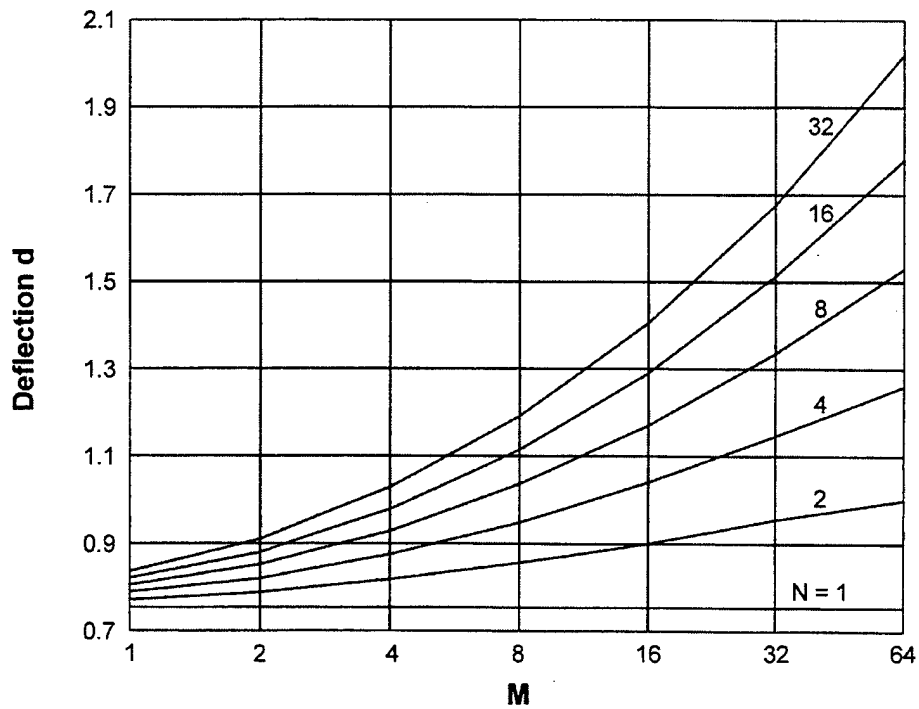


Figure 7. Required Input Deflection $d(K, N, M)$
for $P_f = 1E-6$, $P_d = 0.9$, $KM = 64$, Deterministic Signal

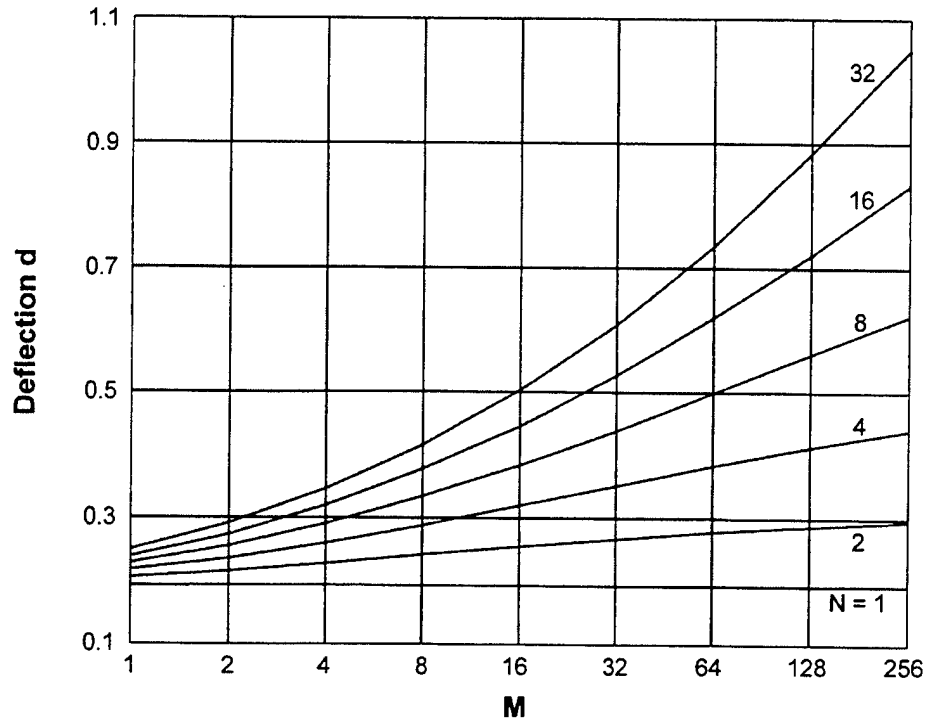


Figure 8. Required Input Deflection $d(K,N,M)$ for $P_i = 1E-3$, $P_d = 0.5$, $KM = 256$, Deterministic Signal

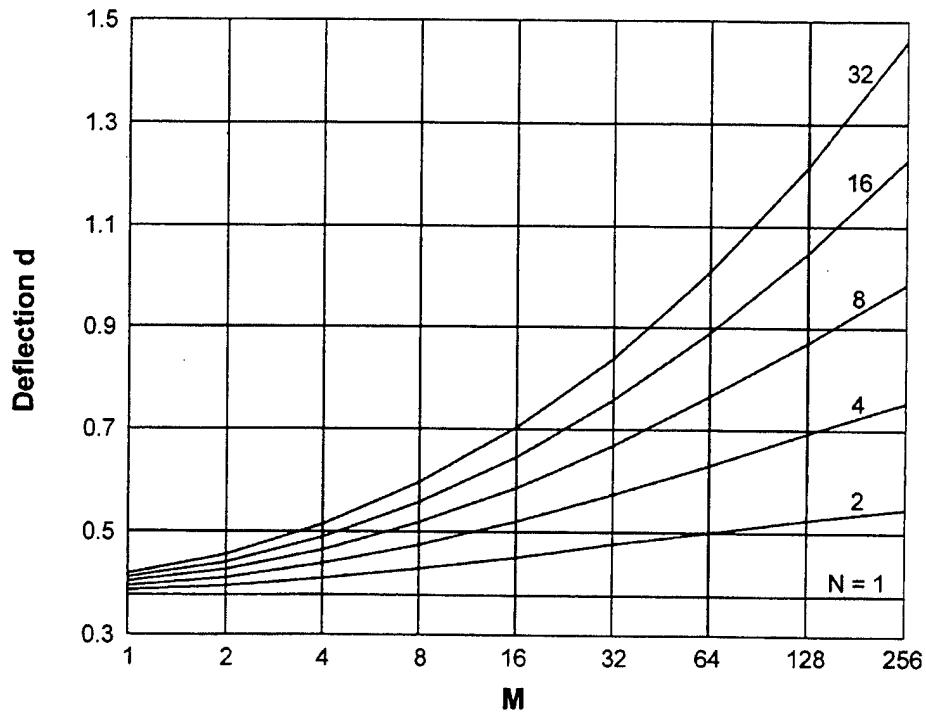


Figure 9. Required Input Deflection $d(K,N,M)$ for $P_i = 1E-6$, $P_d = 0.9$, $KM = 256$, Deterministic Signal

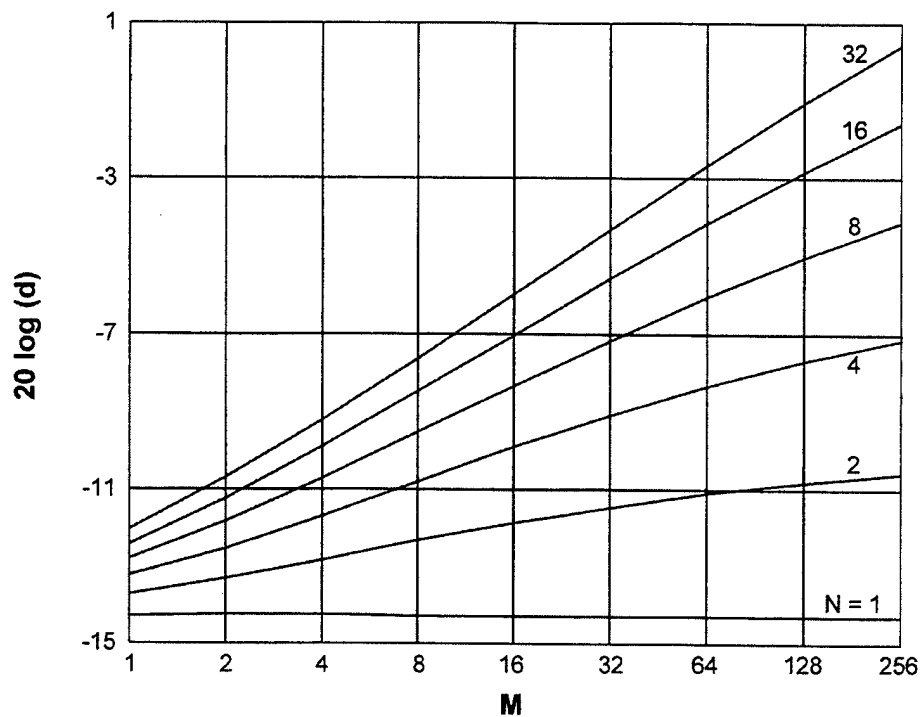


Figure 10. Required Input Deflection $d(K,N,M)$ in Decibels for $P_f = 1E-3$, $P_d = 0.5$, $KM = 256$, Deterministic Signal

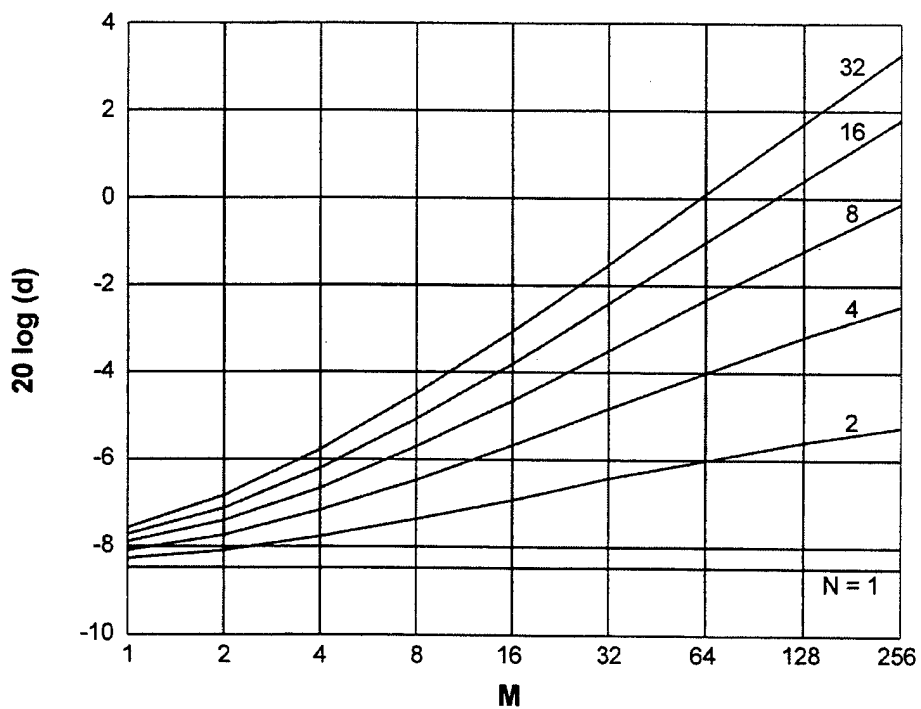


Figure 11. Required Input Deflection $d(K,N,M)$ in Decibels for $P_f = 1E-6$, $P_d = 0.9$, $KM = 256$, Deterministic Signal

The accurate deflection values in tables 1 and 2 were interpolated from the ROCs in appendix A while the false alarm and detection probability numbers, P_f and P_d , were still resident in the computer; eyeball interpolation from the plotted ROCs cannot be accomplished this accurately.

It can be seen from figures 2 through 9, as expected, that the required input deflection d increases monotonically with the number (N) of channels or-ed if K and M are held fixed. Also, the required input deflection increases monotonically with the amount (M) of post-averaging employed if N and product KM are held fixed; alternatively, the required input deflection decreases with the amount (K) of pre-averaging employed if N and product KM are held fixed. The exact rates can be determined from figures 2 through 9 and the ROCs in appendix A.

TRADEOFF BETWEEN PRE- AND POST-AVERAGING

For a fixed amount of total time-bandwidth product, that is, $T = KM = \text{constant}$, it is possible to shift some of the pre-averaging to post-averaging, or vice versa. For example, if $KM = 16$, this shift could be accomplished by taking $K = 16$ and $M = 1$, which corresponds to no post-averaging, and then switching to $K = 1$ and $M = 16$, which corresponds to no pre-averaging. Alternatively, intermediate values such as $K = 4$ and $M = 4$ could be used, still keeping $KM = 16$.

In all cases, increasing M at the sake of K requires larger input deflections to maintain the same operating point; see figures 2 through 9. This is because the optimum processor conducts all pre-averaging before any nonlinear operations; see appendix A of reference 1. For example, to maintain the SOP when $KM = 16$, table 1 and equation (32) indicate that the input deflection must be scaled by factors of 1.24, 1.47, 1.67, 1.86, and 2.01 for $N = 2, 4, 8, 16$, and 32, respectively, if the switch is made from all pre-averaging to all post-averaging. Alternatively, to maintain the HOP, the corresponding scaling ratios from table 2 and equation (32) are smaller (1.17, 1.32, 1.45, 1.57, and 1.68 for $N = 2, 4, 8, 16$, and 32, respectively).

For a HOP such as $P_f = 1E-6$ and $P_d = 0.9$, larger input deflections are naturally required to achieve the higher level of performance. At these larger input deflections, the or-ing process is more frequently dominated by the signal-bearing channel. Therefore, as the number (N) of channels or-ed increases, the required increases in input deflection are less severe than for a lower quality operating point, such as SOP $P_f = 1E-3$ and $P_d = 0.5$. For example, for $K = 16$ and $M = 1$, increasing N from 2 to 32 requires a gain factor of 1.22 in the deflection to maintain the SOP, whereas only a gain factor of 1.08 is needed at the HOP.

A related observation is that, for a given configuration (fixed K and M), the relative increase in input deflection required to maintain the SOP is more severe for the larger M values as the amount of or-ing increases. Thus, for $KM = 16$, as N increases from 2 to 32, a deflection factor increase of 1.22 suffices to maintain the SOP for $M = 1$, whereas a factor of 1.97 is required for $M = 16$. The corresponding relative increases at the HOP are 1.08 for $M = 1$ versus 1.56 for $M = 16$, as N increases from 2 to 32. The behaviors are similar for the other values of KM , although the required input deflection values are smaller as KM increases because of the additional observation times allowed.

Inspection of figures 10 and 11 reveals that the decibel or-ing losses in the input deflection ($20 \log(d)$) are much larger than for the random signal treated in part I (reference 1) and the phase-incoherent signal in part II (reference 2). The reason is that if KM is held fixed and M increases, then K is decreasing. But, since the pre-averager is now (part III) performing coherent (amplitude) addition rather than incoherent addition (that is, sums of envelopes squared in parts I and II), any decrease in K is felt more strongly. So, the tradeoff from pre-averaging (larger K) to post-averaging (larger M , smaller K) is more detrimental to performance for a deterministic signal than for a random signal or a phase-incoherent signal.

SUMMARY

For a deterministic signal in Gaussian noise, closed-form expressions have been derived for the PDFs at the output of a pre-averager followed by an or-ing operation. These forms have been numerically subjected to a cascaded pair of Fourier transforms to yield accurate results for the EDFs at the output of a post-averager, under both hypotheses H_0 and H_1 , for numerous values of the parameters of the complete processor (figure 1). Such results enable investigation of the or-ing processor for false alarm probabilities P_f in the range of $1E-6$ and smaller; there is no need to resort to lengthy simulations.

Numerous ROCs have been generated that enable users or system designers to quickly assess the losses to be expected from employing or-ing in their processors. Also, quantitative evaluation of the tradeoffs between pre-averaging and post-averaging has been conducted. Finally, because the enclosed tabulations will undoubtedly not cover all cases of practical interest, a MATLAB program for the evaluation of additional ROCs is presented in appendix B.

The analytical approach utilized here can be extended to include quantizers on the inputs in figure 1, and accurate ROCs can still be obtained for decision variable $w(t)$. In fact, there can be arbitrary amounts of quantization (L levels), and the input PDFs can be completely arbitrary. This procedure will be documented in a future report.

APPENDIX A - ROCs FOR DETERMINISTIC SIGNAL

This appendix contains the ROCs for or-ing with pre- and post-averaging and a deterministic input signal. In keeping with the discussion in equations (23) and (24), the size of the pre-averager is set at $K = 1$, without loss of generality. The parameters N and M are varied over the ranges

$$N = 1, 2, 4, 8, 16, 32,$$

$$M = 1, 2, 4, 8, 16, 32, 64, 128, 256,$$

giving a total of 54 ROCs. The results in tables 1 and 2 for the SOP and the HOP were extracted from these ROCs. Results for other operating points can also be obtained from these ROCs, if desired.

In the following figures, the ROCs have been computed solely for $K = 1$ and labeled with the corresponding values of input deflection $d_1(N,M)$. However, these labels could be replaced by $\sqrt{K} d(K,N,M)$ for any K , and the same ROCs would still apply for any selected value of integer K . See the discussion on page 11.

To maximize the clear region of the aliased approximations to the CFs and EDFs obtained by FFTs (according to references 3 and 4), a procedure for using shifted RVs is presented in appendix C. This alternative is very useful when a wide range of different input SNR levels is of interest.

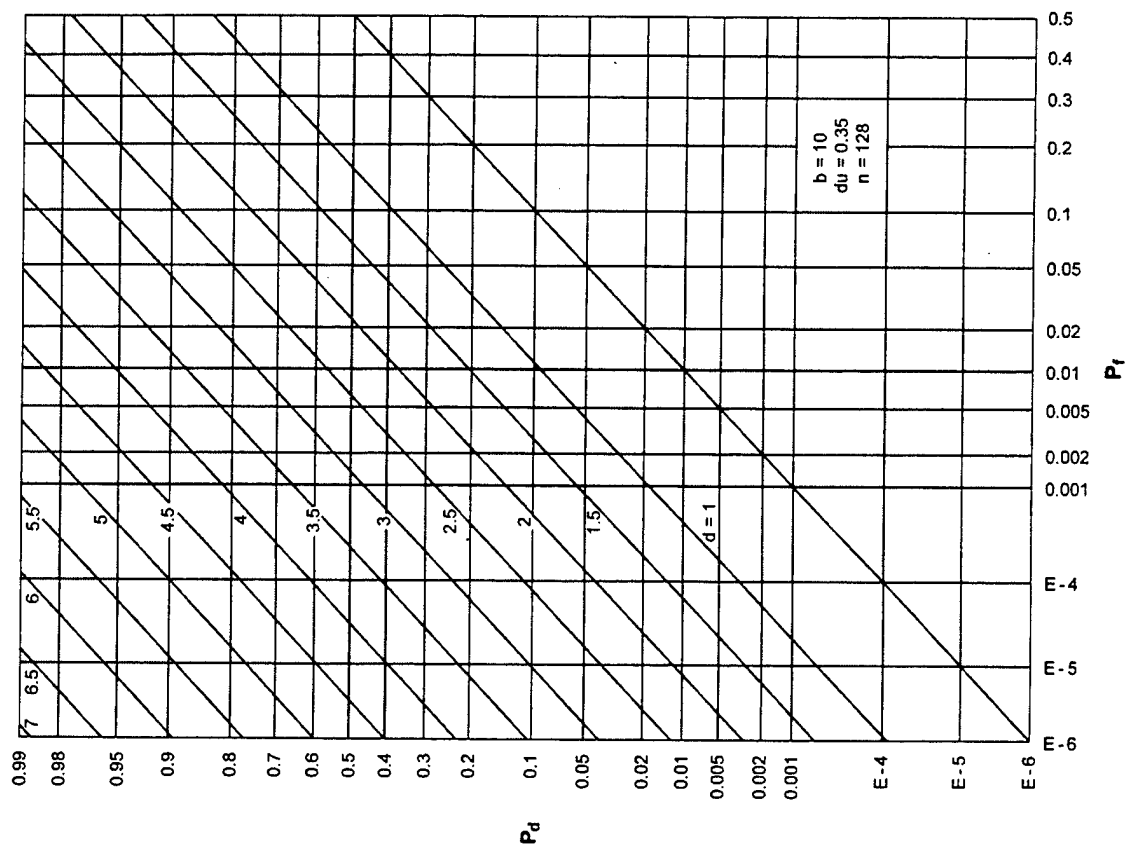


Figure A-1. ROCs for $K = 1$, $N = 1$, $M = 1$

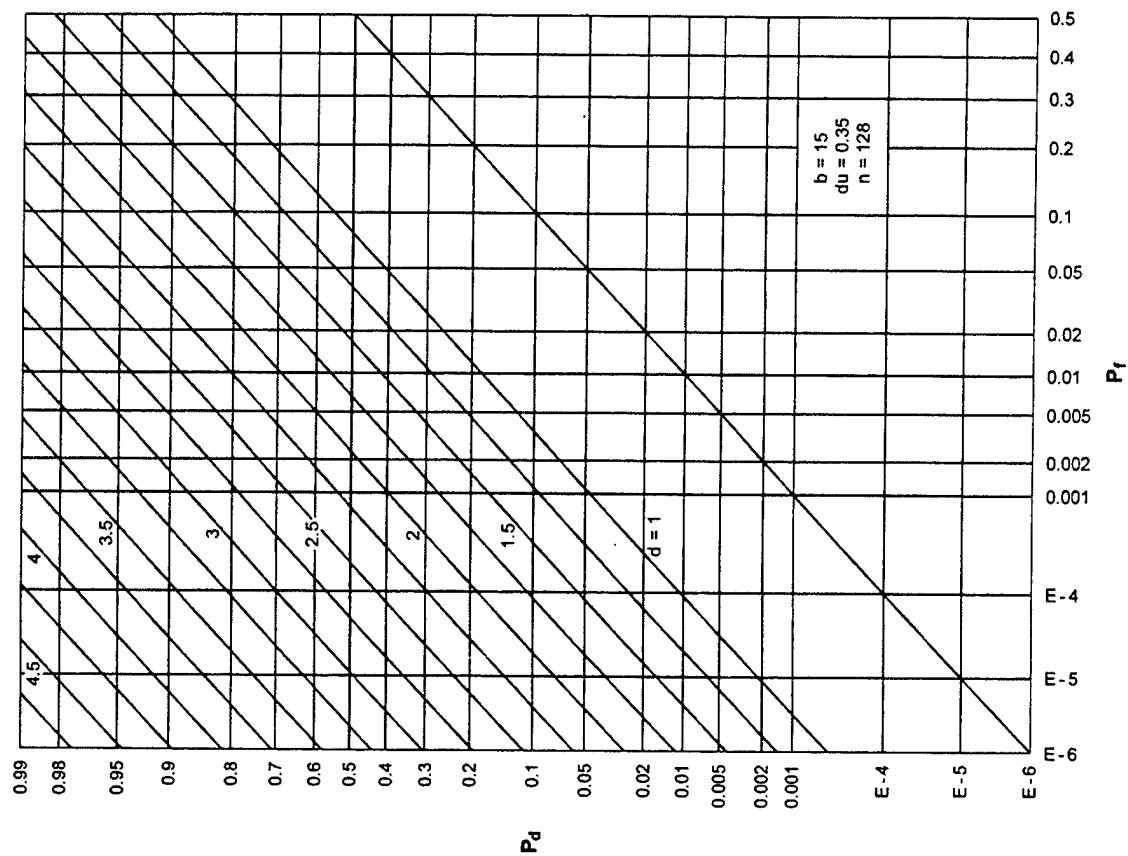


Figure A-2. ROCs for $K = 1$, $N = 1$, $M = 2$

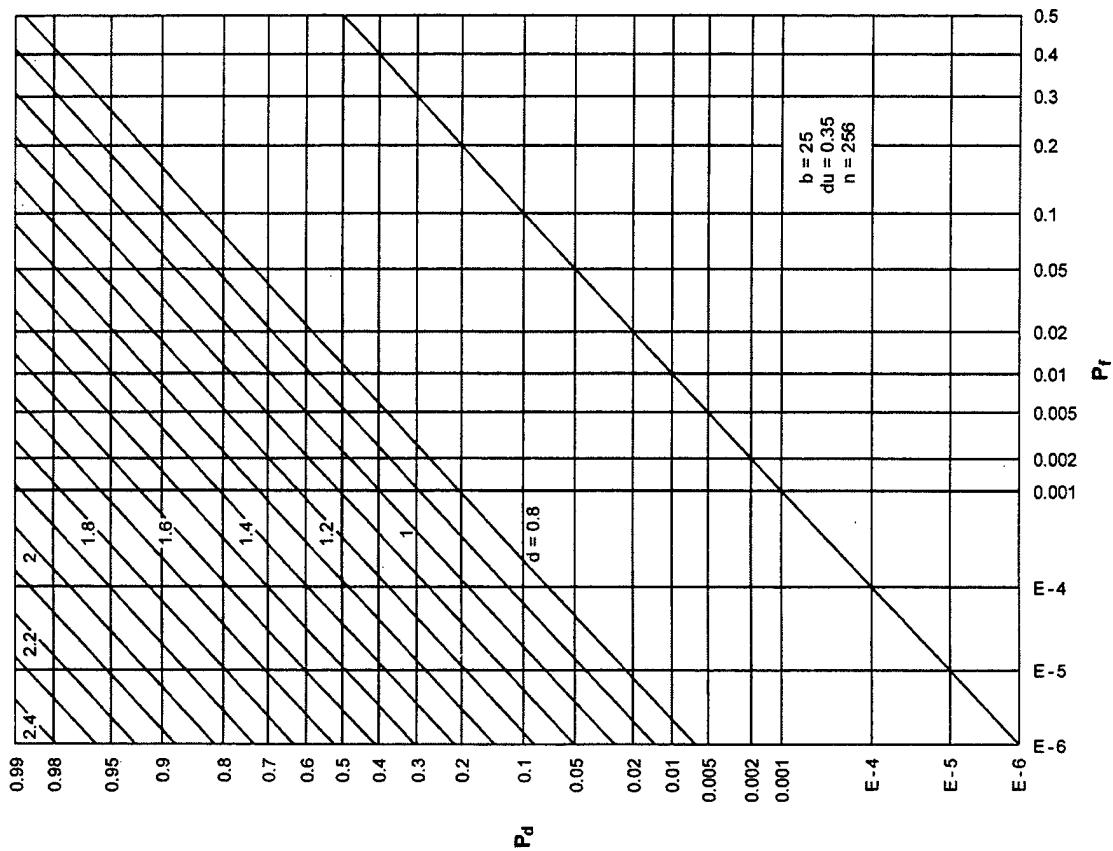


Figure A-4. ROCs for $K = 1, N = 1, M = 8$

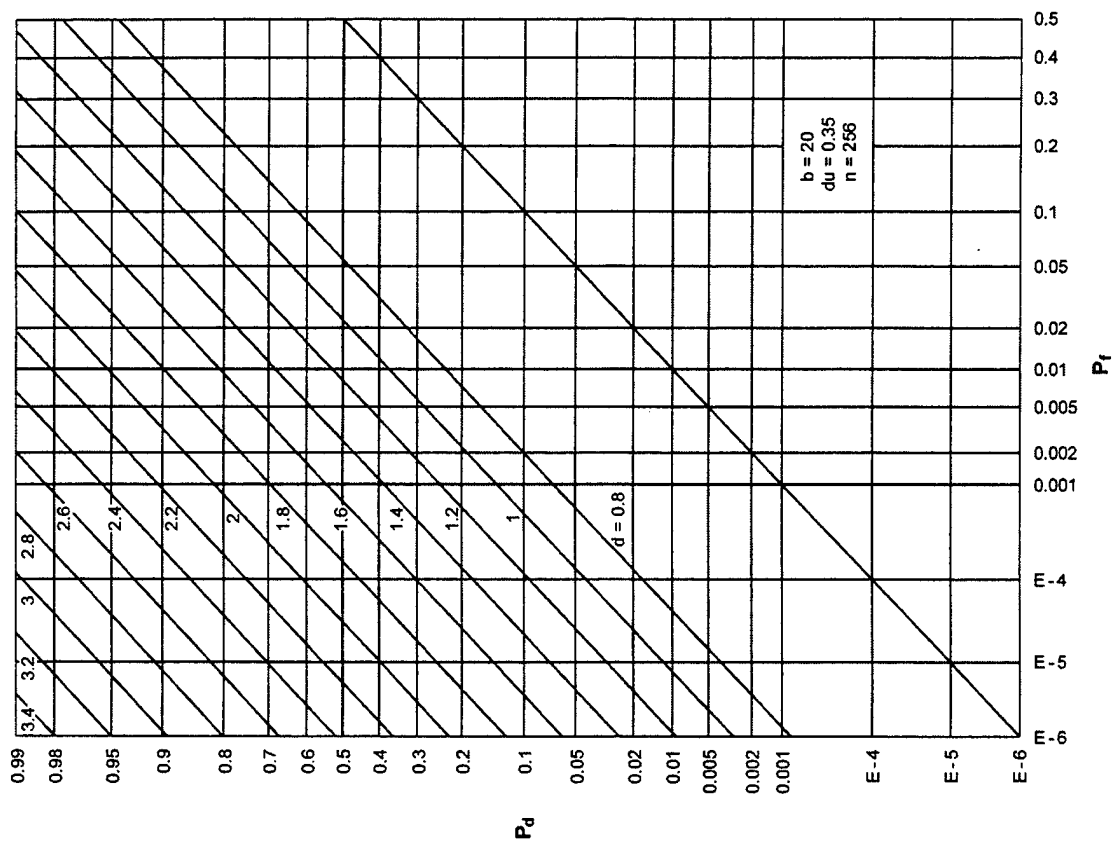


Figure A-3. ROCs for $K = 1, N = 1, M = 4$

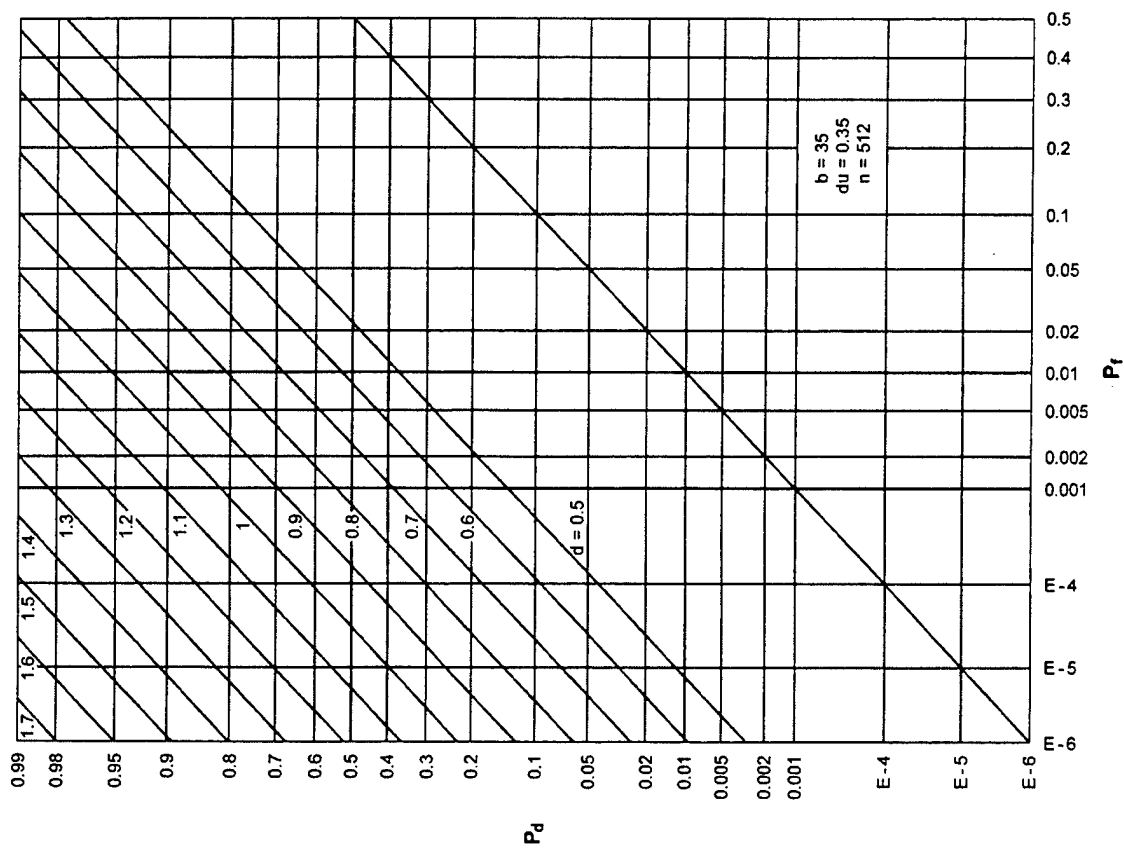


Figure A-5. ROCs for $K = 1, N = 1, M = 16$

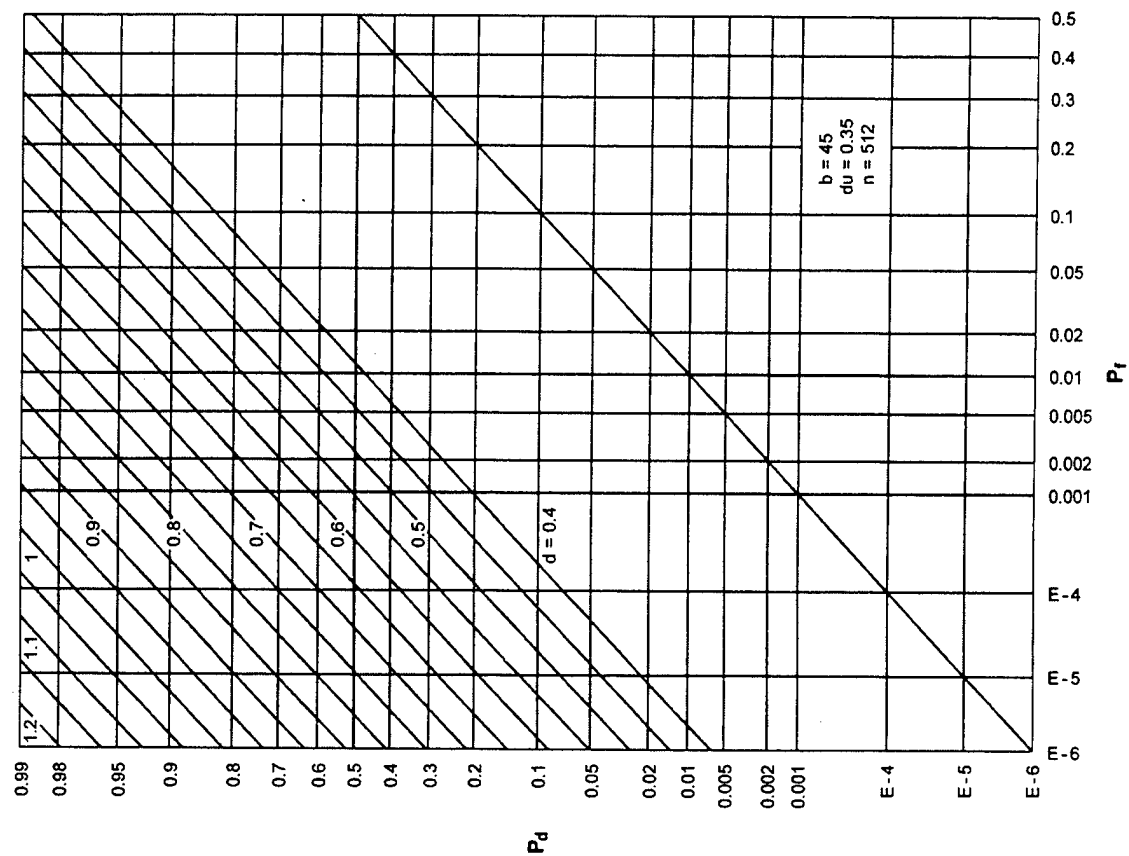


Figure A-6. ROCs for $K = 1, N = 1, M = 32$

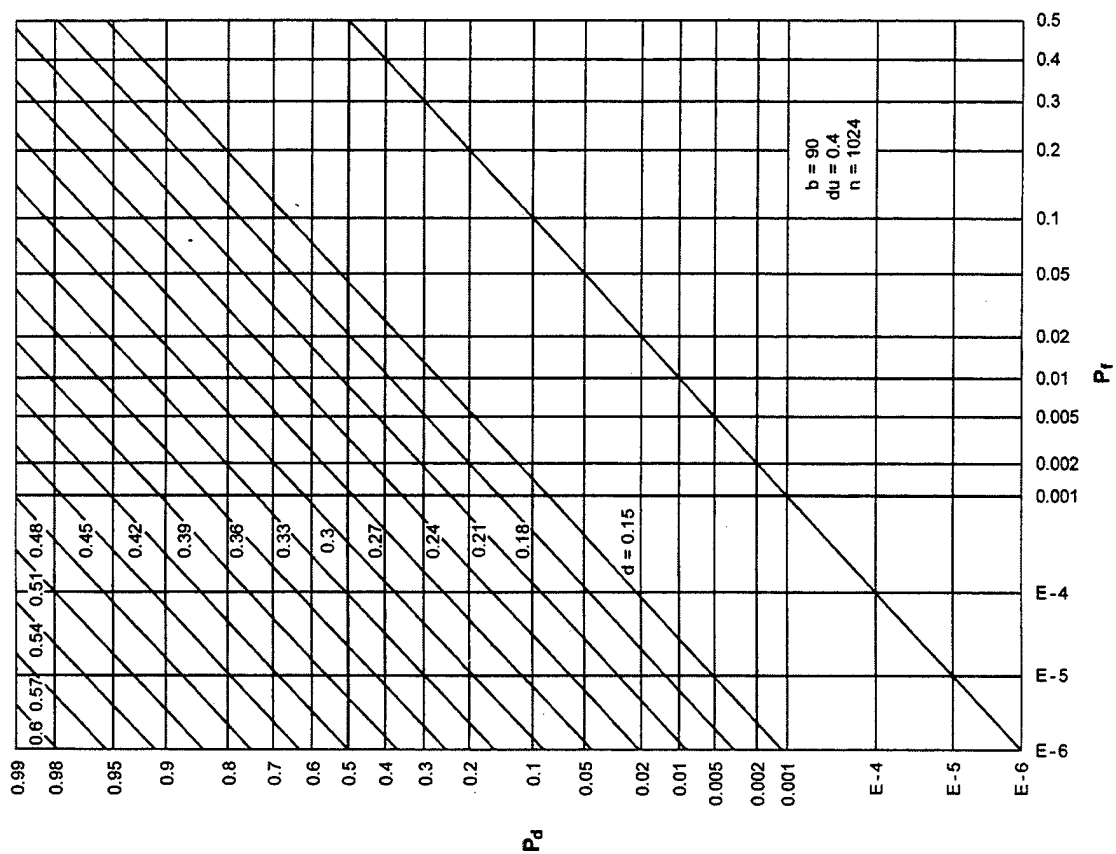


Figure A-8. ROCs for $K = 1$, $N = 1$, $M = 128$

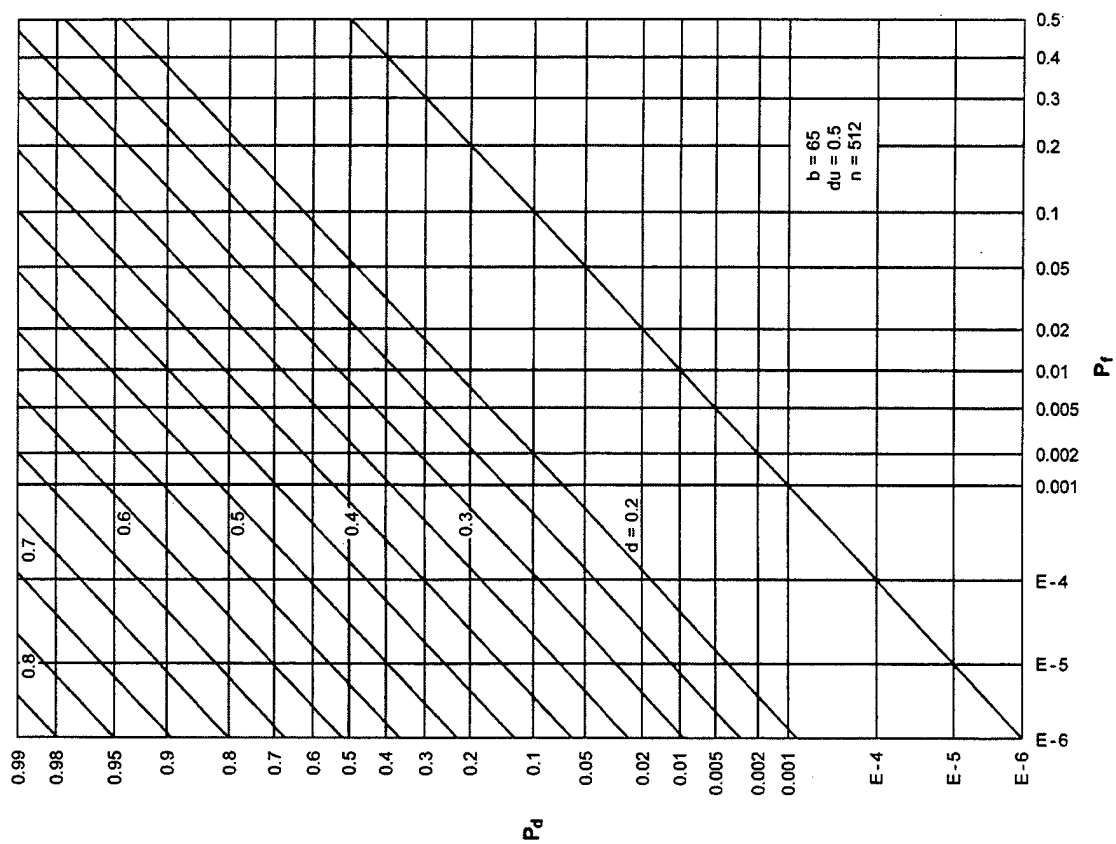


Figure A-7. ROCs for $K = 1$, $N = 1$, $M = 64$

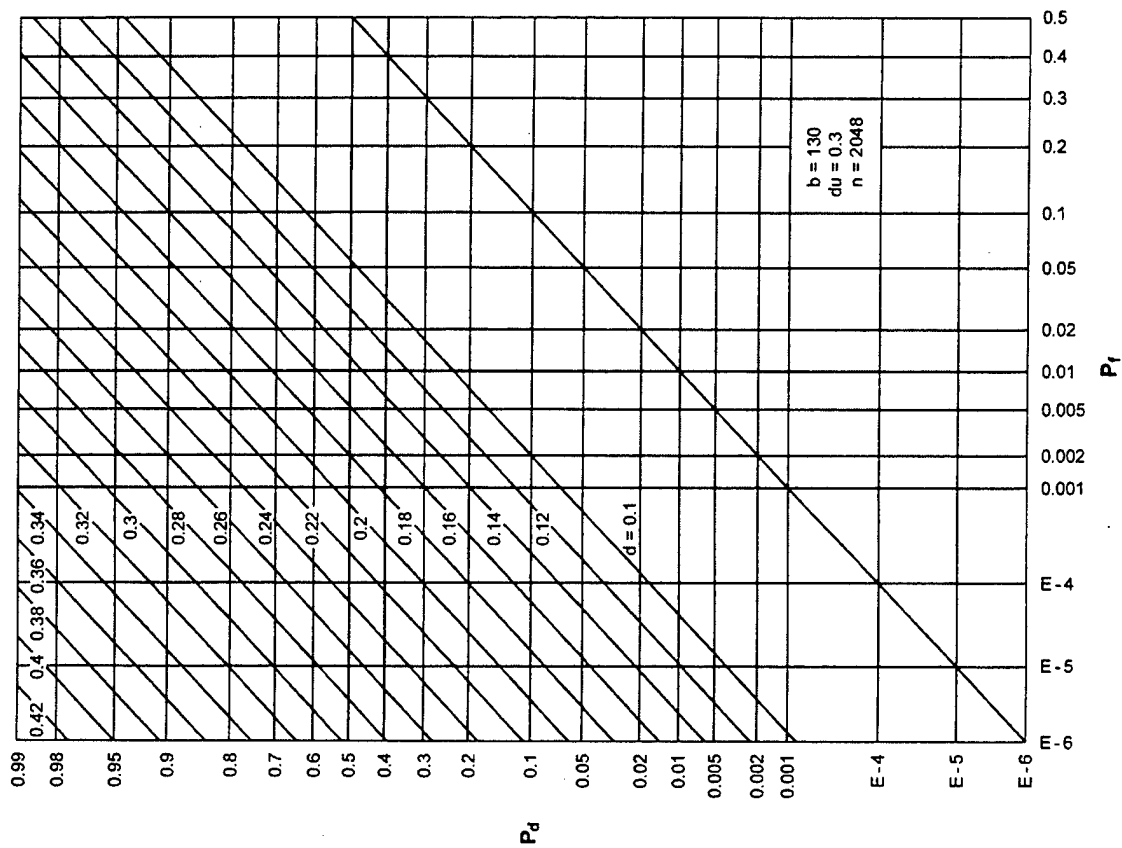


Figure A-9. ROCs for $K = 1$, $N = 1$, $M = 256$

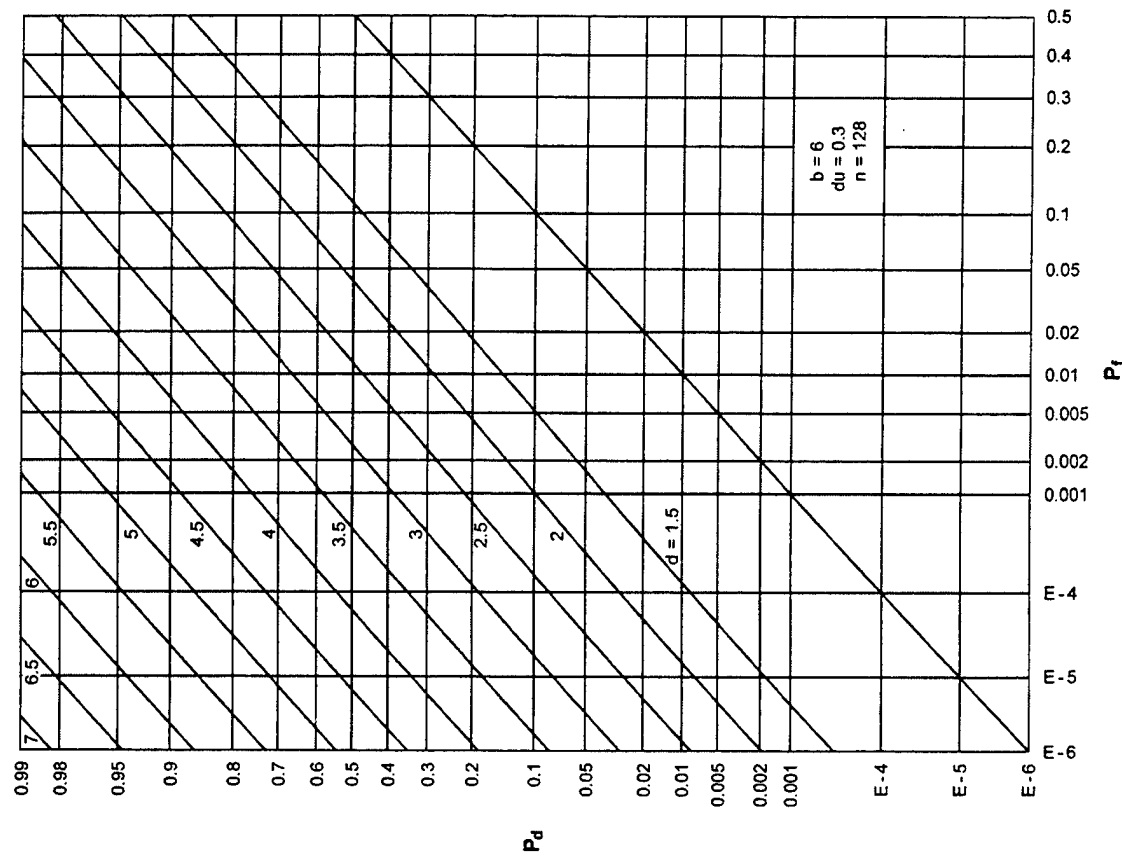


Figure A-10. ROCs for $K = 1$, $N = 2$, $M = 1$

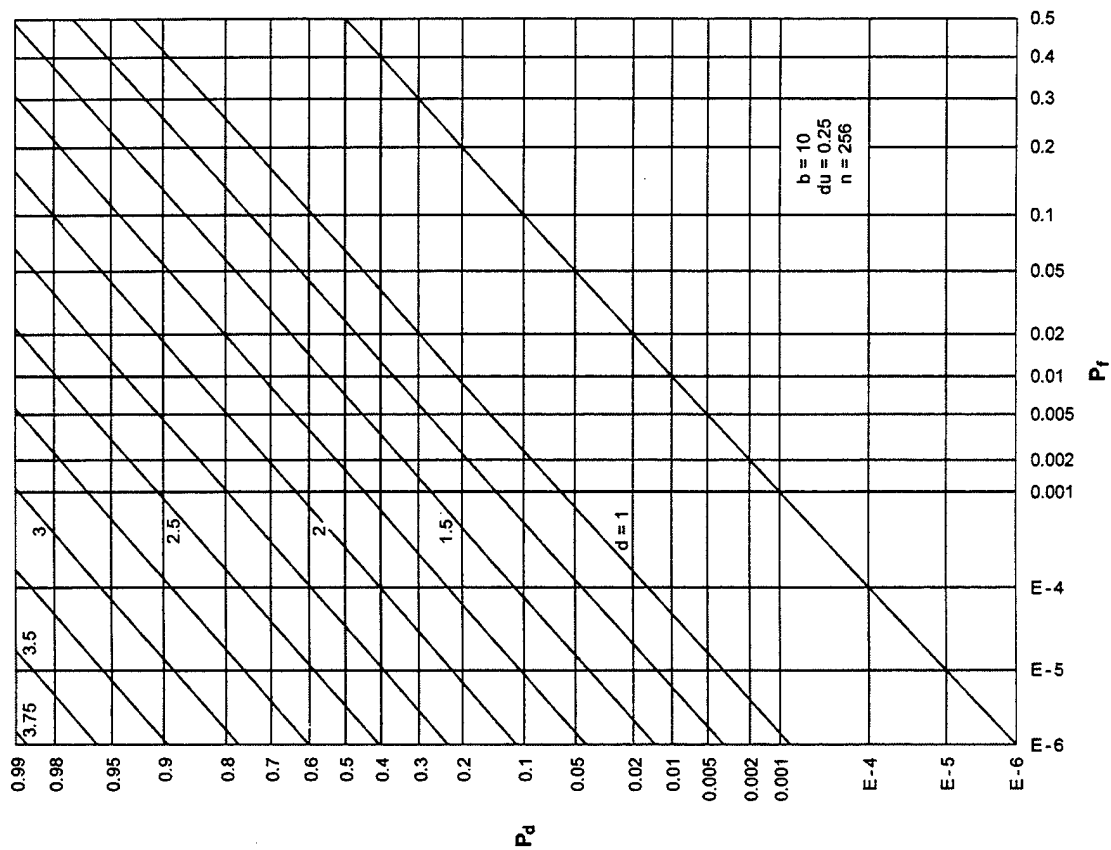


Figure A-12. ROCs for $K = 1$, $N = 2$, $M = 4$

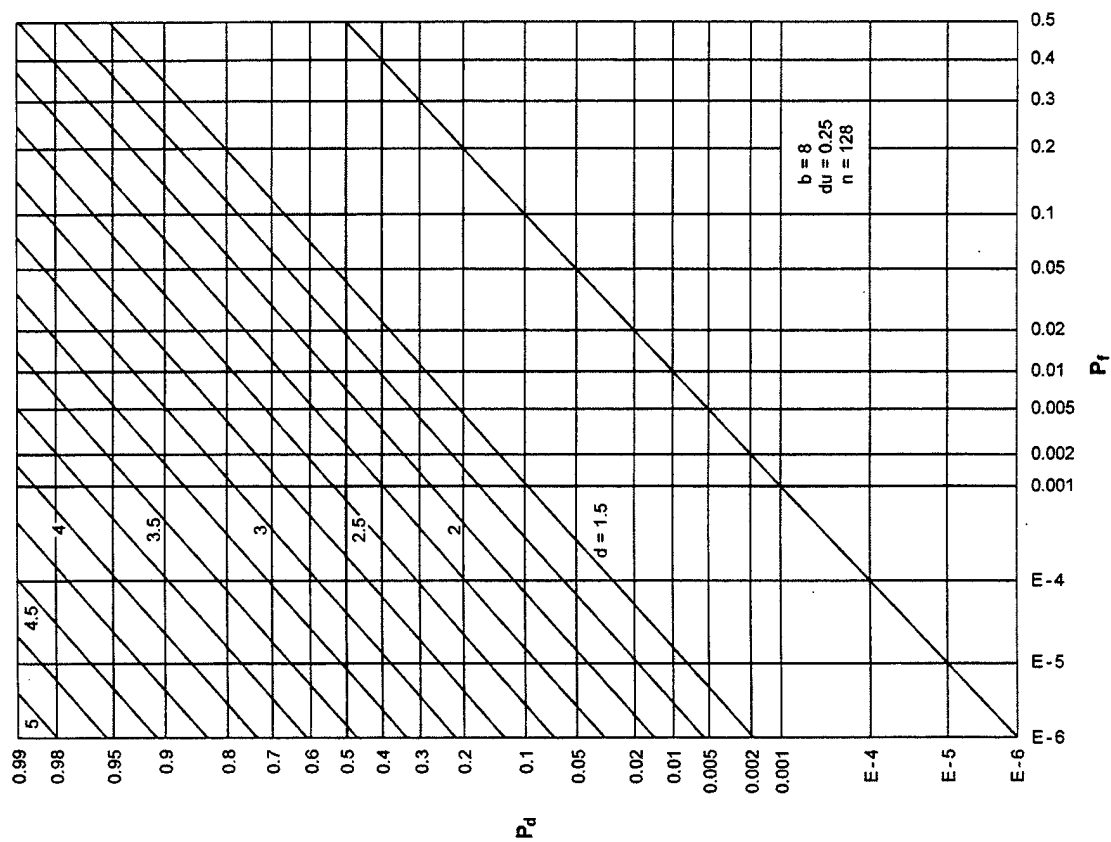


Figure A-11. ROCs for $K = 1$, $N = 2$, $M = 2$

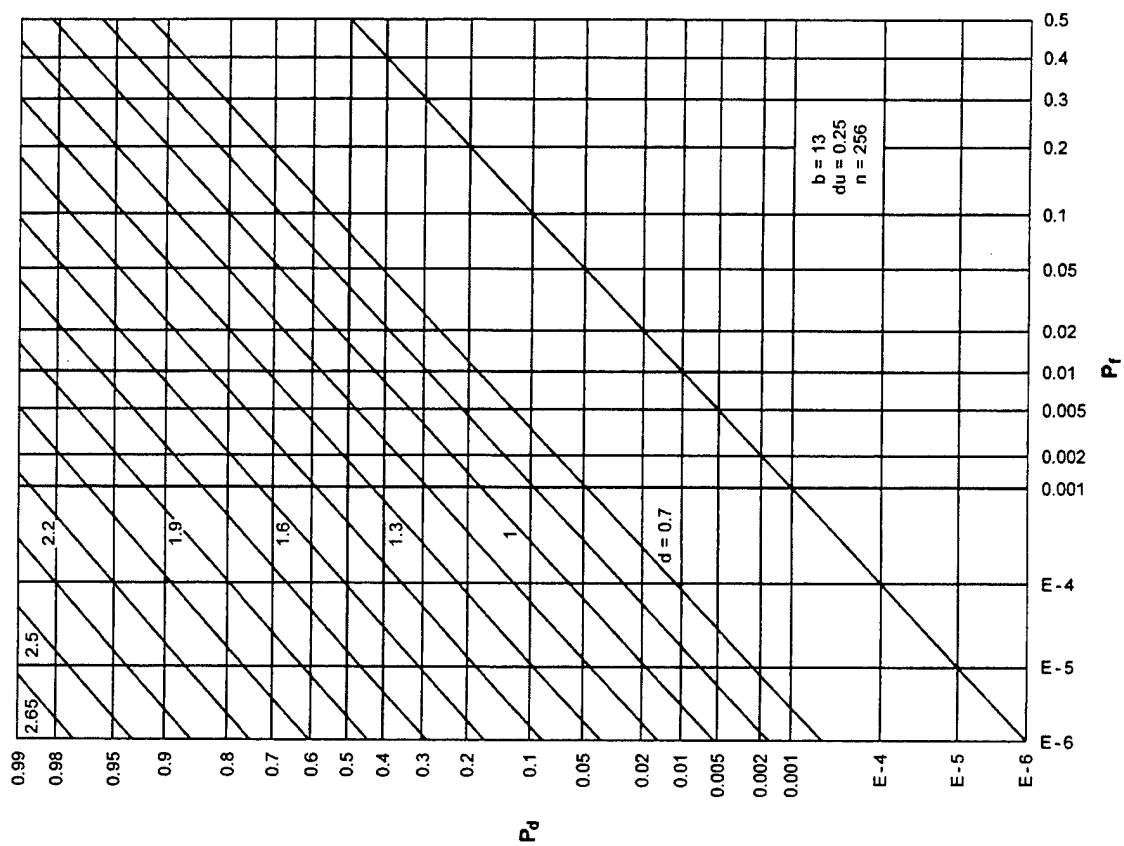


Figure A-13. ROCs for $K = 1$, $N = 2$, $M = 8$

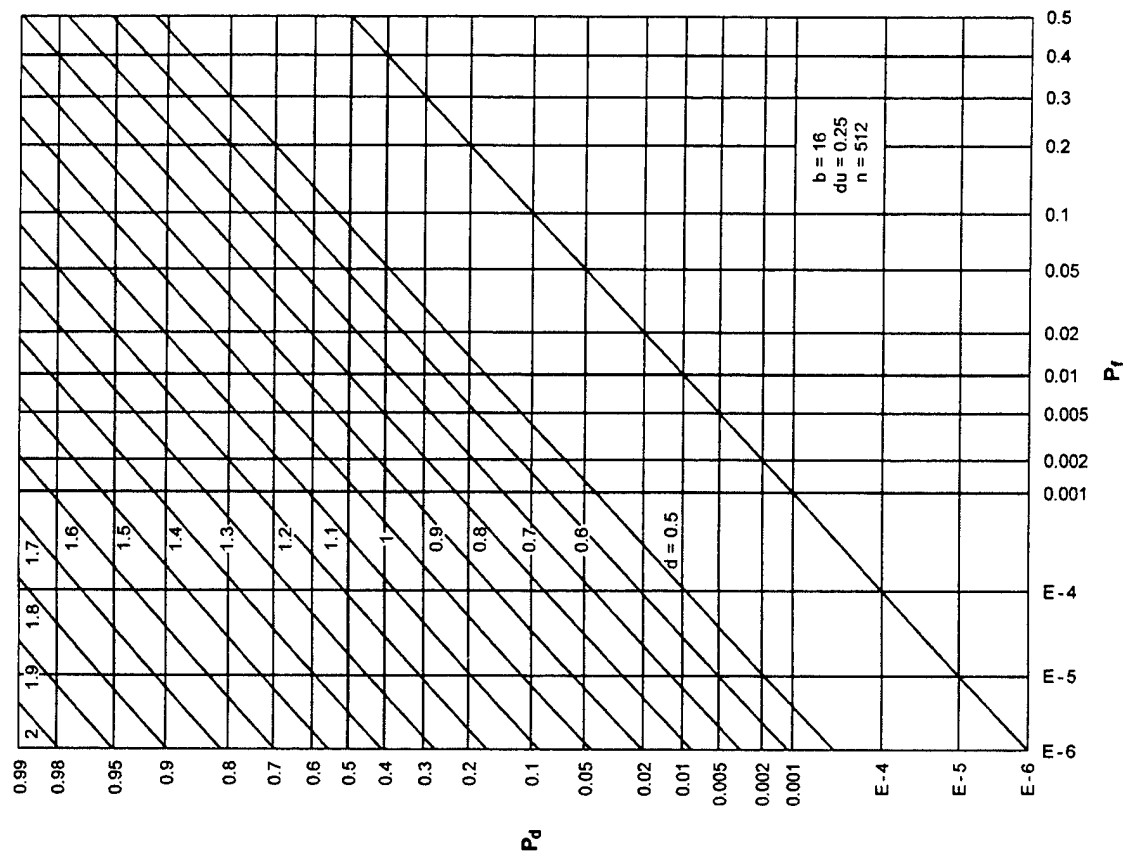


Figure A-14. ROCs for $K = 1$, $N = 2$, $M = 16$

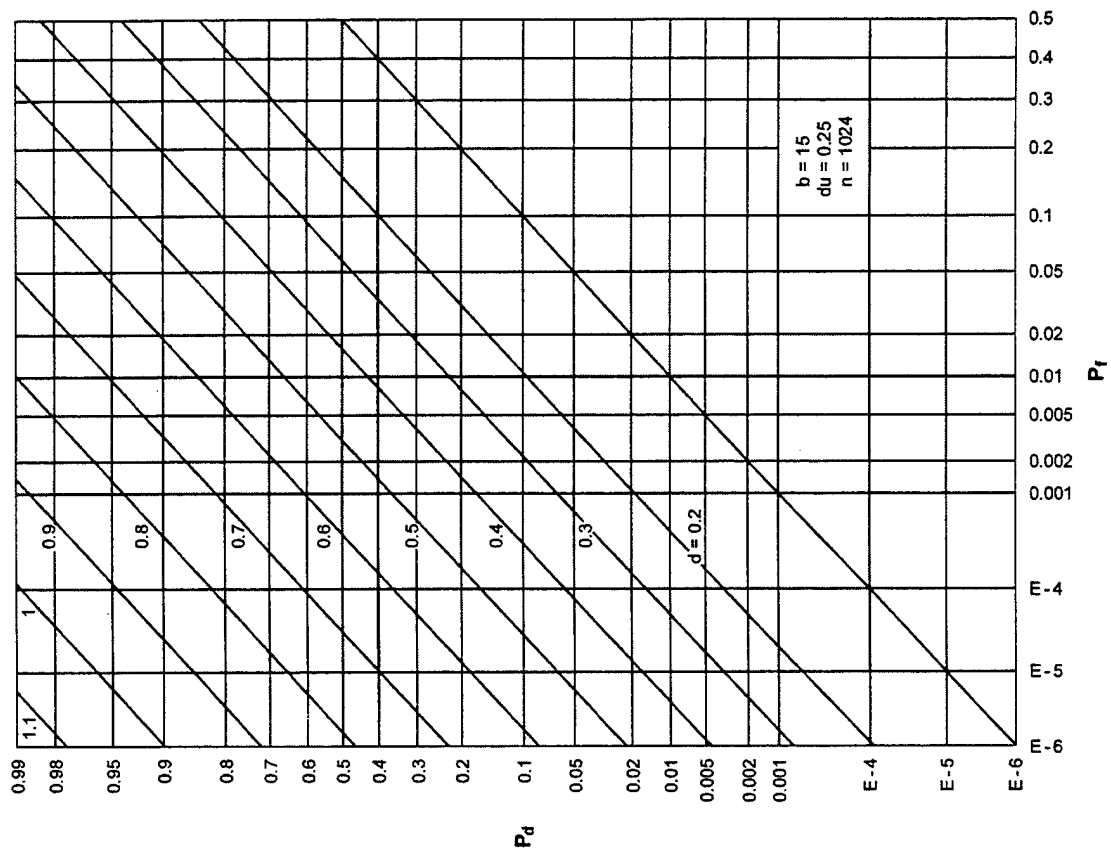


Figure A-16. ROCs for $K = 1$, $N = 2$, $M = 64$

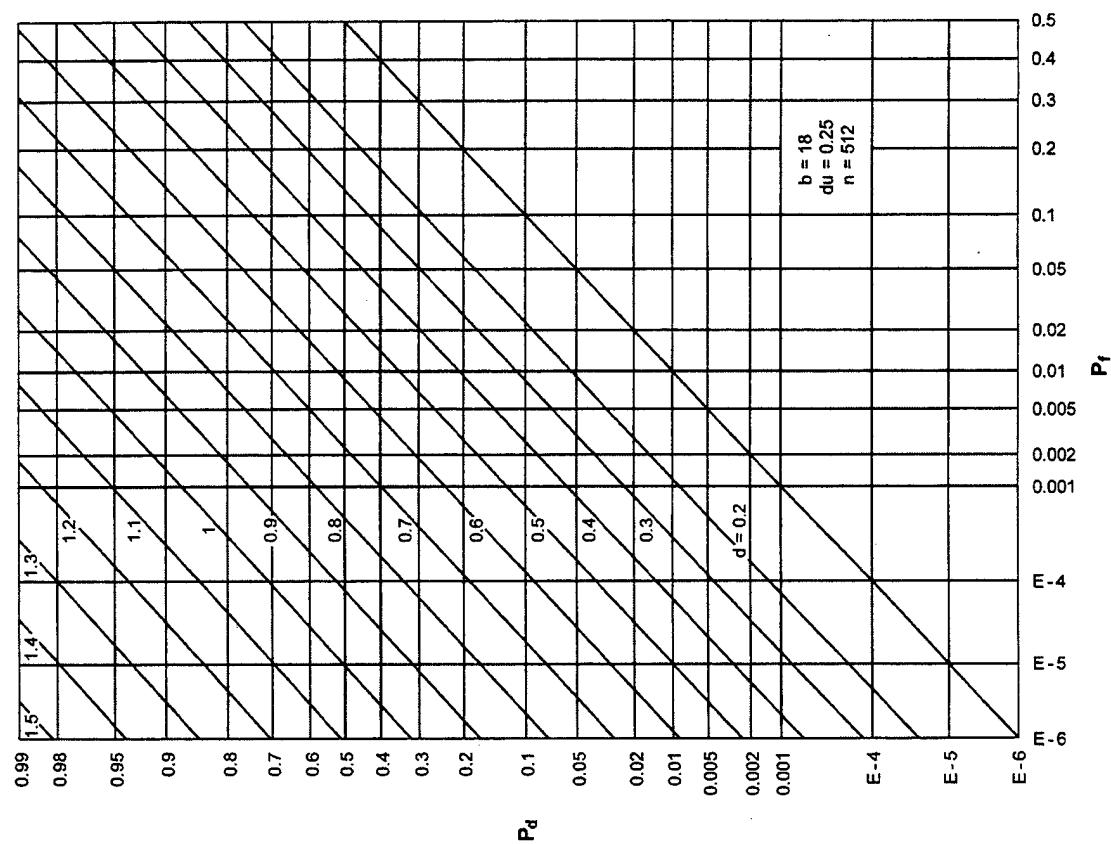


Figure A-15. ROCs for $K = 1$, $N = 2$, $M = 32$

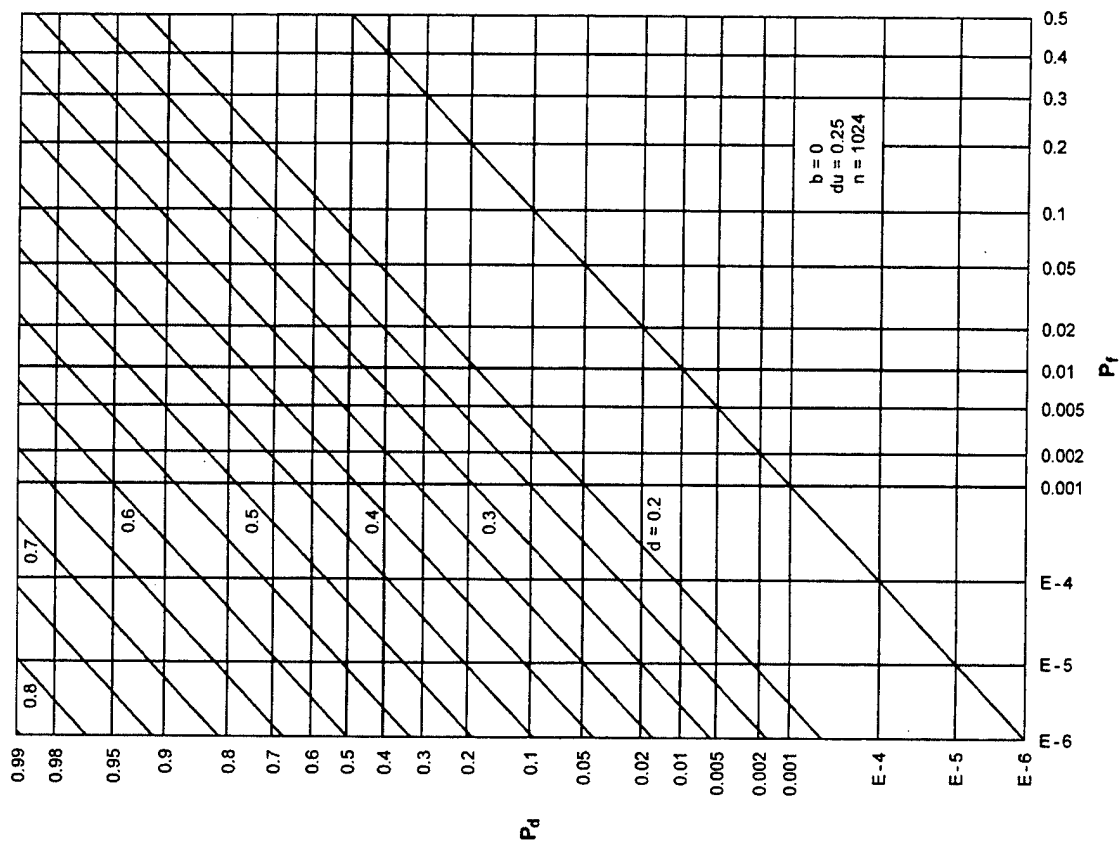


Figure A-17. ROCs for $K = 1$, $N = 2$, $M = 128$

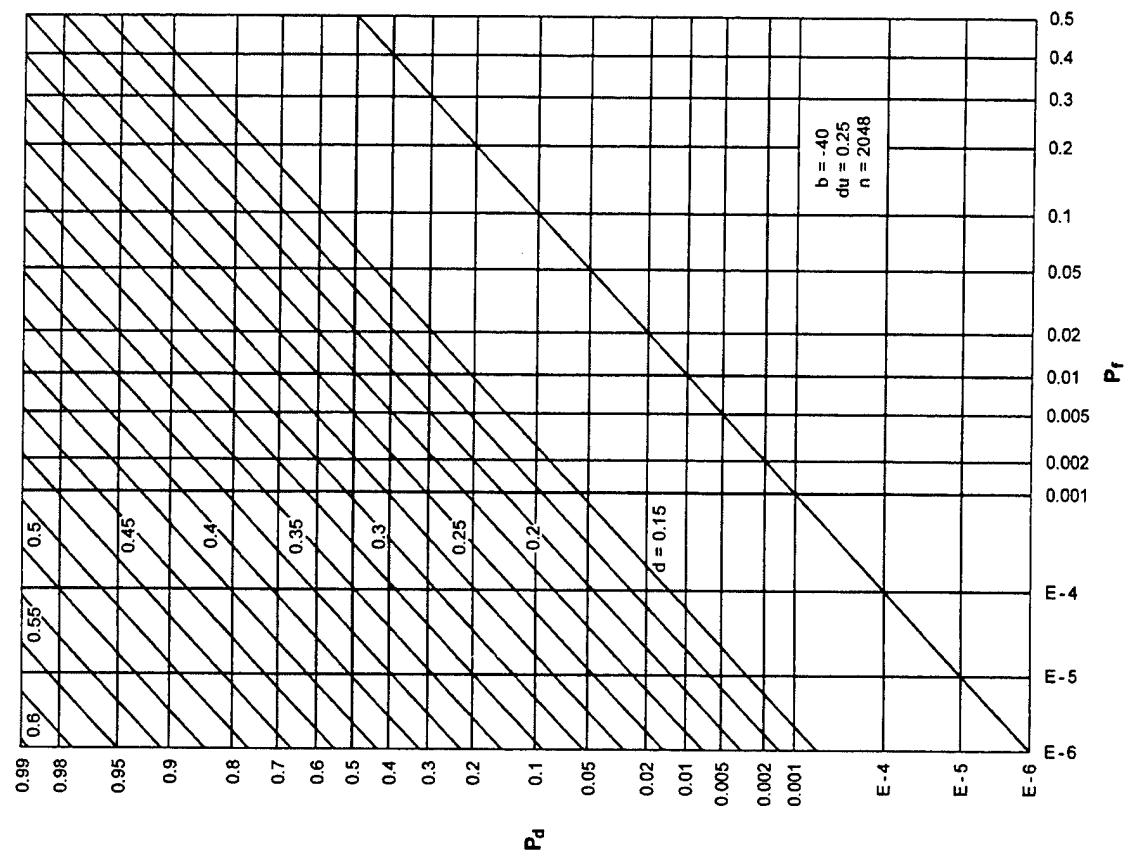


Figure A-18. ROCs for $K = 1$, $N = 2$, $M = 256$

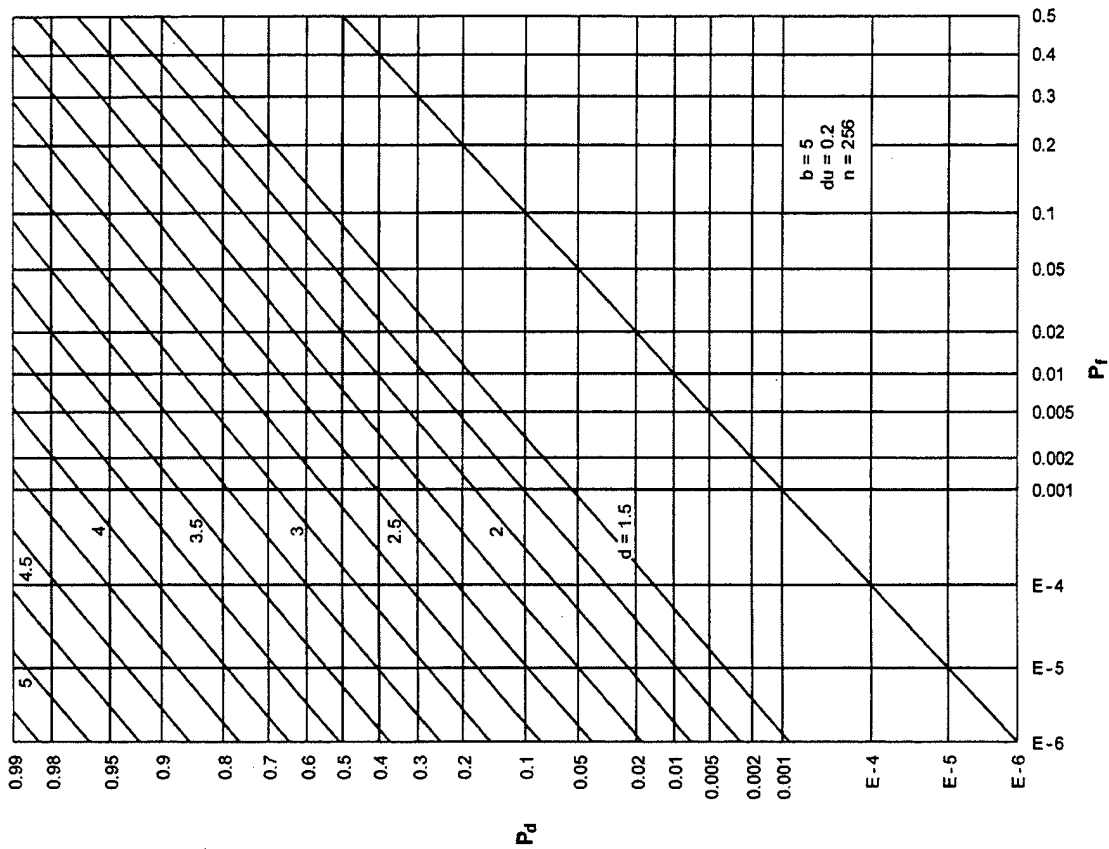


Figure A-20. ROCs for $K = 1, N = 4, M = 2$

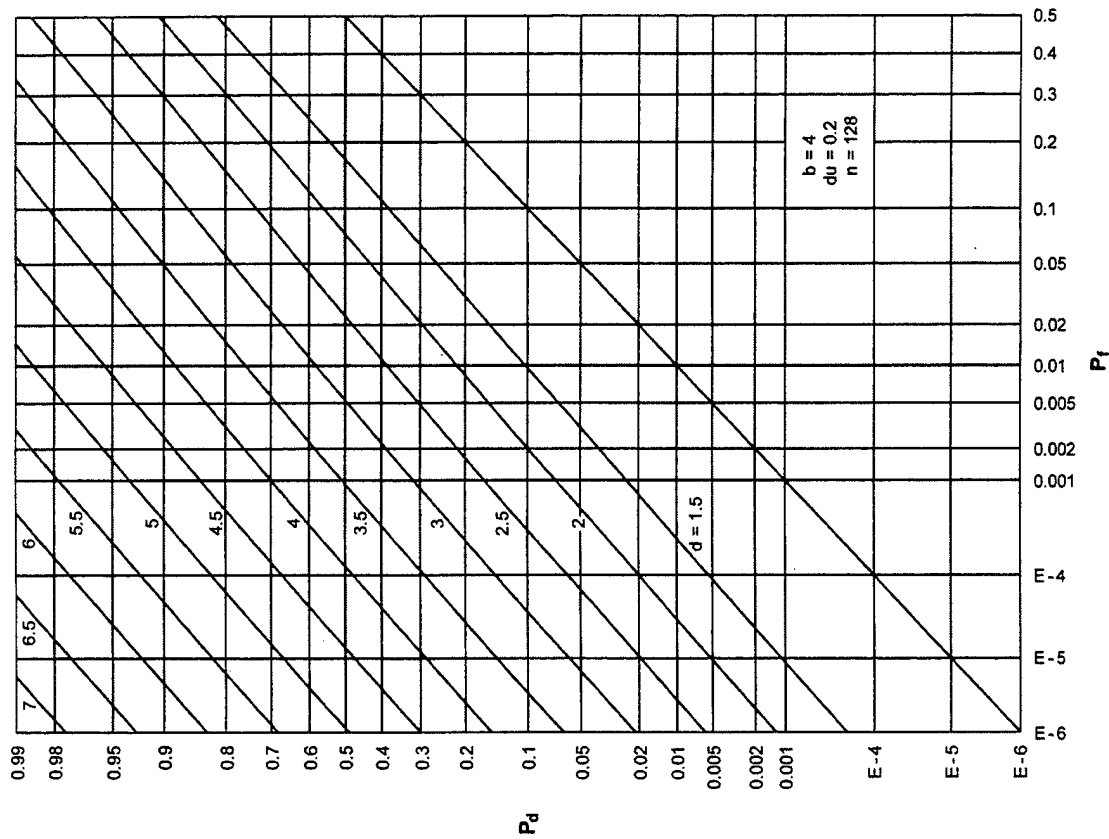


Figure A-19. ROCs for $K = 1, N = 4, M = 1$

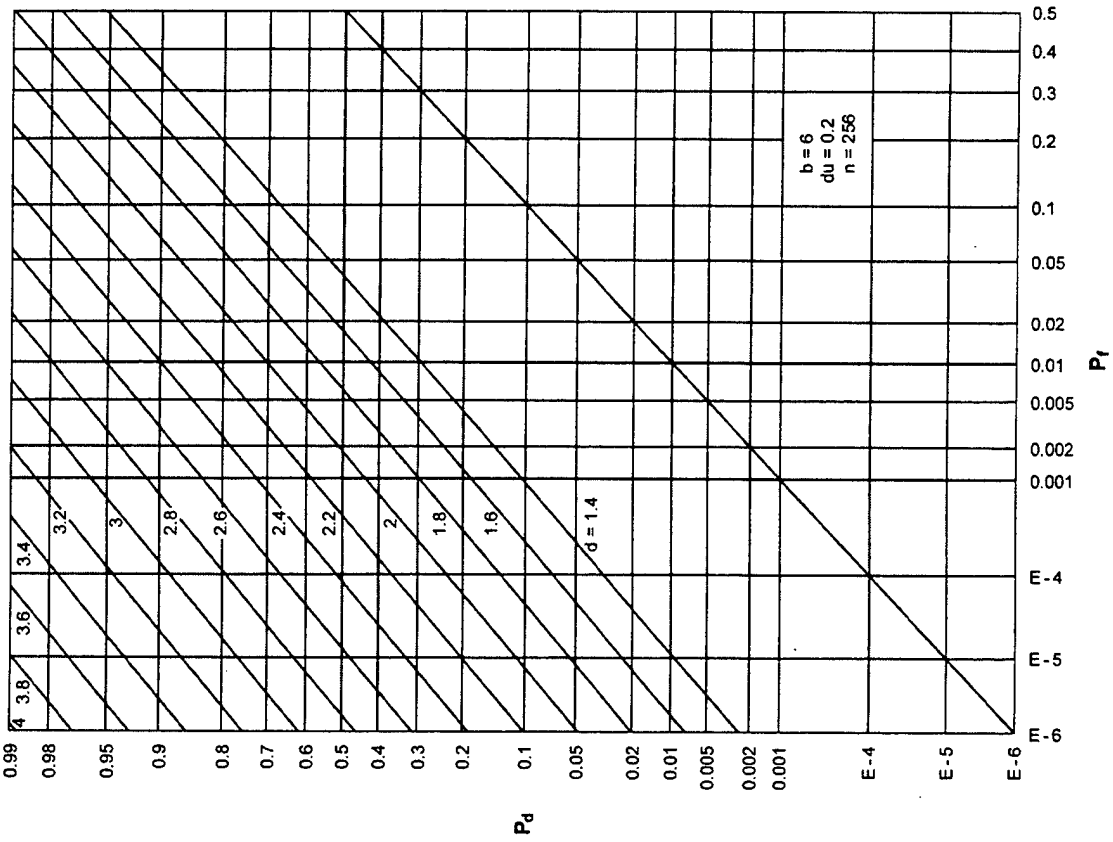


Figure A-21. ROCs for $K = 1$, $N = 4$, $M = 4$

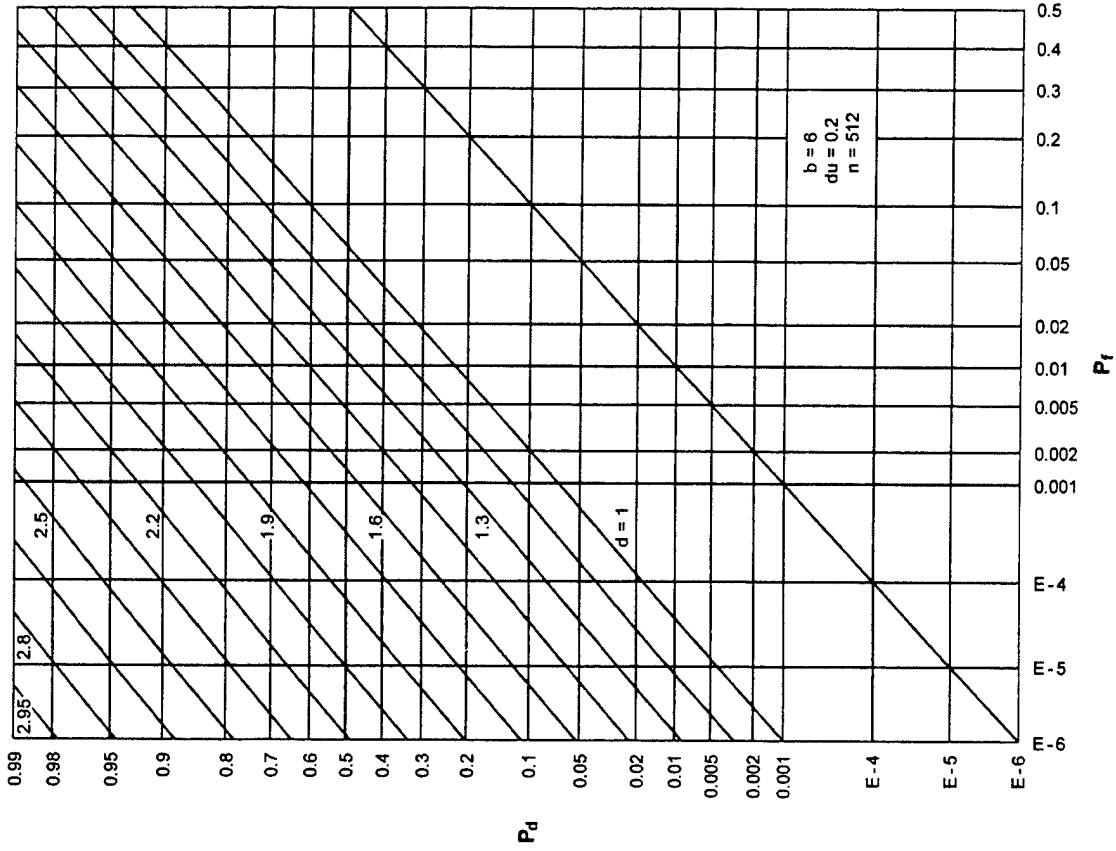


Figure A-22. ROCs for $K = 1$, $N = 4$, $M = 8$

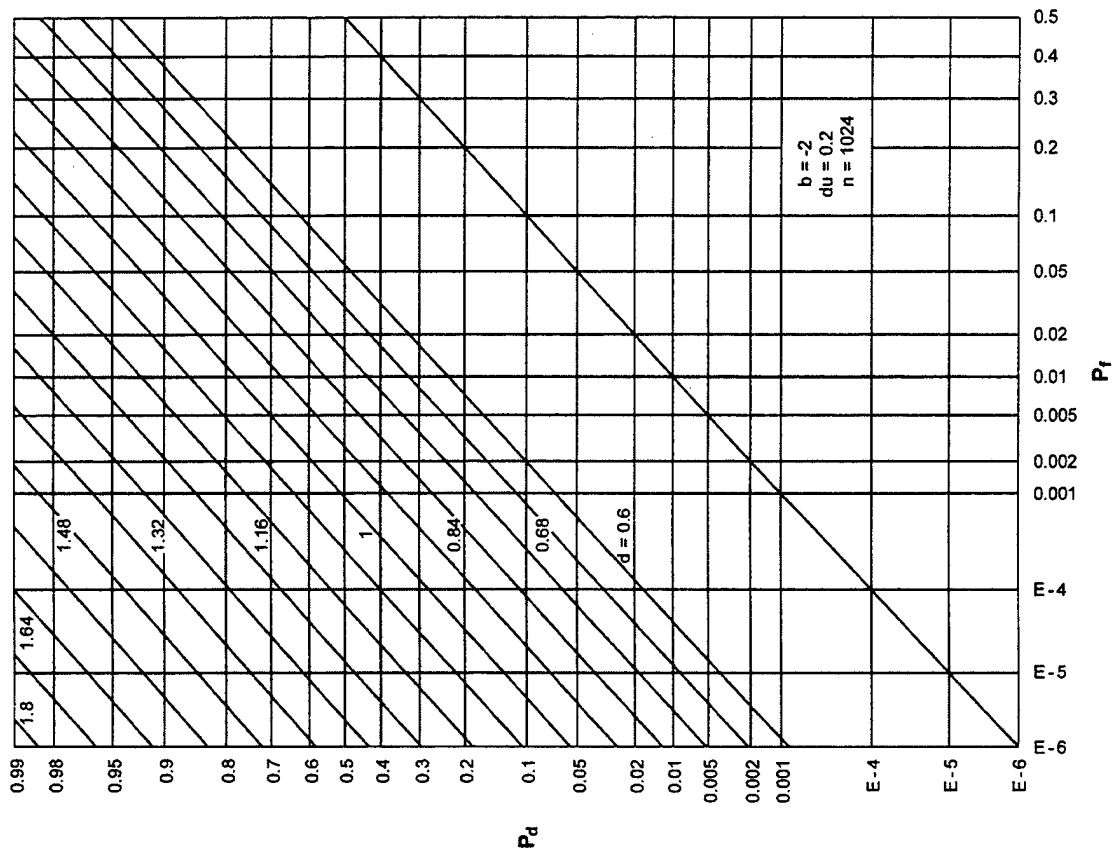


Figure A-24. ROCs for $K = 1$, $N = 4$, $M = 32$

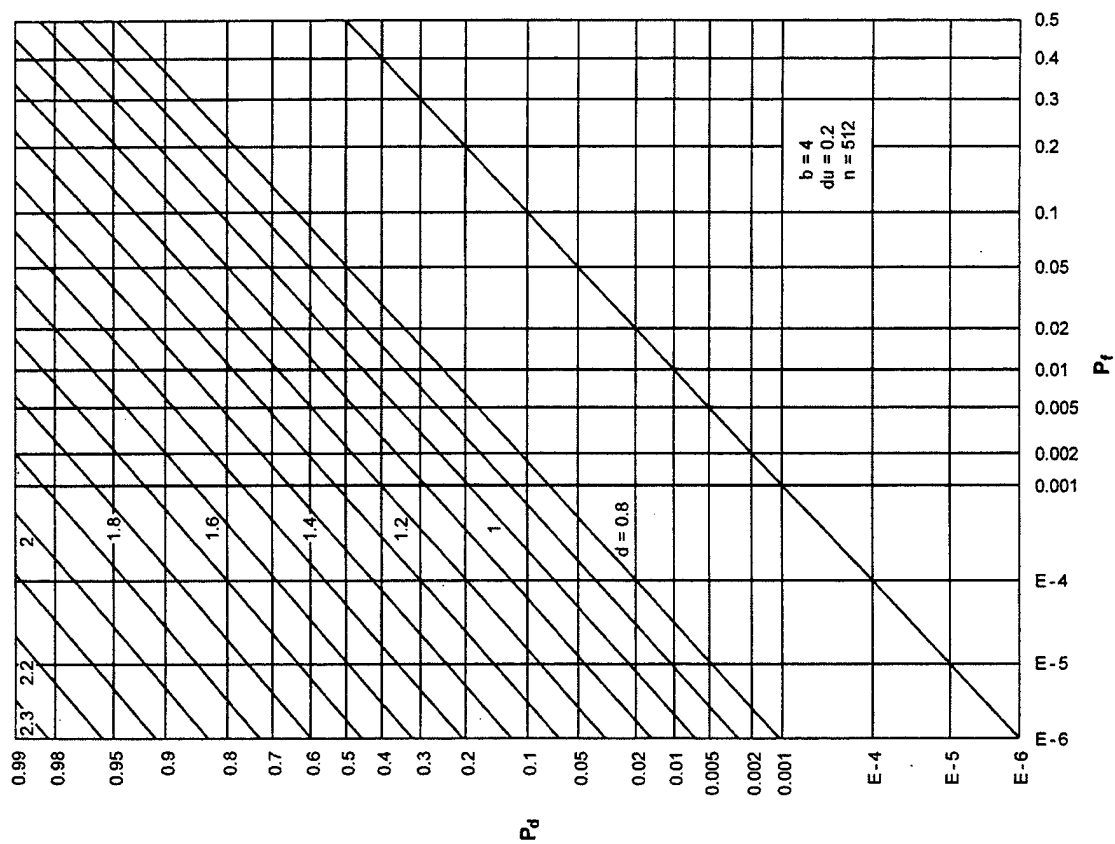


Figure A-23. ROCs for $K = 1$, $N = 4$, $M = 16$

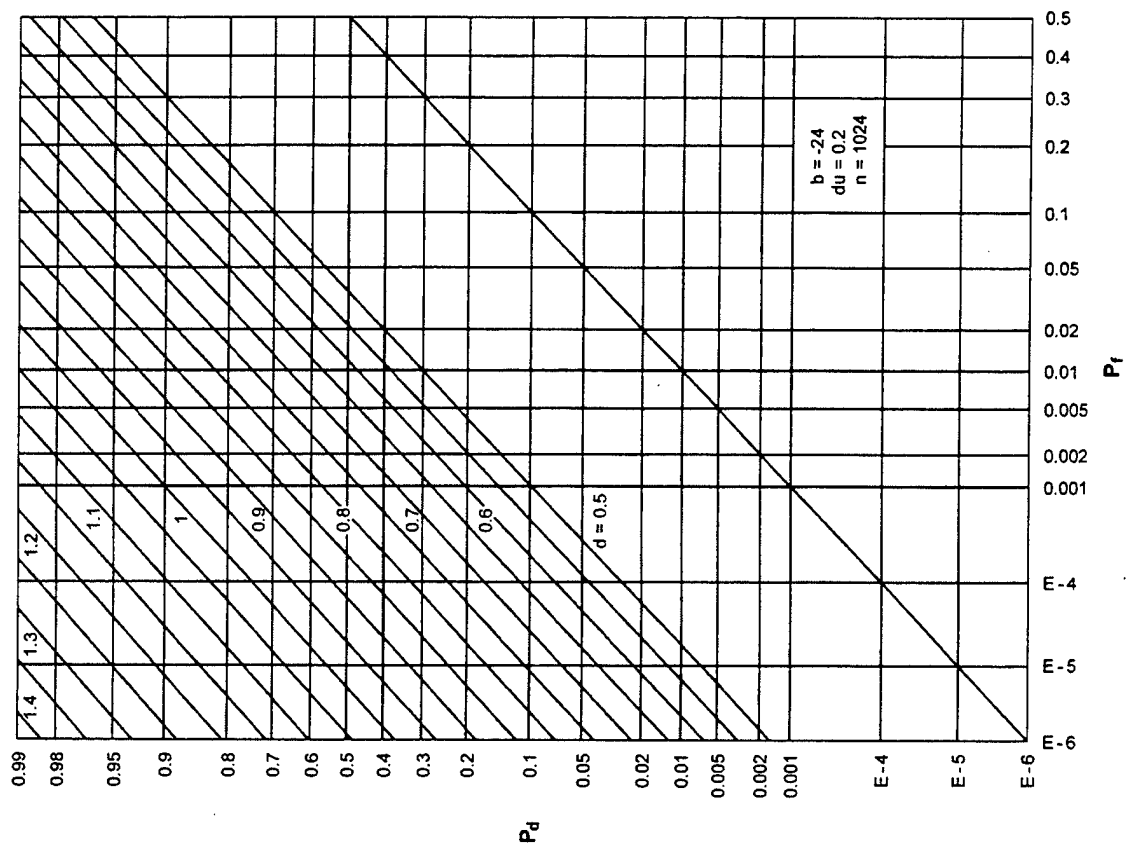


Figure A-25. ROCs for $K = 1$, $N = 4$, $M = 64$

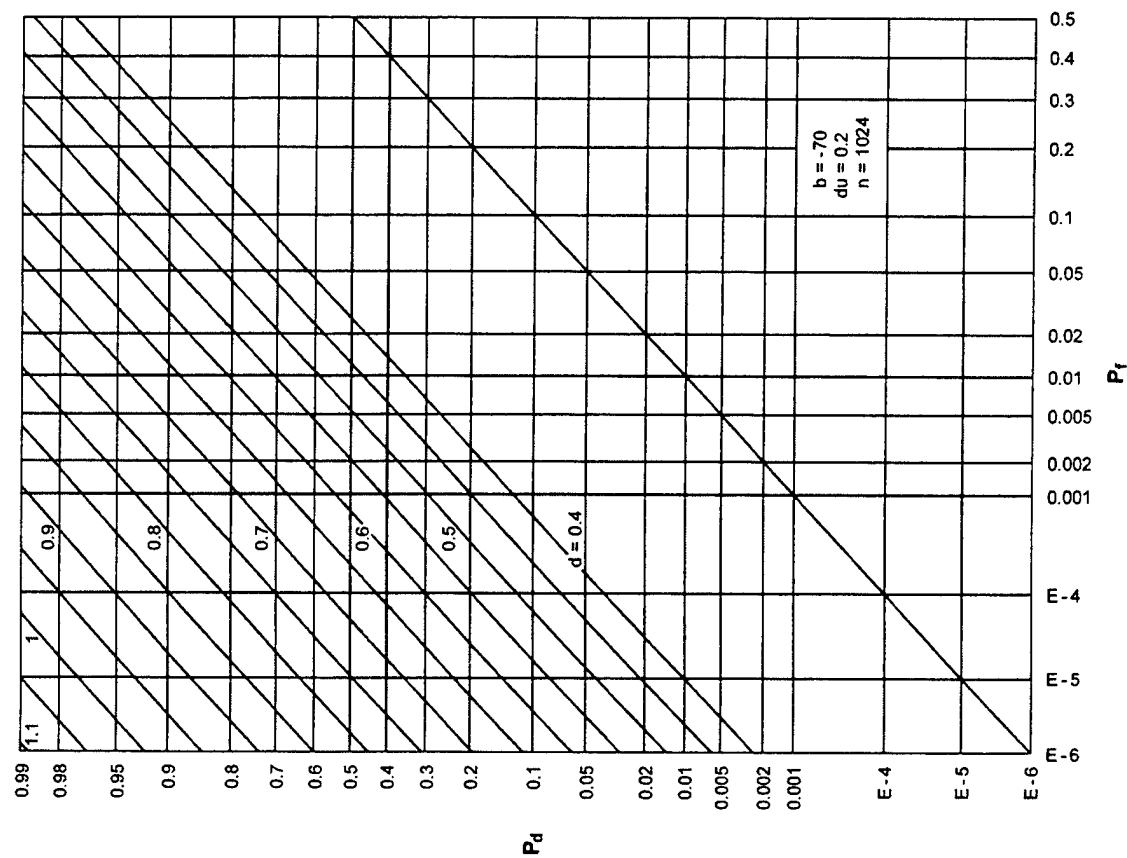


Figure A-26. ROCs for $K = 1$, $N = 4$, $M = 128$

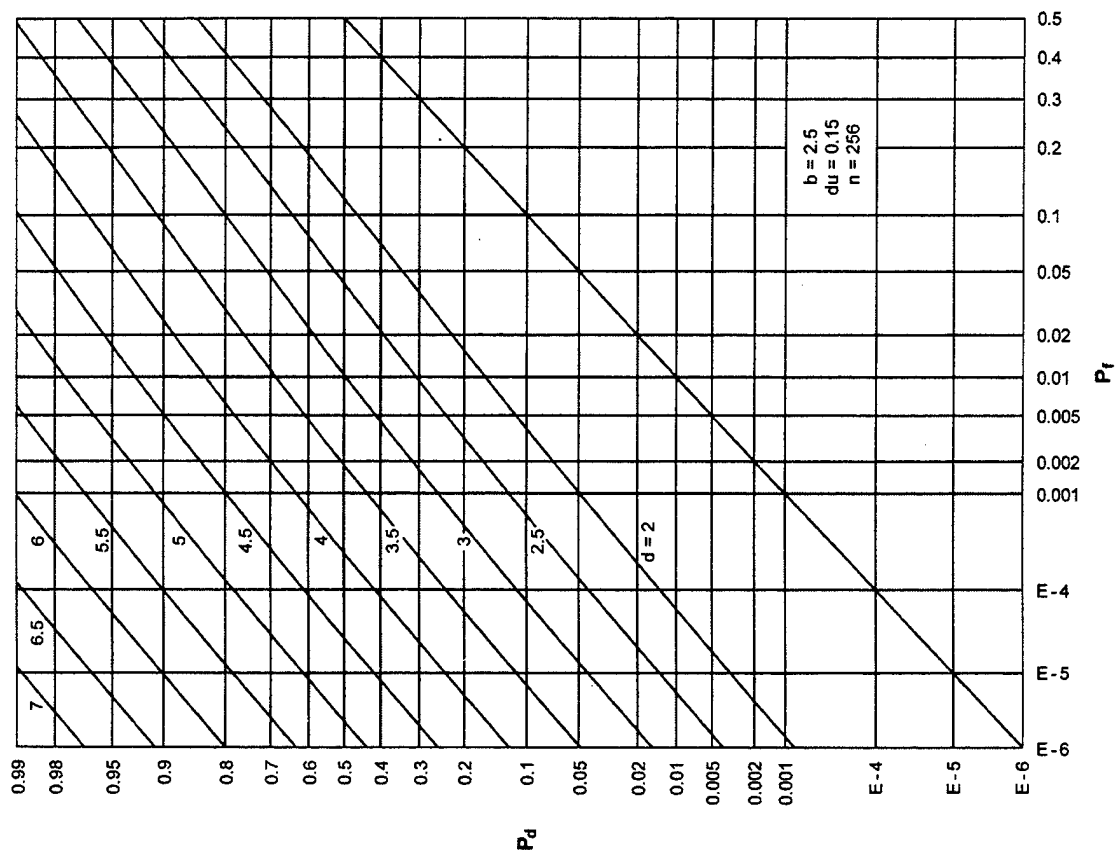


Figure A-28. ROCs for $K = 1$, $N = 8$, $M = 1$

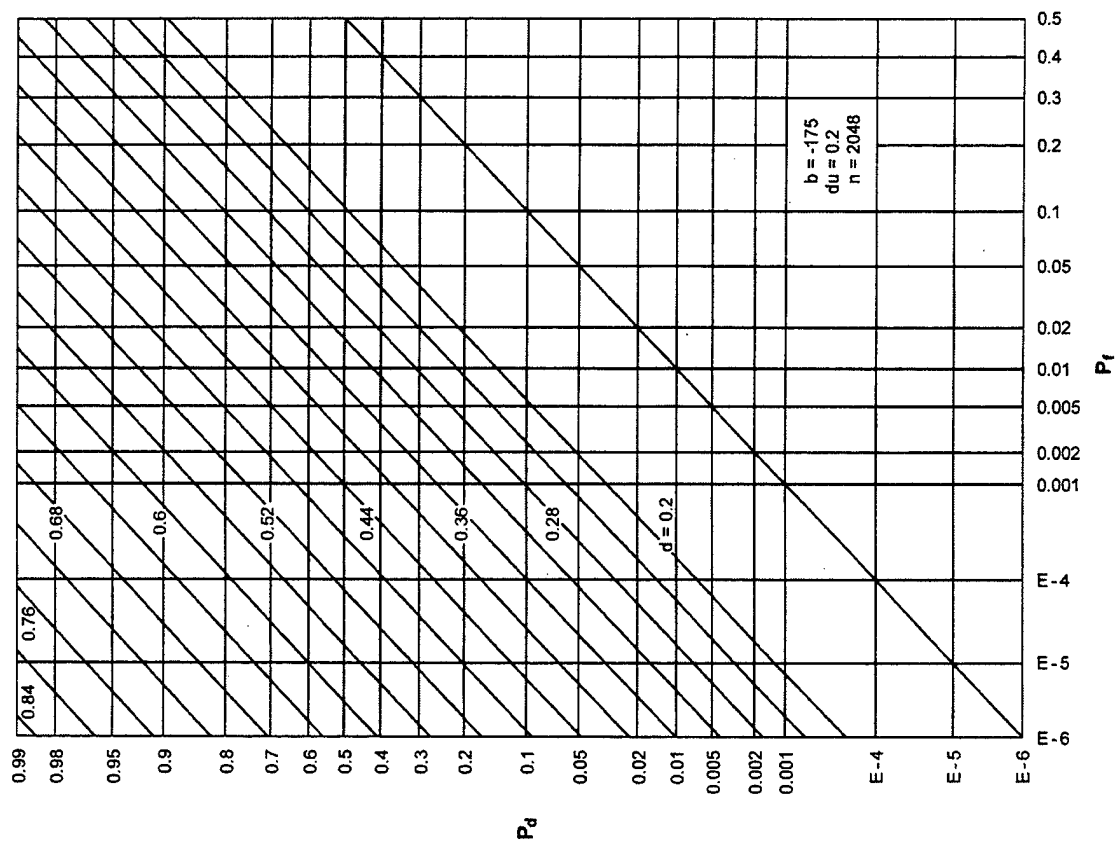


Figure A-27. ROCs for $K = 1$, $N = 4$, $M = 256$

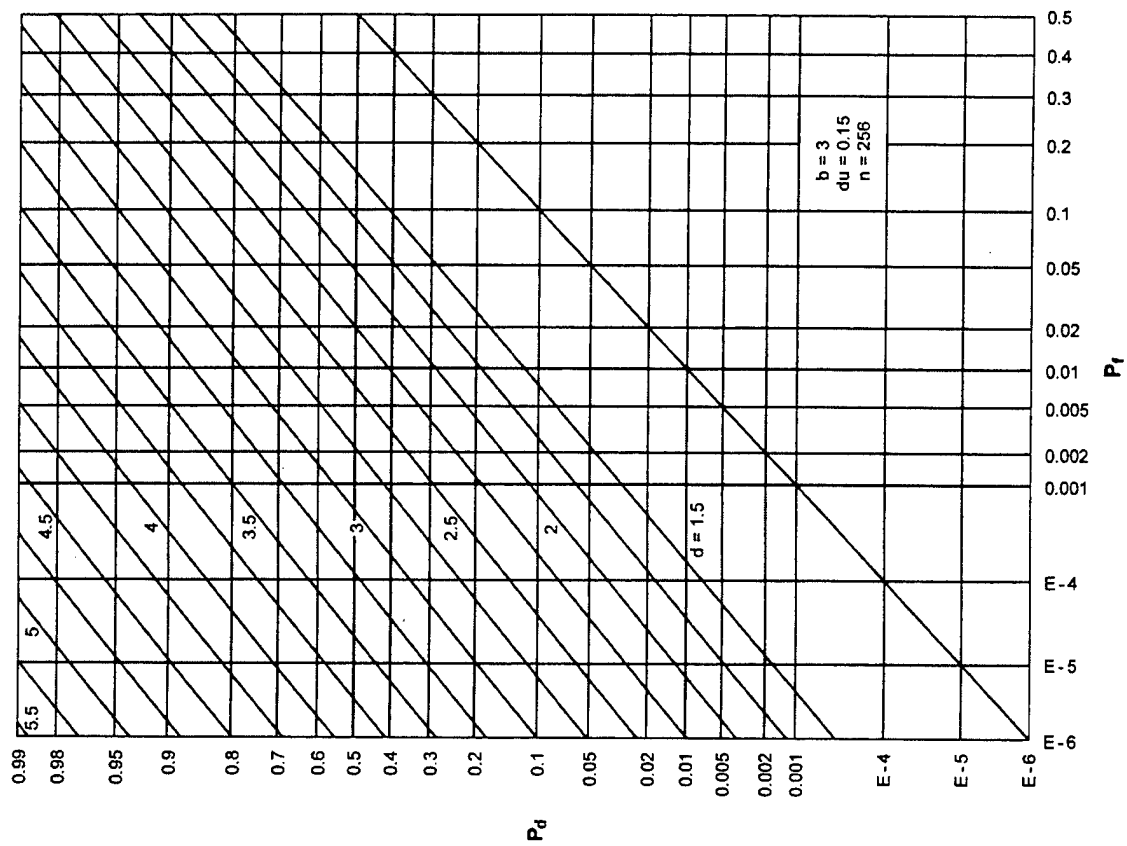


Figure A-29. ROCs for $K = 1$, $N = 8$, $M = 2$

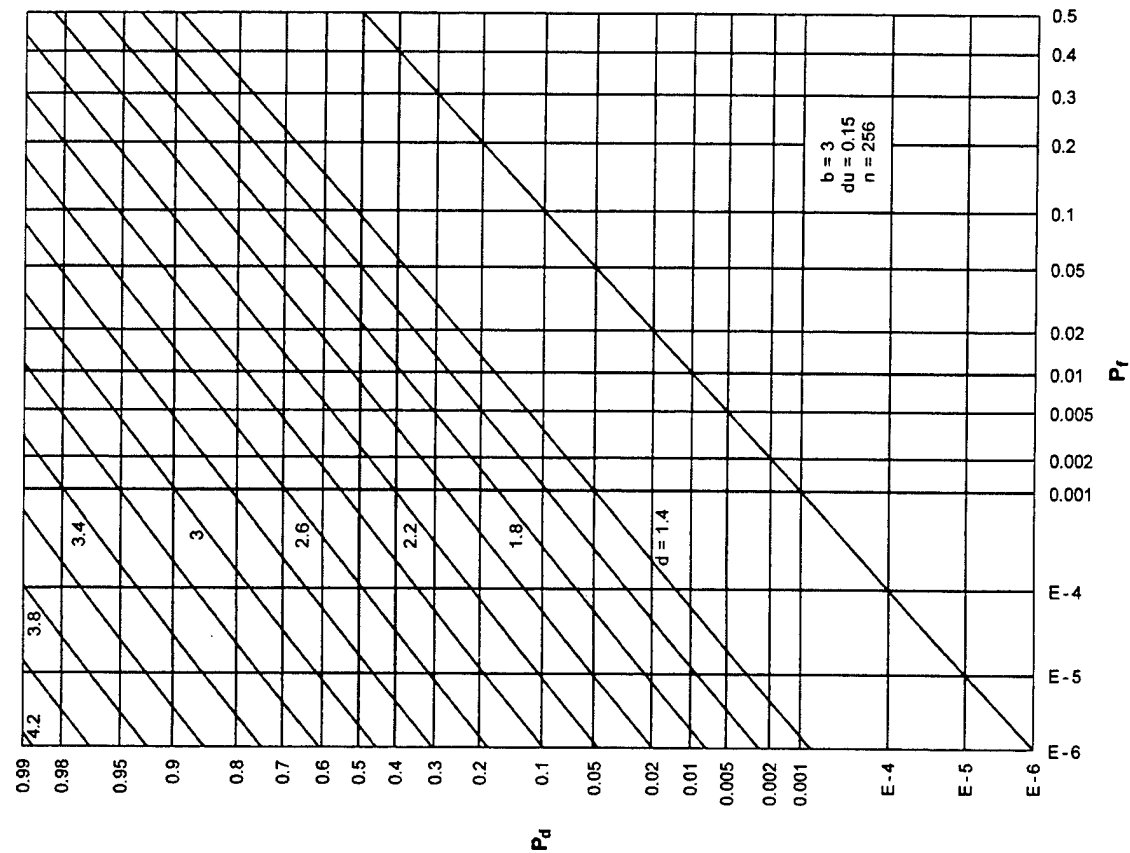


Figure A-30. ROCs for $K = 1$, $N = 8$, $M = 4$

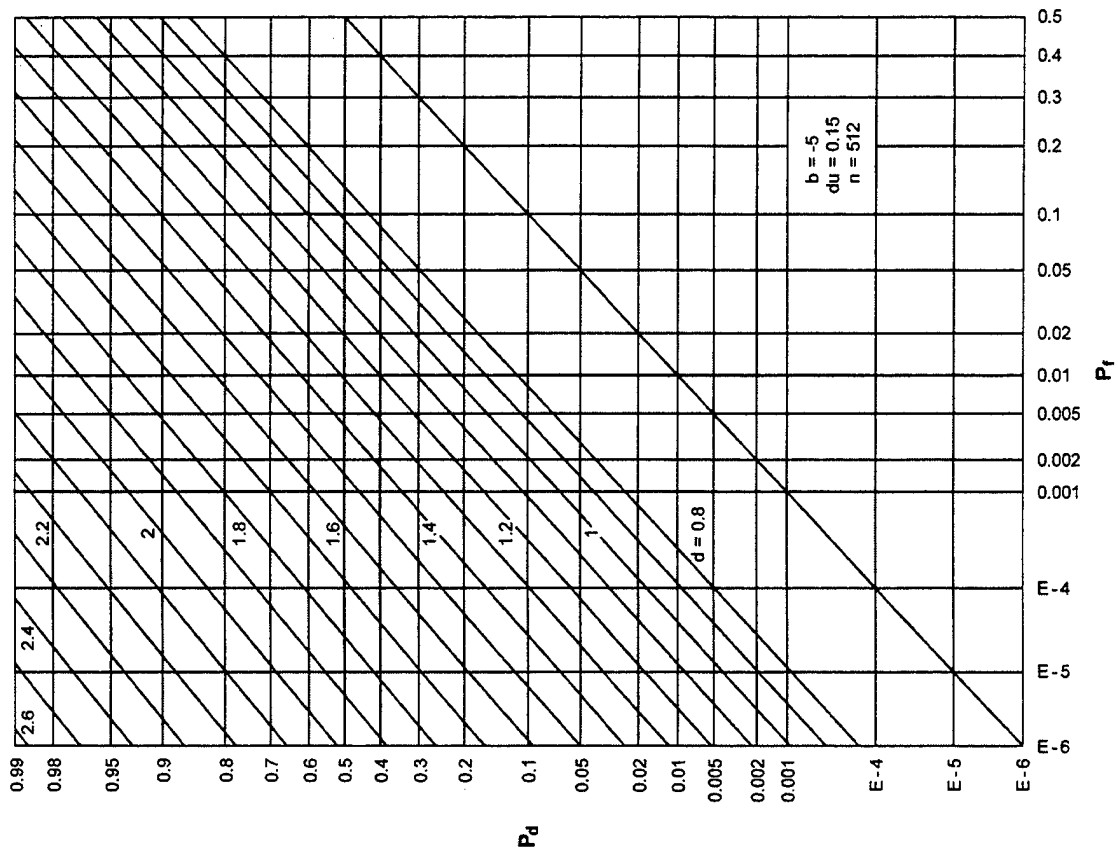


Figure A-32. ROCs for $K = 1$, $N = 8$, $M = 16$

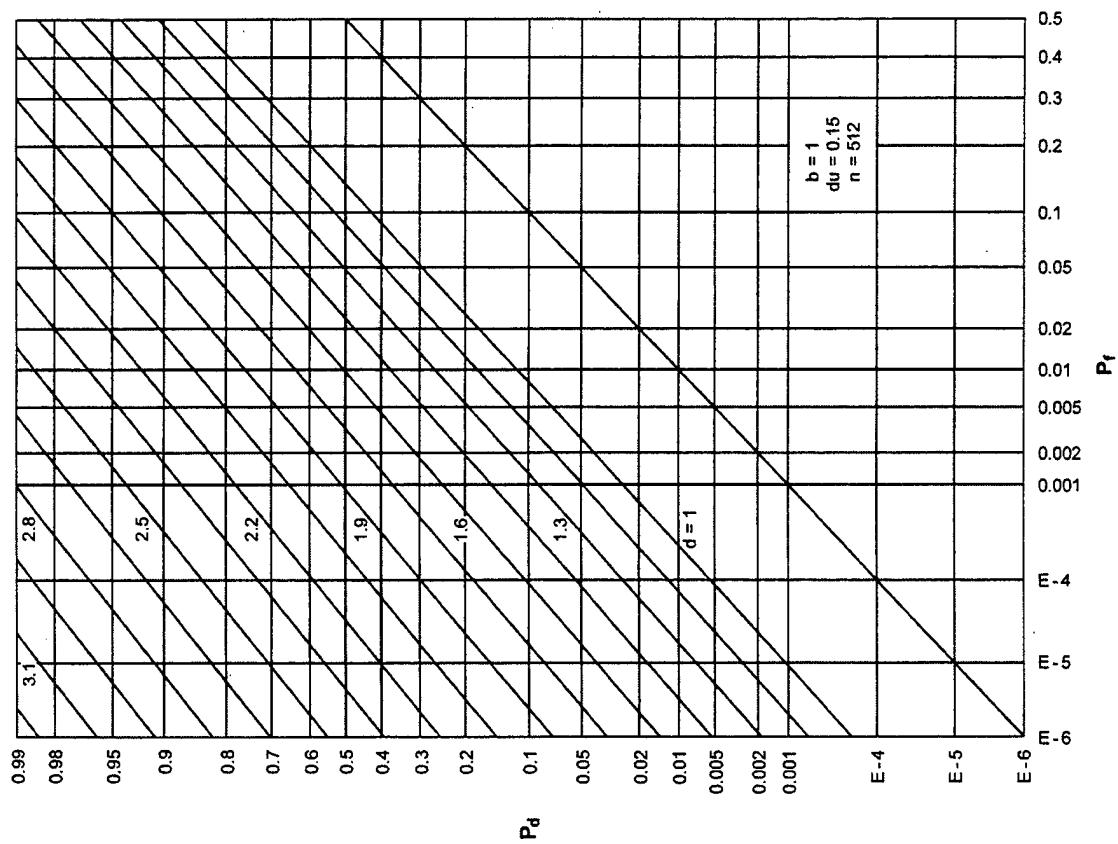


Figure A-31. ROCs for $K = 1$, $N = 8$, $M = 8$

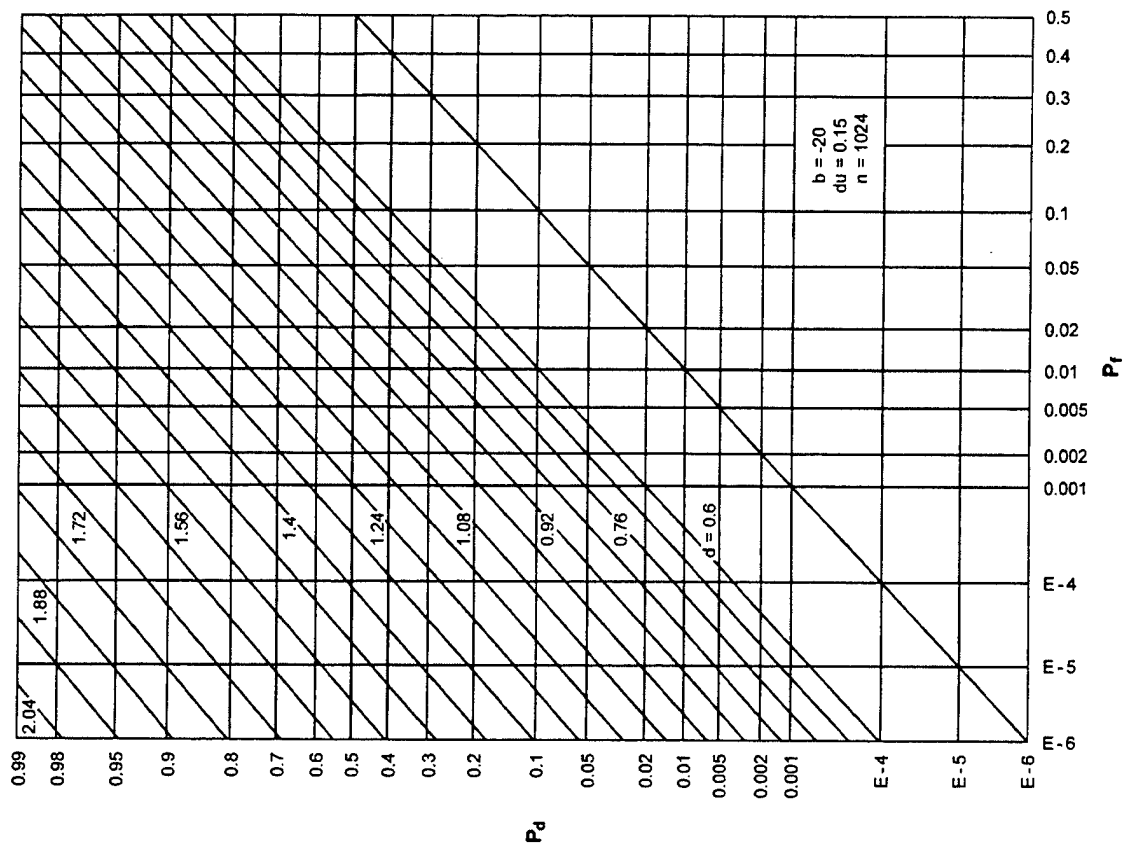


Figure A-33. ROCs for $K = 1$, $N = 8$, $M = 32$

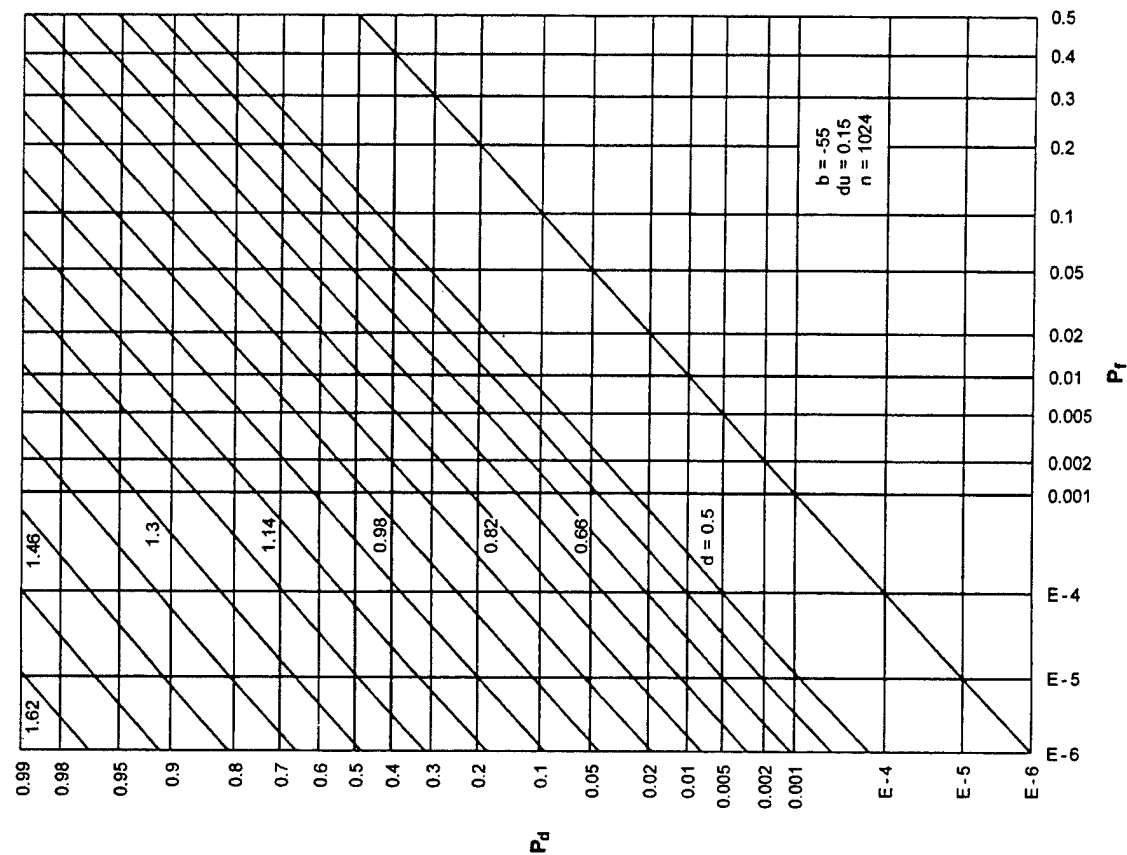


Figure A-34. ROCs for $K = 1$, $N = 8$, $M = 64$

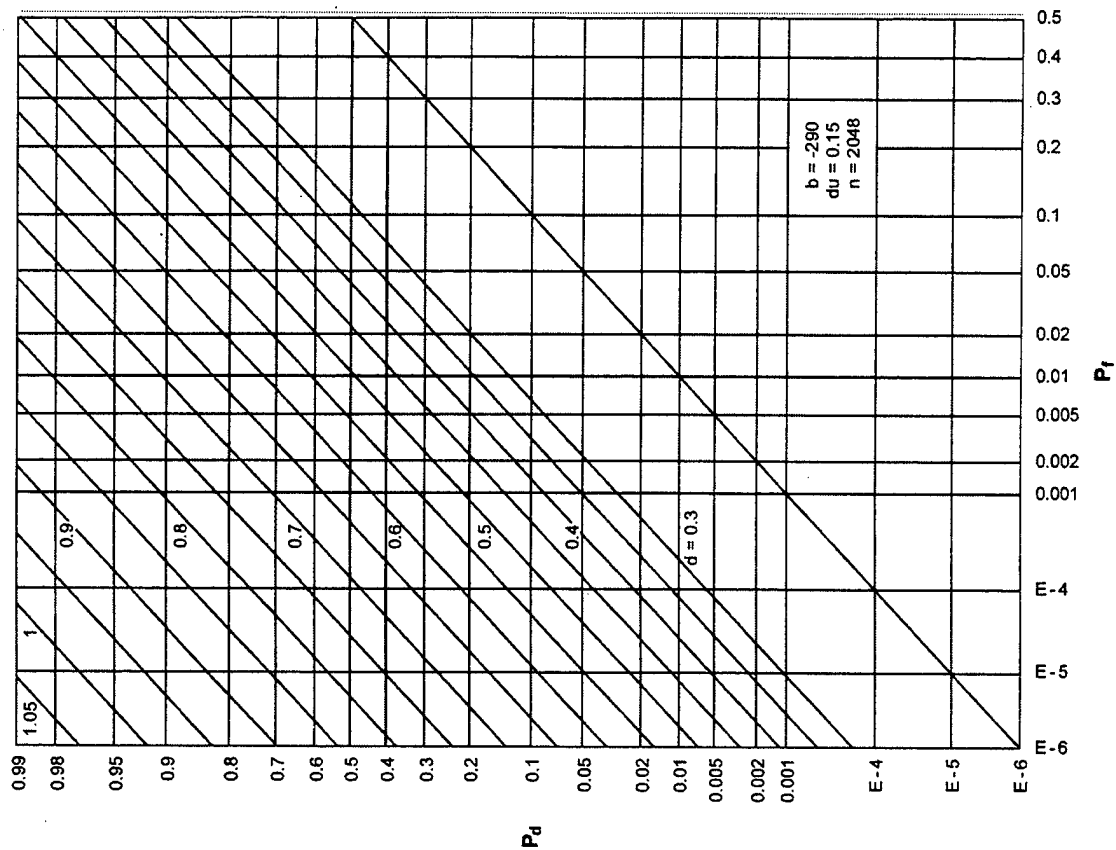


Figure A-36. ROCs for $K = 1$, $N = 8$, $M = 256$

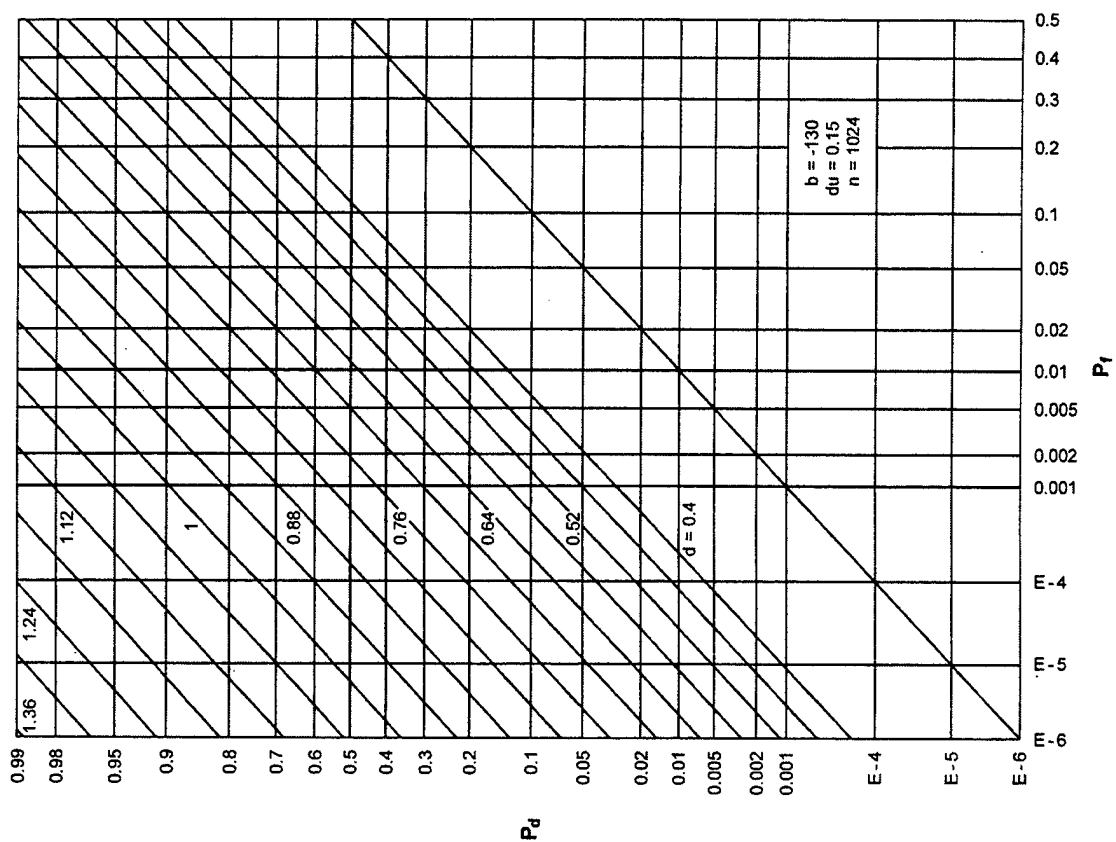


Figure A-35. ROCs for $K = 1$, $N = 8$, $M = 128$

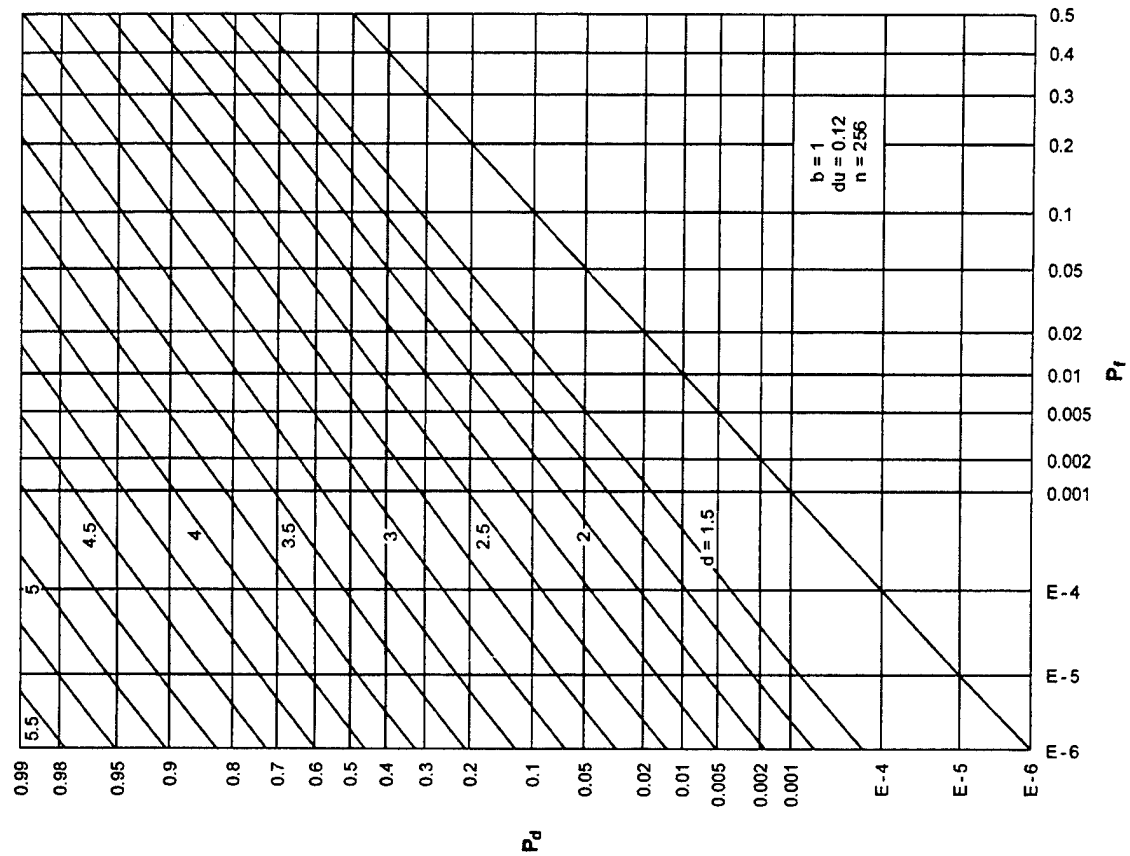


Figure A-38. ROCs for $K = 1$, $N = 16$, $M = 2$

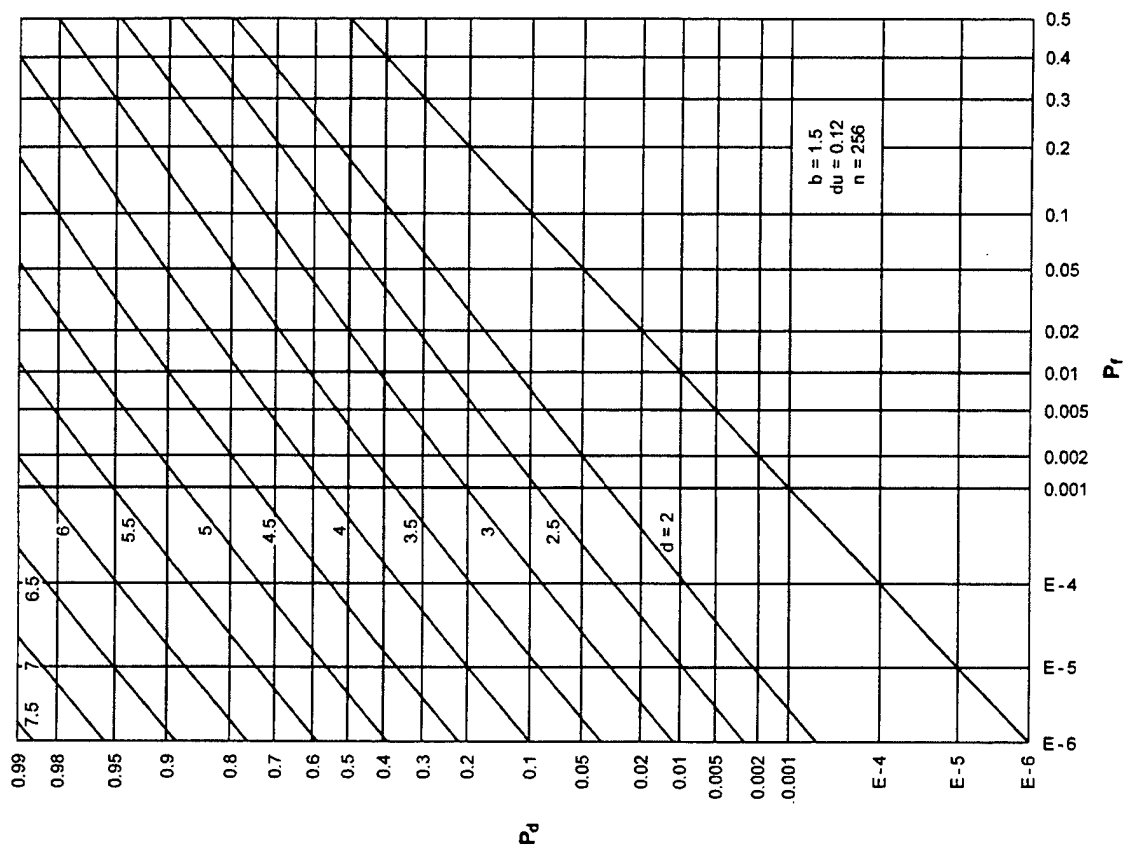


Figure A-37. ROCs for $K = 1$, $N = 16$, $M = 1$

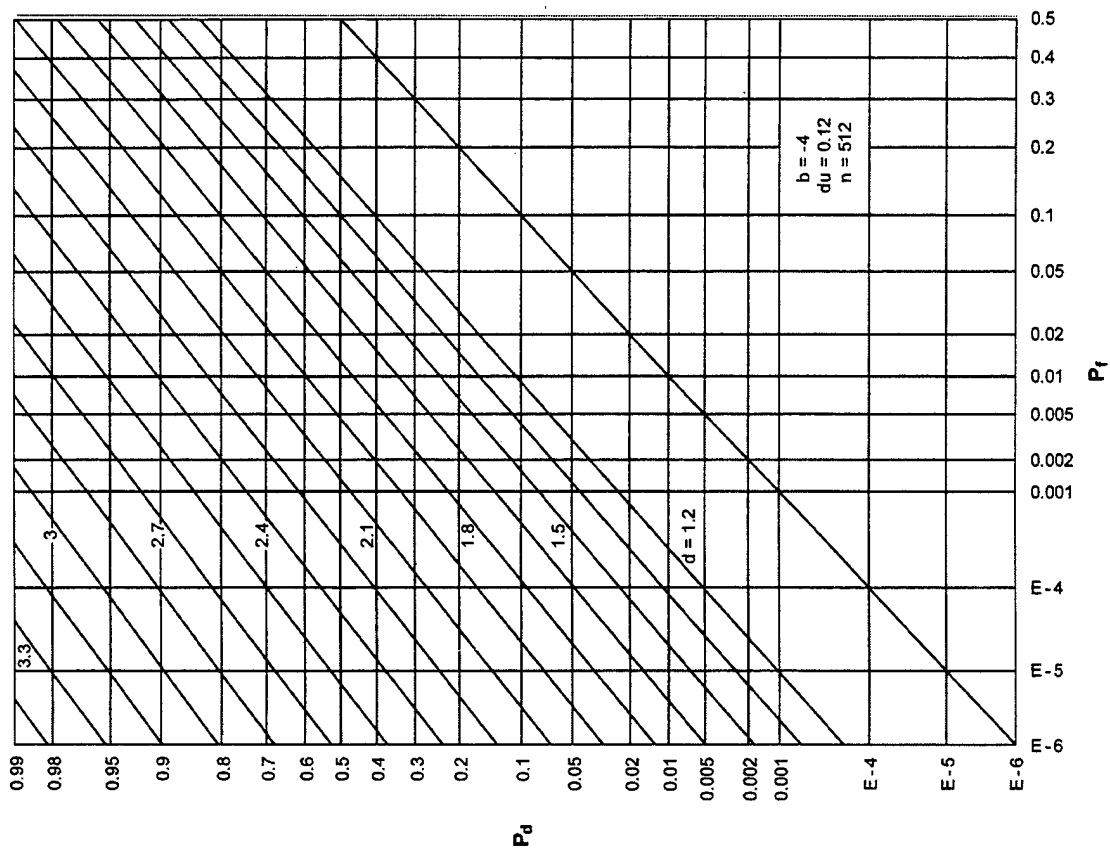


Figure A-40. ROCs for $K = 1$, $N = 16$, $M = 8$

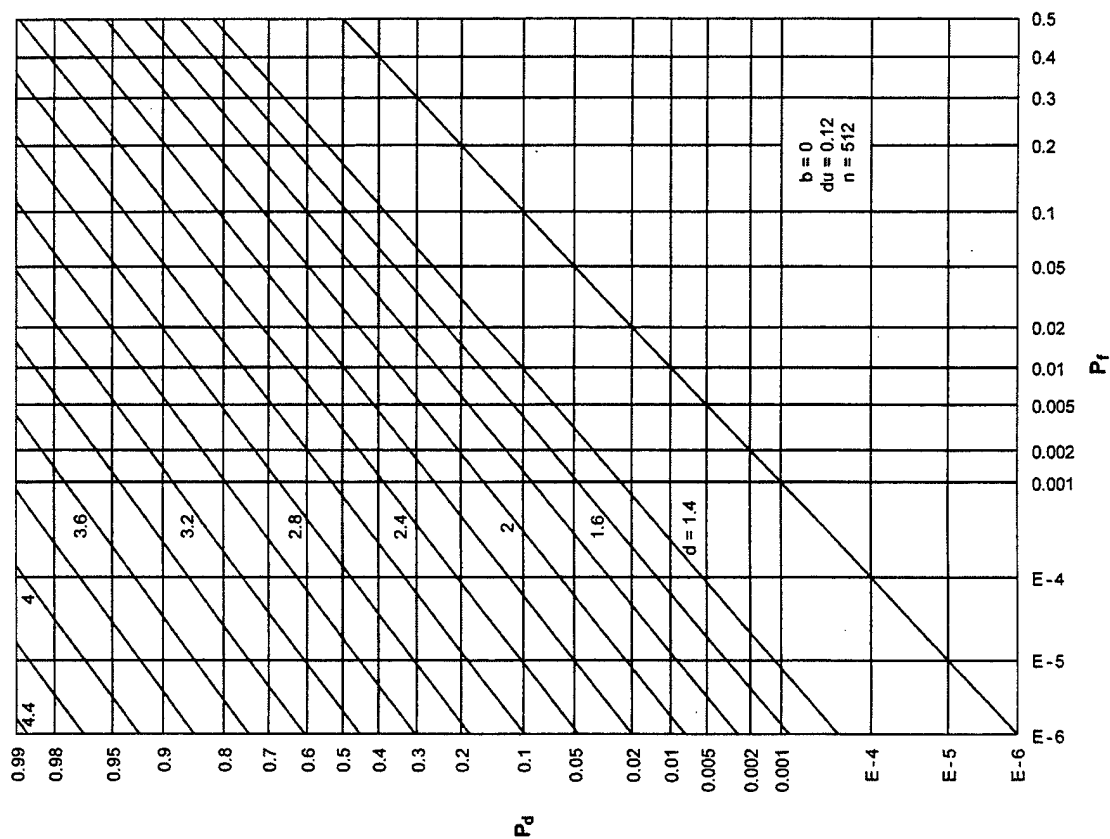


Figure A-39. ROCs for $K = 1$, $N = 16$, $M = 4$

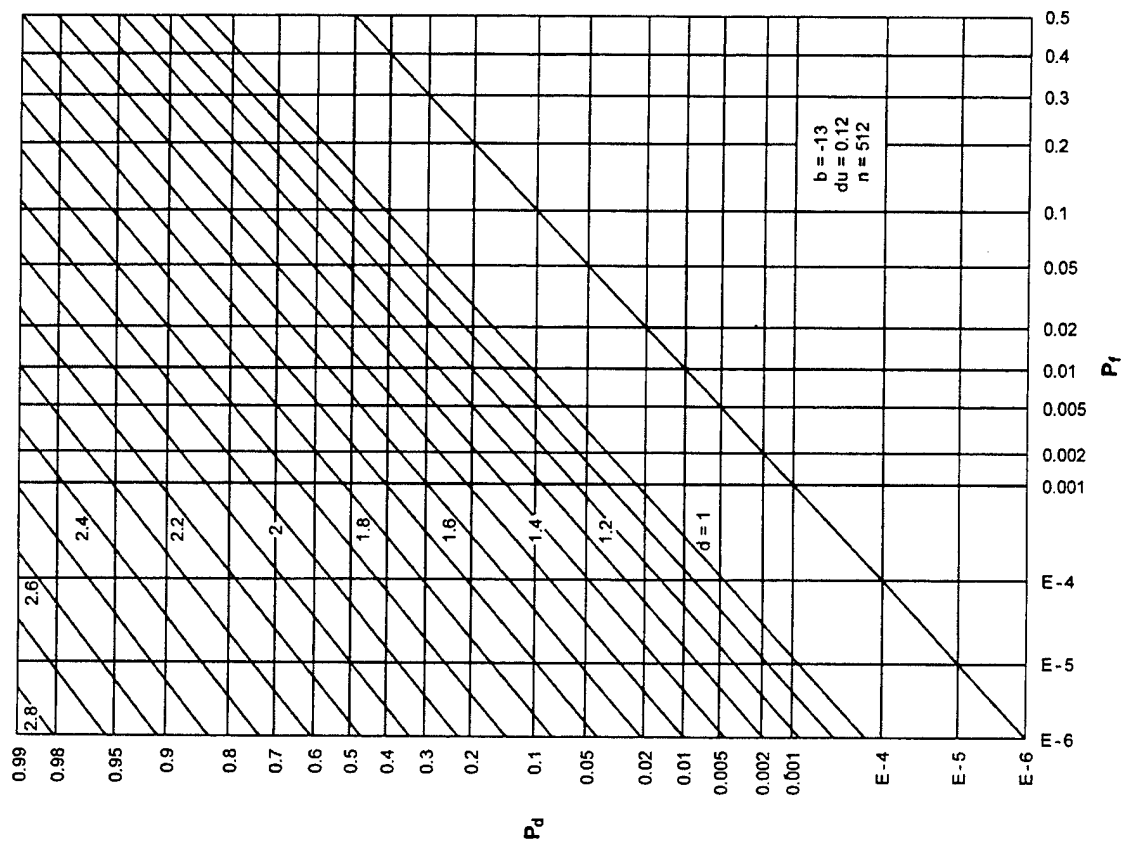


Figure A-41. ROCs for $K = 1$, $N = 16$, $M = 16$

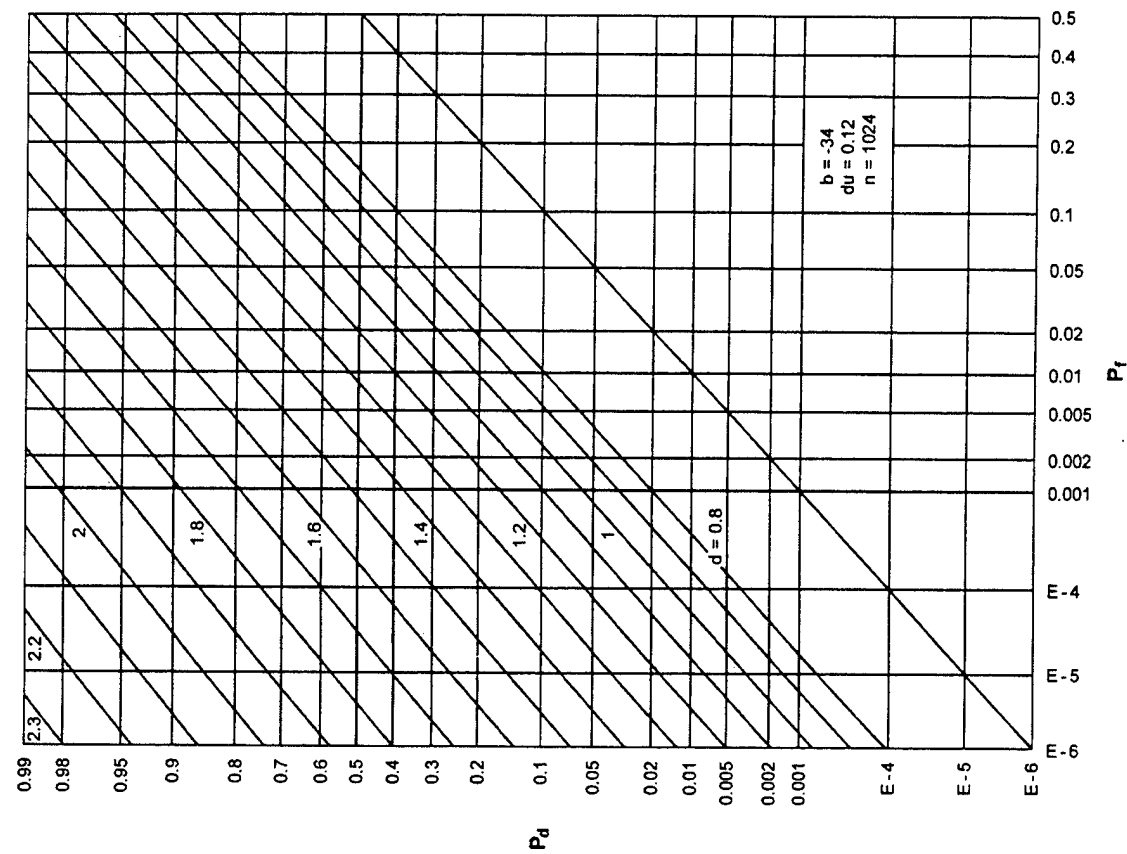


Figure A-42. ROCs for $K = 1$, $N = 16$, $M = 32$

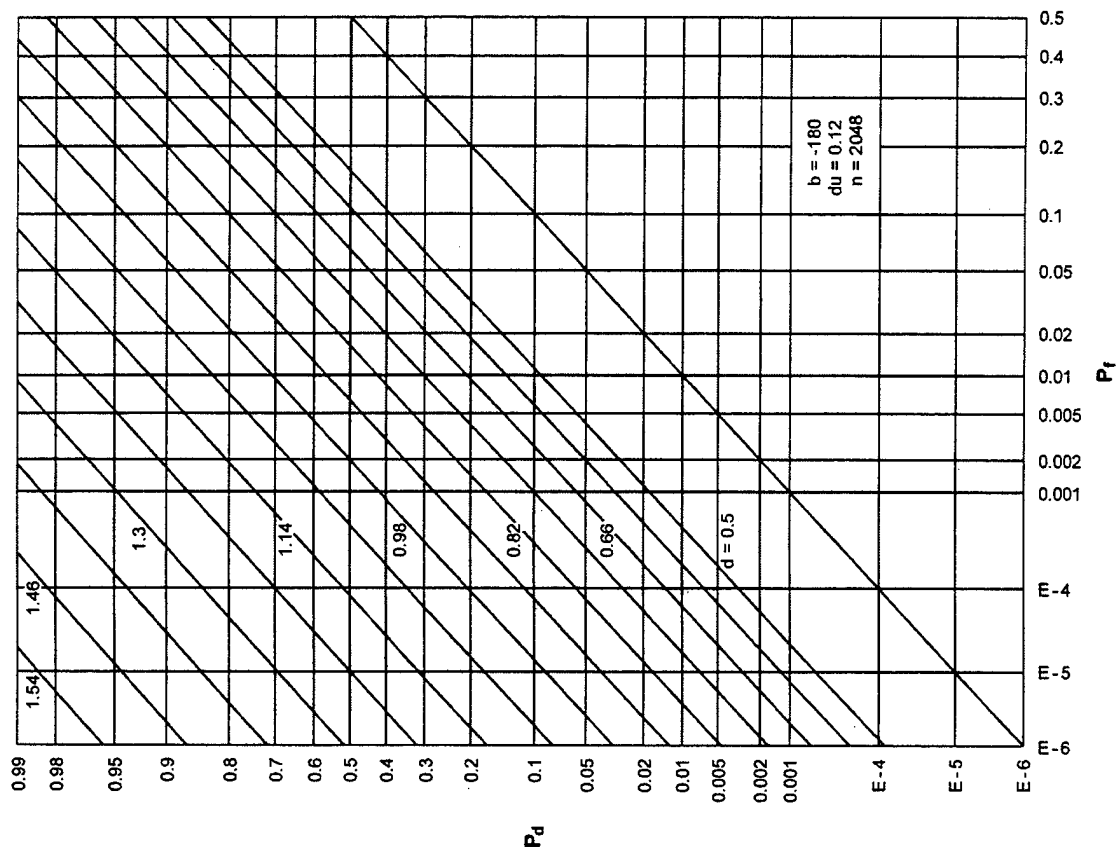


Figure A-44. ROCs for $K = 1$, $N = 16$, $M = 128$

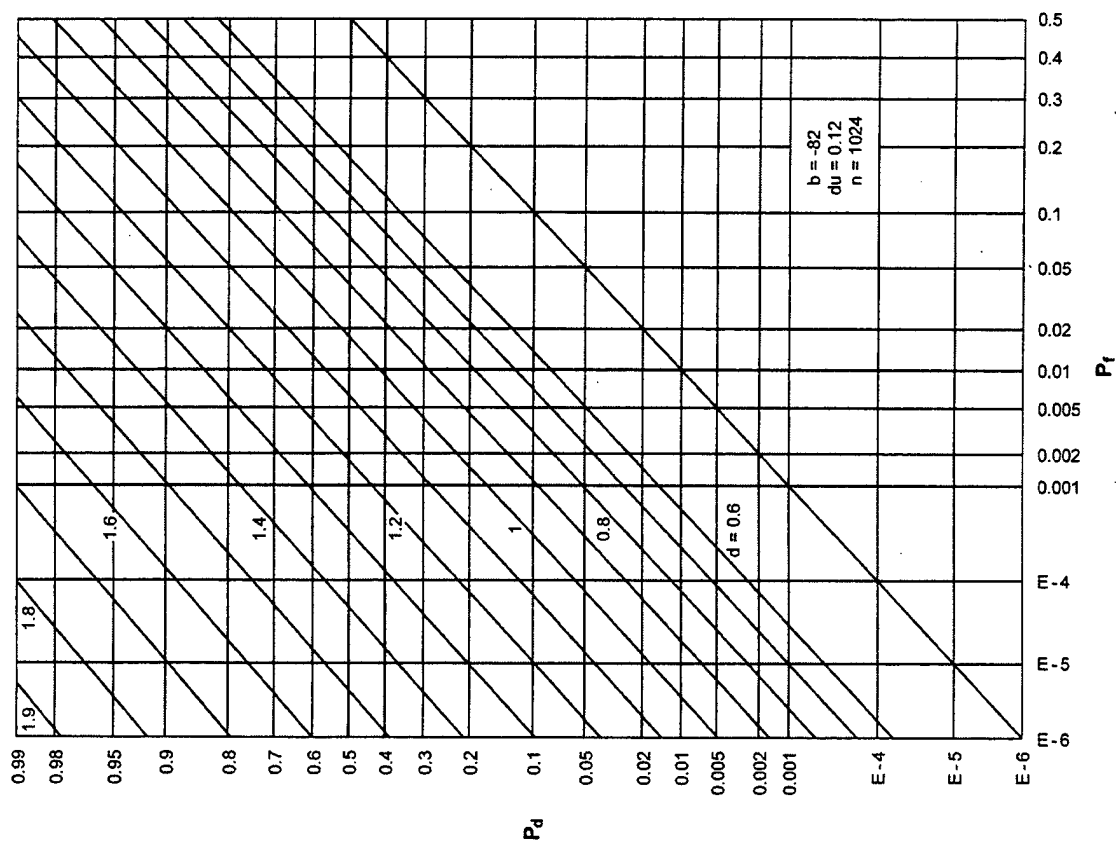


Figure A-43. ROCs for $K = 1$, $N = 16$, $M = 64$

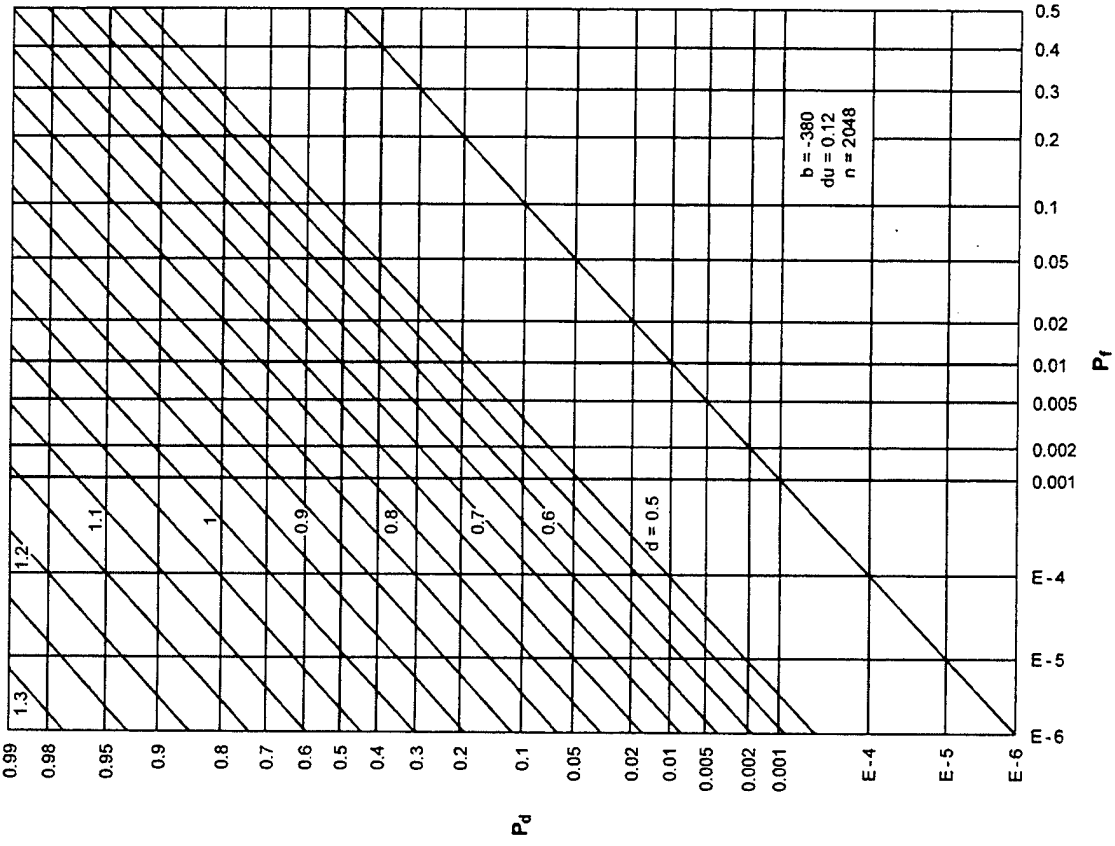


Figure A-45. ROCs for $K = 1$, $N = 16$, $M = 256$

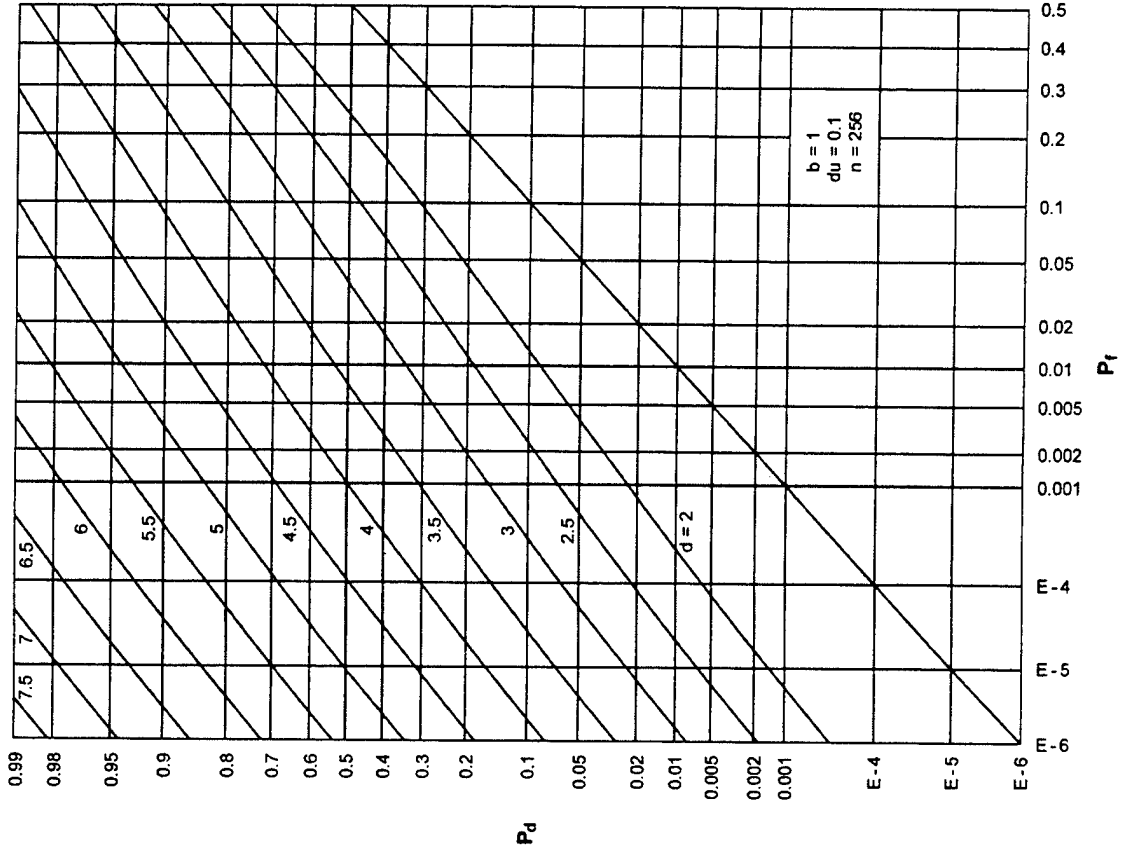


Figure A-46. ROCs for $K = 1$, $N = 32$, $M = 1$

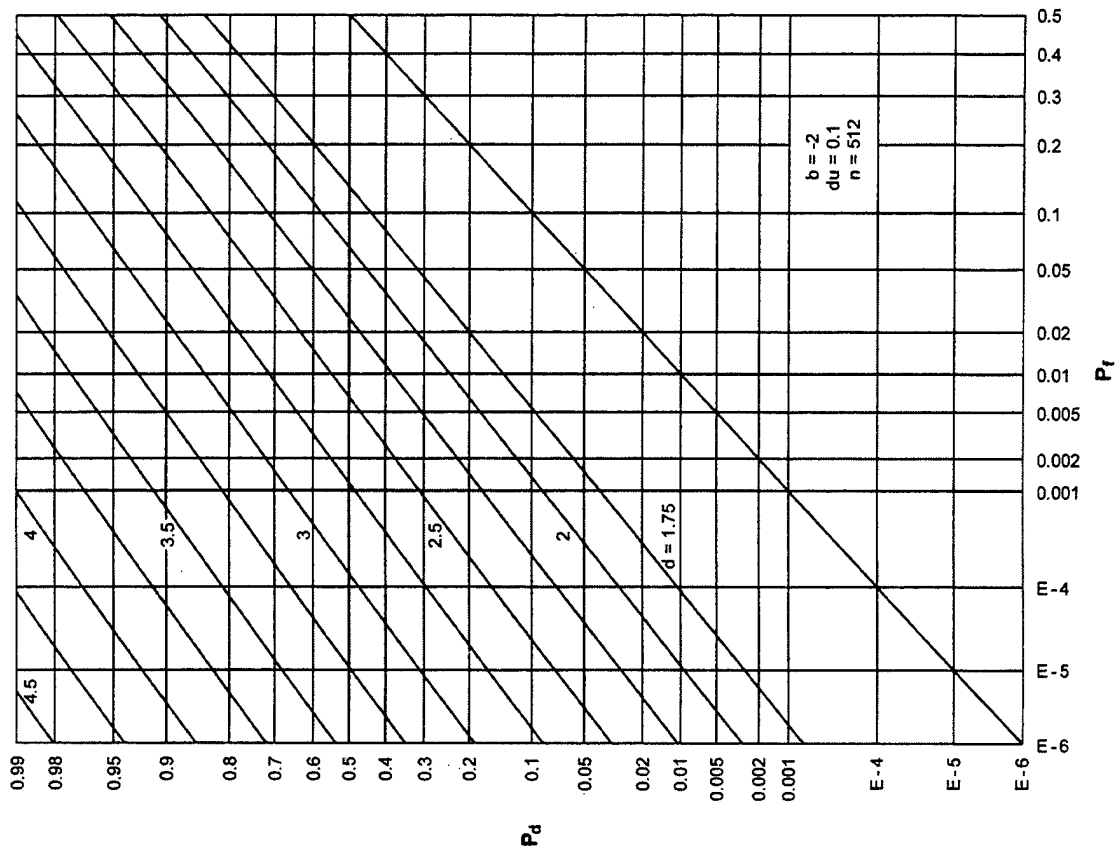


Figure A-48. ROCs for $K = 1$, $N = 32$, $M = 4$

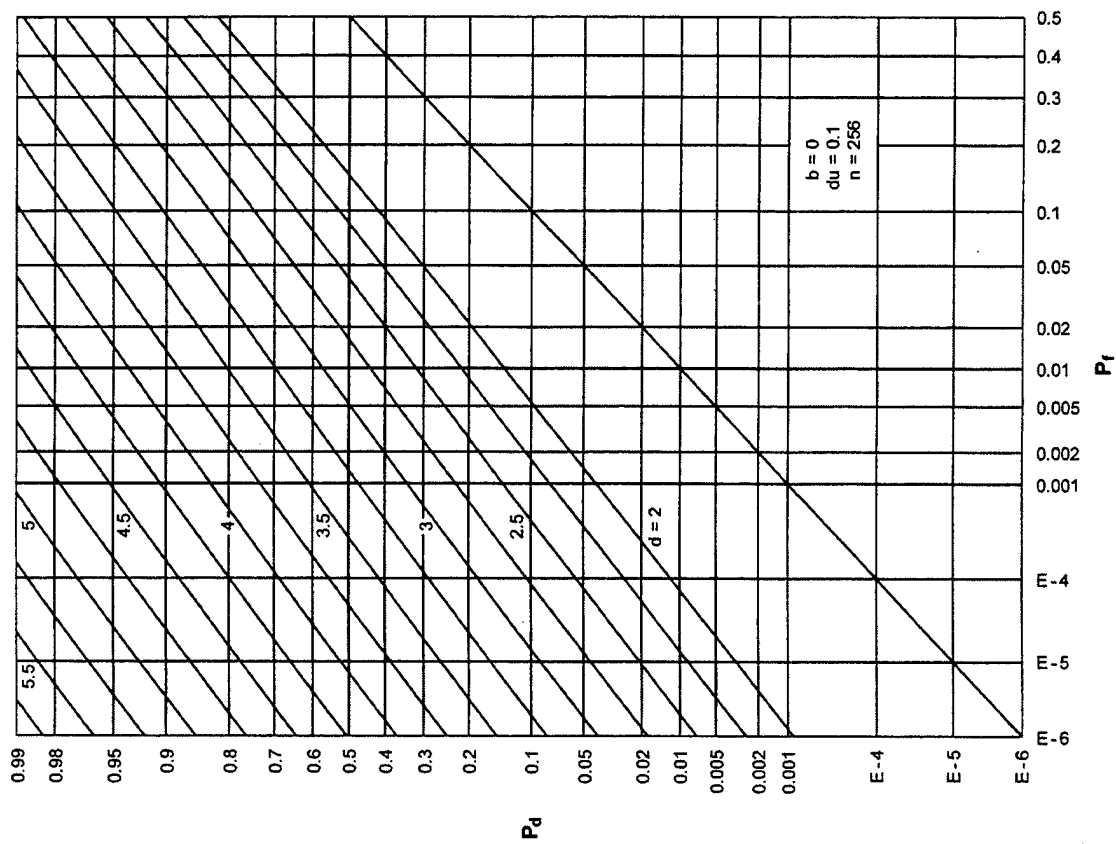


Figure A-47. ROCs for $K = 1$, $N = 32$, $M = 2$

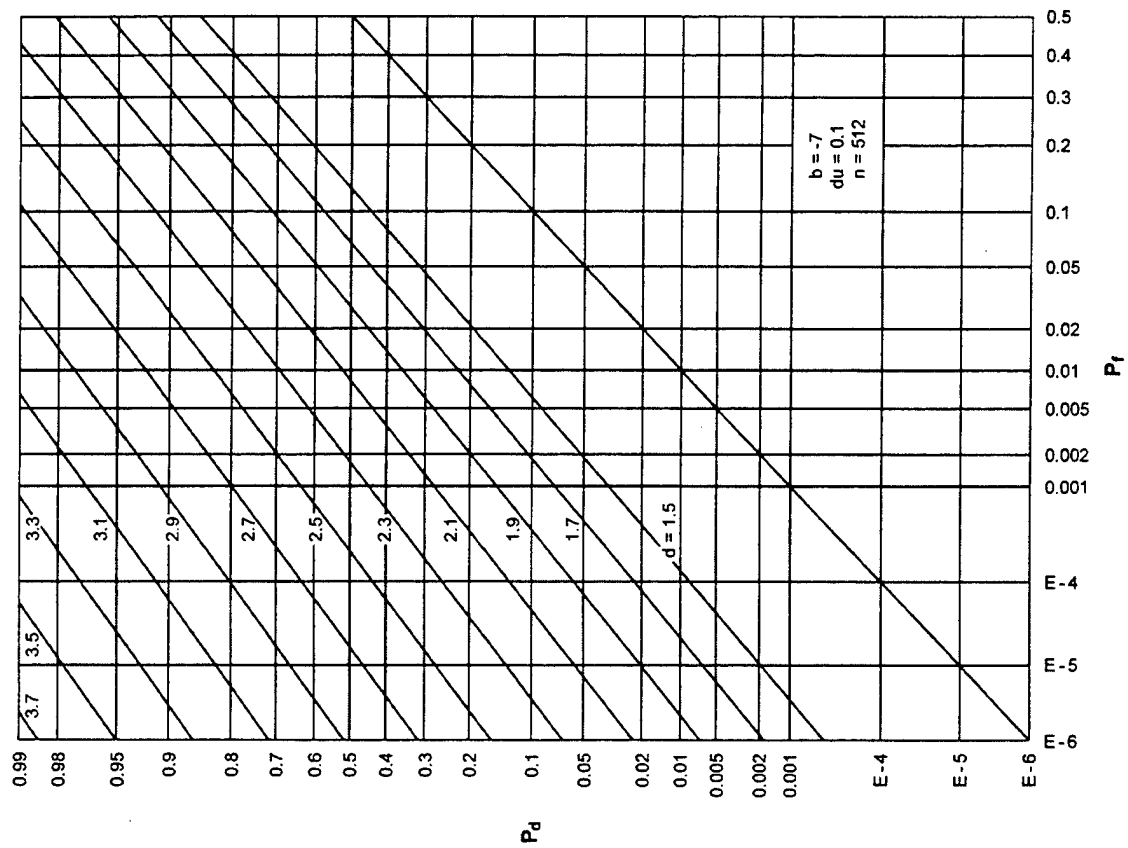


Figure A-49. ROCs for $K = 1$, $N = 32$, $M = 8$

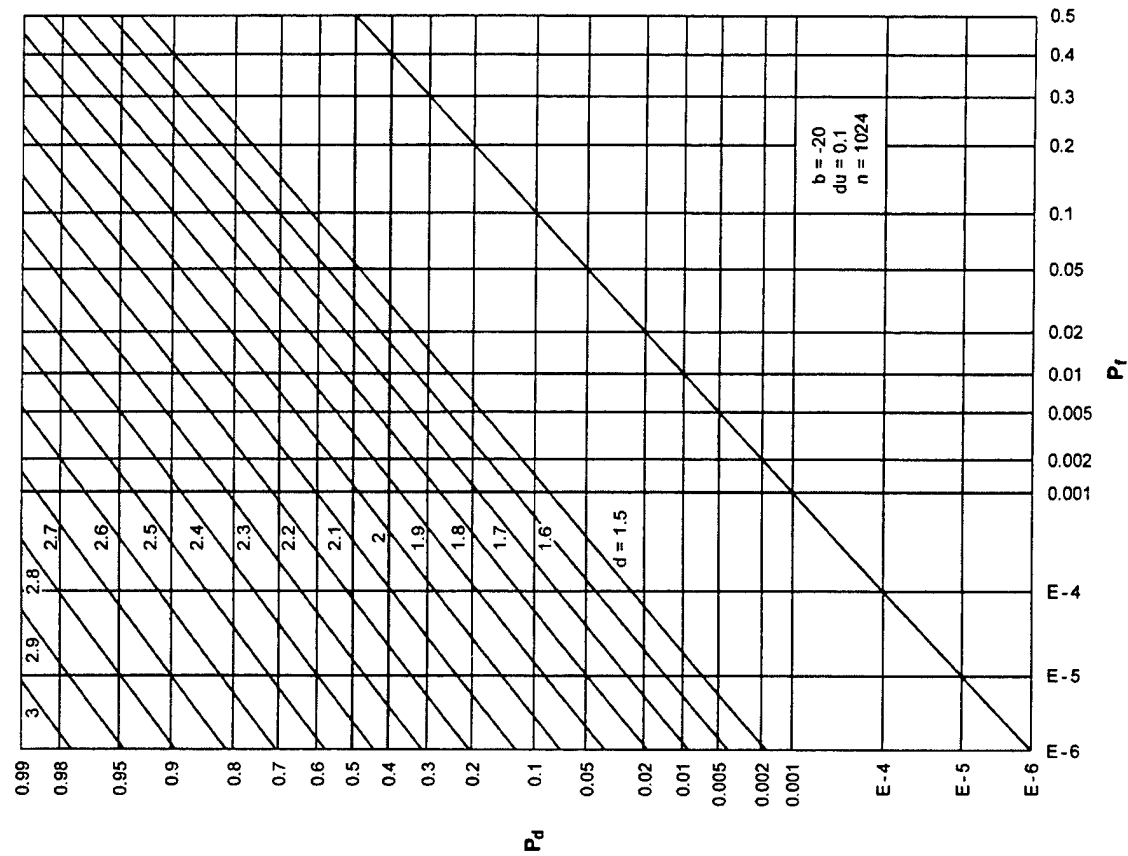


Figure A-50. ROCs for $K = 1$, $N = 32$, $M = 16$

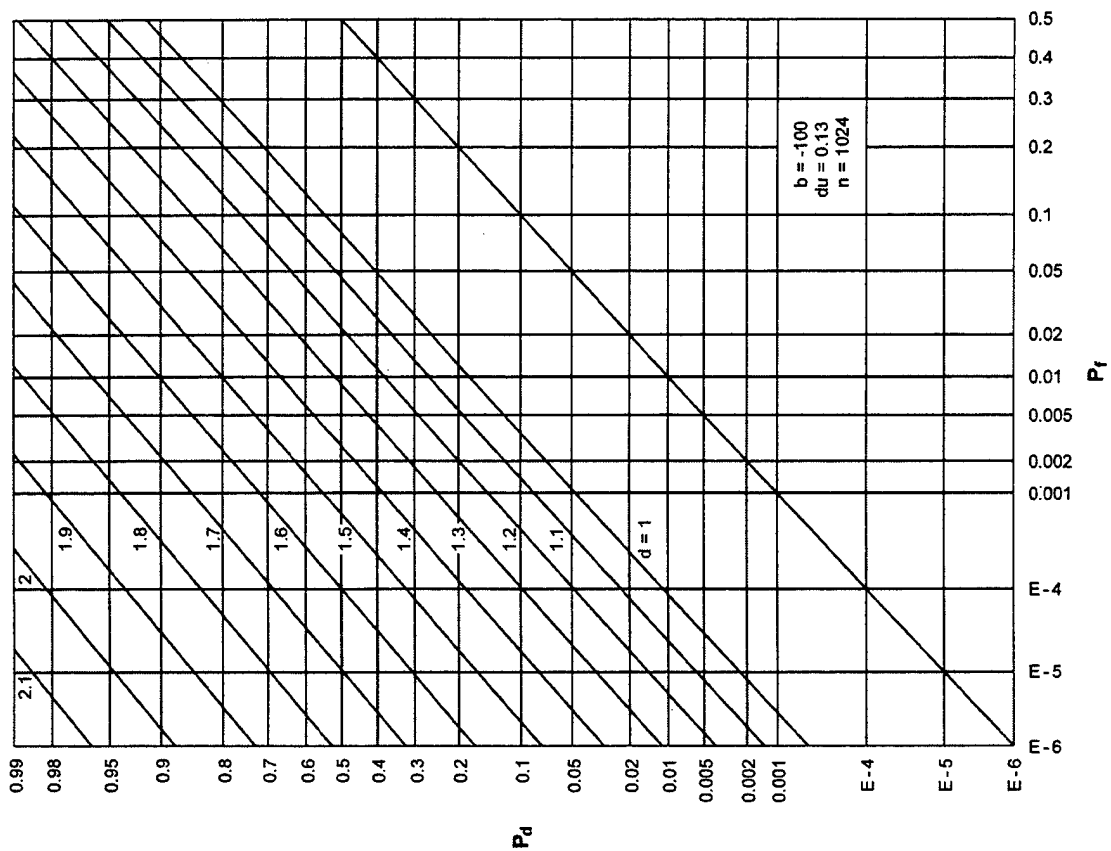


Figure A-52. ROCs for $K = 1$, $N = 32$, $M = 64$

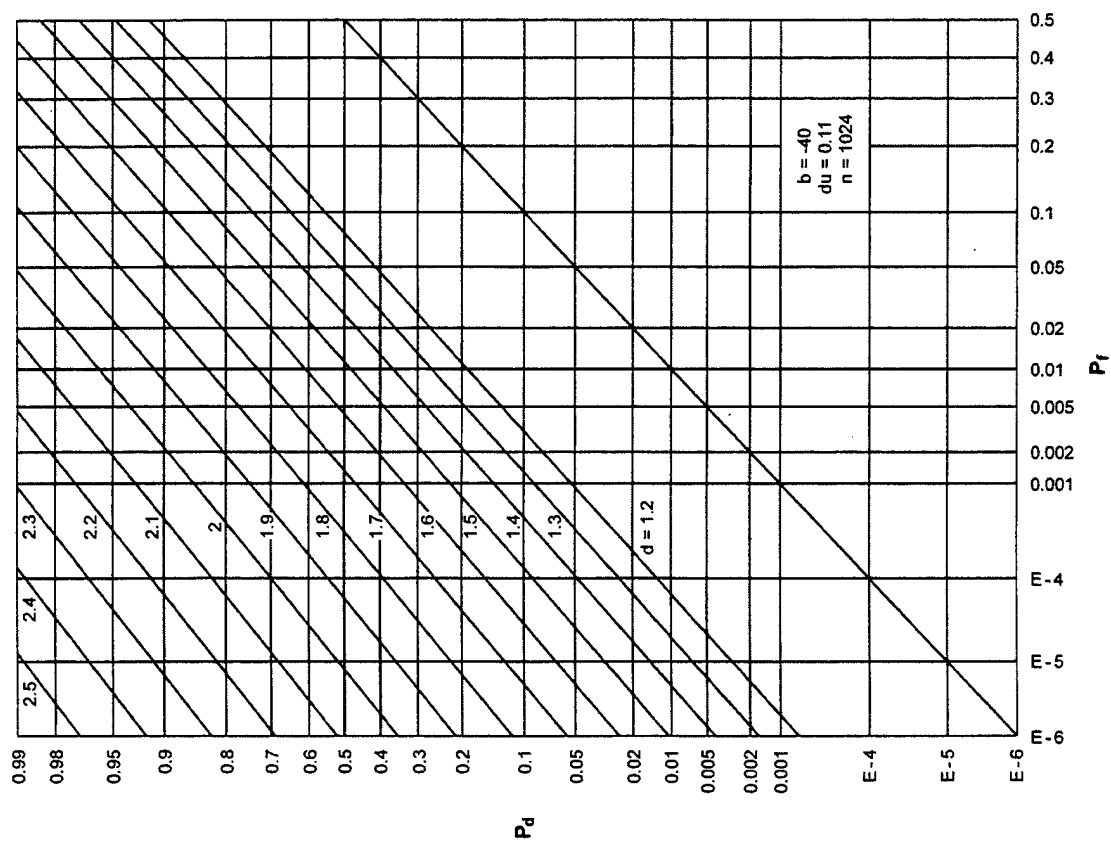


Figure A-51. ROCs for $K = 1$, $N = 32$, $M = 32$

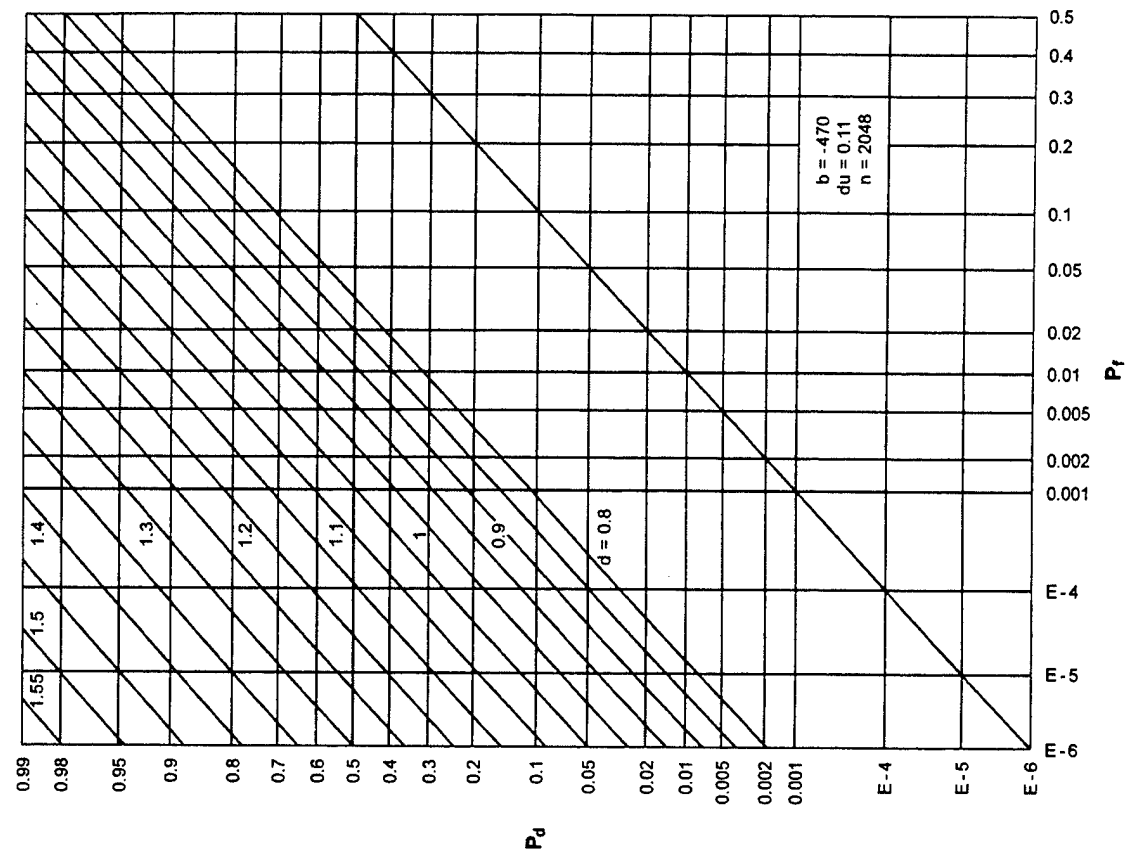


Figure A-54. ROCs for $K = 1$, $N = 32$, $M = 256$

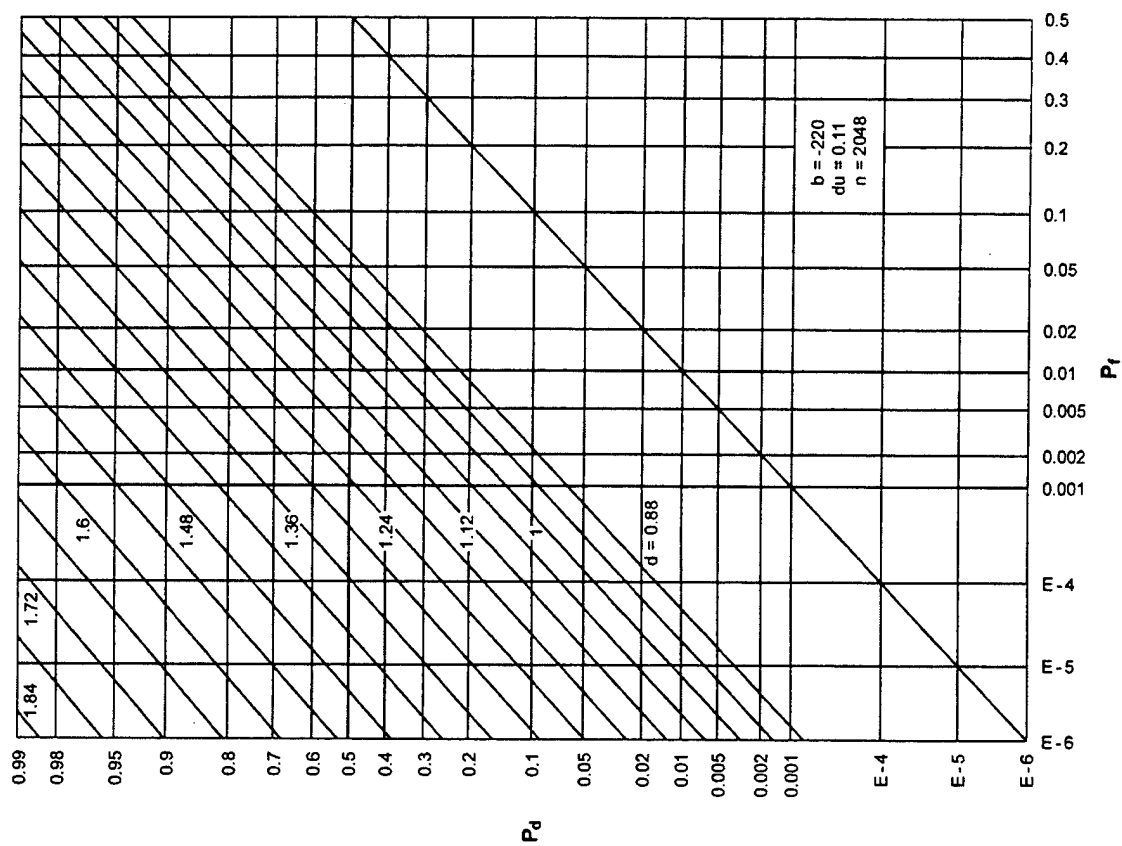


Figure A-53. ROCs for $K = 1$, $N = 32$, $M = 128$

APPENDIX B — MATLAB PROGRAM FOR EVALUATION OF RECEIVER OPERATING CHARACTERISTICS

Every figure in each set of ROCs in appendix A has the three parameter values listed on it that were used to generate those specific curves. They are the bias b , sampling increment du , and FFT size n . Because an additive constant to the decision variable in figure 1 does not change the ROC (reference 1), bias b was added to RV $w(t)$ and chosen so as to make the sum variable as small as possible, but never negative (within roundoff error). This procedure maximizes the unaliased region when the final FFT is conducted from the CF domain, equation (12), to the EDF domain for system output $w(t)$, as well as eases the requirements on sampling increment du and FFT size n .

Sampling increment du is applied in the u domain to equations (19) and (20); increment du must be taken small enough so that the approximation to CF $f_v(\xi)$ in equation (11) is not aliased significantly in the ξ domain. Finally, FFT size n must be taken large enough so that the u -domain span, $n du$, in the final FFT of equation (12), from the CF to the EDF, guarantees insignificant aliasing. Complete details on this cascade procedure are presented in appendix B of reference 1.

All three parameter values (b , du , n) have been chosen by a trial and error procedure, in which intermediate CF $f_v(\xi)$ is observed in the ξ domain and output EDF $e_w(u)$ is observed in the u domain. Repeated trials led to the tight parameter values listed on each set of ROCs. These listed parameter values can serve as starting or reference points for the evaluation of additional ROCs with different values of K , N , M , and d that are of interest to a user. The following listing of the MATLAB program corresponds to figure A-45.

```
clear, clf % Part III, NUWC TR 11,248
b=-380;    % Additive bias to w
du=.12;    % Sampling increment in u
n=2^11;    % FFT size
kc=1;%FIXED % K, amount of pre-averaging
nc=16;     % N, amount of or-ing
mc=256;    % M, amount of post-averaging
dmin=.5;   % Minimum deflection d
dinc=.05;  % Increment in deflection d
num=17;    % Number of ROCs
disp('b du n; kc nc mc:')
disp([b du n; kc nc mc])
xg=[1e-6 1e-5 1e-4 .001 .002 .005 .01 .02...
    .05 .1 .2 .3 .4 .5];
yg=[1e-6 1e-5 1e-4 .001 .002 .005 .01 .02...
    .05 .1 .2 .3 .4 .5 .6 .7 .8 .9 .95 .98 .99];
xg=phiinv(xg);
yg=phiinv(yg);
[Xg,Yg]=meshgrid(xg,yg);
Magcf=zeros(n,1);
EDF=zeros(n,1);
Pd=zeros(n,num+1);
n1=n-1; n2=n/2; n3=n2+1; nc1=nc-1;
pn=pi/n; d2=du/2; dxi=2*pi/(n*du);
arg=pn.*(1:n2)';
rsinc=arg./sin(arg);
ex=exp(b*dxi*(0:n2) '*i);
disp('          isnr   edf(0)-1')
```

```

for isnr=0:num
    d=dmin+dinc*(isnr-1);
    if(isnr==0), d=0; end
    X=zeros(n,1)+zeros(n,1)*i;
    meanv=0; cdfk=0; area=0;
    u0=phiinv(10^(-16/nc)); k=floor(u0/du);
    while(cdfk < .5 | area > 1e-20)
        k=k+1; uk=du*k; u2=uk+d2;
        c0=phi(u2);
        if(d==0), c1=c0;
        else c1=phi(u2-d);
        end
        cdfo=cdfk; cdfk=c1*c0^nc1;
        area=cdfk-cdfo;
        j=mod(k,n);
        X(j+1)=X(j+1)+area;
        meanv=meanv+area*uk; % uk, not u2
    end
    X=fftgreen(X);
    Magcf=log10(magsq(X)+1e-50)*.5;
    plot(Magcf, 'r')
    axis([1 n+1 -16 0]); grid on
    pause(1)
    X(2:n3)=conj(X(2:n3)).*rsinc(1:n2);
    X(n2+2:n)=0;
    X=X.^mc;
    X(1:n3)=X(1:n3).*ex;
    meanw=meanv*mc+b;
    X(1)=0;
    X(2:n3)=X(2:n3)./(1:n2)';
    X=fftgreen(X);
    a=.5+meanw/(n*du);
    edf0=a+imag(X(1))/pi;
    disp([isnr edf0-1])
    k=(1:n)';
    edf=a-(k-1)./n+imag(X(k))./pi;
    X=edf;
    EDF=log10(abs(edf)+1e-30);
    plot(EDF, 'r')
    axis([1 n+1 -18 0]); grid on
    pause(1)

```



```

        edf=real(X(k));
        edf=min(edf,1-1e-12);
        edf=max(edf,1e-12);
        Pd(:,isnr+1)=phiinv(edf);
    end
    beep
    pause
    clf
    hold on
    set(gcf,'PaperPosition',[.25 .25 8 10.5])
    plot(xg,Yg,'k')
    plot(Xg,yg,'k')
    plot(xg,xg,'k') % zero SNR ROC
    plot(Pd(:,1),Pd(:,[2:num+1]),'k')
    axis([xg(1) xg(14) yg(1) yg(21)])
    axis off
    while 1
        T=input('pf pd isnr: ');
        if(T(1)==0), break, end
        pft=phiinv(T(1));
        pdt=phiinv(T(2));
        isnr=T(3);
        for j=0:n1
            if(Pd(j+1,1)<pft), break, end
        end
        x1=Pd(j+1,1);
        x2=Pd(j,1);
        as=Pd(j+1,isnr+1);
        bs=Pd(j+1,isnr+2);
        cs=Pd(j,isnr+1);
        ss=(cs-as)/(x2-x1);
        a1=pdt-ss*pft;
        fs=(a1+ss*x1-as)/(bs-as);
        dc=dmin+dinc*(isnr-1+fs);
        disp([T fs dc])
    end

% function y=phiinv(x) % 0 < x < 1
% y=1.414213562373095*erfinv(2*x-1);

% function y=phi(x)
% y=.5*erfc(-x*.7071067811865476,1);

```

APPENDIX C - SHIFTED DECISION VARIABLES

Suppose that the ROCs for decision variables w_0 and w_1 under hypotheses H_0 and H_1 , respectively, are of interest. That is, a plot of exceedance probability $P_d(k) = \text{Prob}(w_1 > k\Delta)$ versus exceedance probability $P_f(k) = \text{Prob}(w_0 > k\Delta)$ is desired. Let shifted decision variables

$$z_0 = w_0 + I_0\Delta, \quad z_1 = w_1 + I_1\Delta, \quad (C-1)$$

where I_0 and I_1 are integers. Then,

$$\begin{aligned} P_f(k) &= \text{Prob}(z_0 > (k + I_0)\Delta) \equiv Q_0(k + I_0), \\ P_d(k) &= \text{Prob}(z_1 > (k + I_1)\Delta) \equiv Q_1(k + I_1), \end{aligned} \quad (C-2)$$

where exceedance probabilities Q_0 and Q_1 are computed and stored for decision variables z_0 and z_1 under hypotheses H_0 and H_1 , respectively. That is, probabilities $Q_0(n) = \text{Prob}(z_0 > n\Delta)$ and $Q_1(n) = \text{Prob}(z_1 > n\Delta)$ are available.

Then, to obtain the ROC for variables w_0 and w_1 , plot $Q_1(k + I_1)$ versus $Q_0(k + I_0)$, or, equivalently, $Q_1(k + I_1 - I_0)$ versus $Q_0(k)$. The integers I_0 and I_1 should be taken with as large negative values as possible, but still keeping the shifted RVs z_0 and z_1 positive. This procedure enables maximum use of the fundamental "cleared region" in the EDF plot obtained by an FFT procedure; see references 3 and 4. In fact, for best results, I_1 can be a function of (SNR measure) deflection d .

REFERENCES

1. Albert H. Nuttall, "Detection Performance of Or-ing Device with Pre- and Post-Averaging: Part I - Random Signal," NUWC-NPT Technical Report 11,150, Naval Undersea Warfare Center Division, Newport, RI, 26 July 1999.
2. Albert H. Nuttall, "Detection Performance of Or-ing Device with Pre- and Post-Averaging: Part II - Phase-Incoherent Signal," NUWC-NPT Technical Report 11,166, Naval Undersea Warfare Center Division, Newport, RI, 28 September 1999.
3. Albert H. Nuttall, "Accurate Efficient Evaluation of Cumulative or Exceedance Probability Distributions Directly From Characteristic Functions," NUSC Technical Report 7023, Naval Underwater Systems Center, New London, CT, 1 October 1983.
4. Albert H. Nuttall, "Evaluation of Small Tail Probabilities Directly from the Characteristic Function," NUWC-NPT Technical Report 10,840, Naval Undersea Warfare Center Division, Newport, RI, 15 September 1997.
5. **Handbook of Mathematical Functions**, U.S. Department of Commerce, National Bureau of Standards, Applied Mathematics Series, no. 55, U.S. Government Printing Office, Washington, DC, June 1964.

INITIAL DISTRIBUTION LIST

Addressee	No. of Copies
Center for Naval Analyses, VA	1
Coast Guard Academy, CT	
J. Wolcin	1
Commander Submarine Force, U.S. Pacific Fleet, HI	
W. Mosa, CSP N72	1
Defense Technical Information Center	2
Griffiss Air Force Base, NY	
Documents Library	1
J. Michels	1
Hanscom Air Force Base, MA	
M. Rangaswamy	1
National Radio Astronomy Observatory, VA	
F. Schwab	1
National Security Agency, MD	
J. Maar	1
National Technical Information Service, VA	10
Naval Environmental Prediction Research Facility, CA	1
Naval Intelligence Command, DC	1
Naval Oceanographic and Atmospheric Research Laboratory, MS	
B. Adams	1
R. Fiddler	1
E. Franchi	1
R. Wagstaff	1
Naval Oceanographic Office, MS	1
Naval Personnel Research and Development Center, CA	1
Naval Postgraduate School, CA	
Superintendent	1
C. Therrien	1
Naval Research Laboratory, DC	
W. Gabriel	1
E. Wald	1
N. Yen	1
Naval Surface Warfare Center, FL	
E. Linsenmeyer	1
D. Skinner	1
Naval Surface Warfare Center, VA	
J. Gray	1
Naval Technical Intelligence Center, DC	
Commanding Officer	1
D. Rothenberger	1
Naval Undersea Warfare Center, FL	
Officer in Charge	1
Naval Weapons Center, CA	1
Office of the Chief of Naval Research, VA	
ONR 321 (D. Johnson)	1
ONR 321US (N. Harned)	1
ONR 322 (R. Tipper)	1
ONR 334 (P. Abraham)	1

INITIAL DISTRIBUTION LIST (Cont'd)

Addressee	No. of Copies
Office of Naval Research	
ONR 31 (R. R. Junker)	1
ONR 311 (A. M. van Tilborg)	1
ONR 312 (M. N. Yoder)	1
ONR 313 (N. L. Gerr)	1
ONR 32 (S. E. Ramberg)	1
ONR 321 (F. Herr)	1
ONR 33 (S. G. Lekoudis)	1
ONR 334 (A. J. Tucker)	1
ONR 342 (W. S. Vaughan)	1
ONR 343 (R. Cole)	1
ONR 362 (M. Sponder)	1
Program Executive Office, Undersea Warfare (ASTO), VA	
J. Thompson, A. Hommel, R. Zarnich	3
U.S. Air Force, Maxwell Air Force Base, AL	
Air University Library	1
Vandenberg Air Force Base, CA	
CAPT R. Leonard	1
Brown University, RI	
Documents Library	1
Catholic University of America, DC	
J. McCoy	1
Drexel University, PA	
S. Kesler	1
Duke University, NC	
J. Krolik	1
Harvard University, MA	
Gordon McKay Library	1
Johns Hopkins University, Applied Physics Laboratory, MD	
H. M. South	1
T. N. Stewart	1
Lawrence Livermore National Laboratory, CA	
L. Ng	1
Los Alamos National Laboratory, NM	1
Marine Biological Laboratory, MA	
Library	1
Massachusetts Institute of Technology, MA	
Barker Engineering Library	1
Massachusetts Institute of Technology, Lincoln Laboratory, MA	
V. Premus	1
J. Ward	1
Northeastern University, MA	
C. Nikias	1
Pennsylvania State University, Applied Research Laboratory, PA	
R. Hettche	1
E. Liszka	1
F. Symons	1
Princeton University, NJ	
S. Schwartz	1
Rutgers University, NJ	
S. Orfanidis	1

INITIAL DISTRIBUTION LIST (Cont'd)

Addressee	No. of Copies
San Diego State University, CA	
F. Harris	1
Sandia National Laboratory, NM	
J. Claasen	1
Scripps Institution of Oceanography, Marine Physical Laboratory, CA	
Director	1
Syracuse University, NY	
D. Weiner	1
Engineering Societies Information Center, Kansas City, MO	
Linda Hall Library-East	1
University of Colorado, CO	
L. Scharf	1
University of Connecticut, CT	
Wilbur Cross Library	1
C. Knapp	1
P. Willett	1
University of Florida, FL	
D. Childers	1
University of Hartford	
Science and Engineering Library	1
University of Illinois, IL	
D. Jones	1
University of Illinois at Chicago, IL	
A. Nehorai	1
University of Massachusetts, MA	
C. Chen	1
University of Michigan, MI	
Communications and Signal Processing Laboratory	1
W. Williams	1
University of Minnesota, MN	
M. Kaveh	1
University of Rhode Island, RI	
Library	1
G. Boudreaux-Bartels	1
S. Kay	1
D. Tufts	1
University of Rochester, NY	
E. Titlebaum	1
University of Southern California, CA	
W. Lindsey	1
A. Polydoros	1
University of Texas, TX	
Applied Research Laboratory	1
C. Penrod	1
University of Washington, WA	
Applied Physics Laboratory	1
D. Lytle	1
J. Ritcey	1
R. Spindel	1

INITIAL DISTRIBUTION LIST (Cont'd)

Addressee	No. of Copies
Villanova University, PA	
M. Amin	1
Woods Hole Oceanographic Institution, MA	
Director	1
T. Stanton	1
Yale University, CT	
Kline Science Library	1
P. Schultheiss	1
Analysis and Technology, CT	
Library	1
Analysis and Technology, VA	
D. Clark	1
Atlantic Aerospace Electronics Corp.	
R. Stahl	1
Bell Communications Research, NJ	
D. Sunday	1
Berkeley Research, CA	
S. McDonald	1
Bolt, Beranek, and Newman, CT	
P. Cable	1
Bolt, Beranek, and Newman, MA	
H. Gish	1
DSR, Inc., VA	
M. Bozek-Kuzmicki	1
EG&G Services, CT	
J. Pratt	1
Engineering Technology Center	
D. Lerro	1
General Electric, NJ	
H. Urkowitz	1
Harris Scientific Services, NY	
B. Harris	1
Hughes Defense Communications, IN	
R. Kenefic	1
Kildare Corporation, CT	
R. Mellen	1
Lincom Corporation, MA	
T. Schonhoff	1
Lockheed Martin, Undersea Systems, VA	
M. Flicker	1
Lockheed Martin, Ocean Sensor Systems, NY	
R. Schumacher	1
Marconi Aerospace Defense Systems, TX	
R. D. Wallace	1
MITRE Corporation, VA	
S. Pawlukiewicz	1
R. Bethel	1
Neural Technology, Inc., SC	
E. A. Tagliarini	1
Orincon Corporation, VA	
H. Cox	1

INITIAL DISTRIBUTION LIST (Cont'd)

Addressee	No. of Copies
Philips Research Laboratory, Netherlands	
A. J. E. M. Janssen	1
Planning Systems, Inc., CA	
W. Marsh	1
Prometheus, RI	
M. Barrett	1
J. Byrnes	1
Raytheon, RI	
R. Conner	1
S. Reese	1
Schlumberger-Doll Research, CT	
R. Shenoy	1
Science Applications International Corporation, CA	
C. Katz	1
Science Applications International Corporation, VA	
P. Mikhalevsky	1
Toyon Research, CA	
M. Van Blaricum	1
Tracor, TX	
T. Leih	1
TRW, VA	
R. Prager	1
G. Maher	1
Westinghouse Electric, MA	
R. Kennedy	1
Westinghouse Electric, Annapolis, MD	
H. Newman	1
Westinghouse Electric, Baltimore, MD	
R. Park	1
K. Harvel, Austin, TX	1